

---

Dépôt Institutionnel de l'Université libre de Bruxelles /  
Université libre de Bruxelles Institutional Repository  
**Thèse de doctorat/ PhD Thesis**

**Citation APA:**

Daems, D. (1998). *Probabilistic and thermodynamic aspects of dynamical systems* (Unpublished doctoral dissertation). Université libre de Bruxelles, Faculté des sciences, Bruxelles.

**Disponible à / Available at permalink :** <https://dipot.ulb.ac.be/dspace/bitstream/2013/212048/1/a16bb414-976b-48a9-9437-2906003a086a.txt>

---

(English version below)

Cette thèse de doctorat a été numérisée par l'Université libre de Bruxelles. L'auteur qui s'opposerait à sa mise en ligne dans DI-fusion est invité à prendre contact avec l'Université (di-fusion@ulb.be).

**Dans le cas où une version électronique native de la thèse existe, l'Université ne peut garantir que la présente version numérisée soit identique à la version électronique native, ni qu'elle soit la version officielle définitive de la thèse.**

DI-fusion, le Dépôt Institutionnel de l'Université libre de Bruxelles, recueille la production scientifique de l'Université, mise à disposition en libre accès autant que possible. Les œuvres accessibles dans DI-fusion sont protégées par la législation belge relative aux droits d'auteur et aux droits voisins. Toute personne peut, sans avoir à demander l'autorisation de l'auteur ou de l'ayant-droit, à des fins d'usage privé ou à des fins d'illustration de l'enseignement ou de recherche scientifique, dans la mesure justifiée par le but non lucratif poursuivi, lire, télécharger ou reproduire sur papier ou sur tout autre support, les articles ou des fragments d'autres œuvres, disponibles dans DI-fusion, pour autant que :

- Le nom des auteurs, le titre et la référence bibliographique complète soient cités;
- L'identifiant unique attribué aux métadonnées dans DI-fusion (permalink) soit indiqué;
- Le contenu ne soit pas modifié.

L'œuvre ne peut être stockée dans une autre base de données dans le but d'y donner accès ; l'identifiant unique (permalink) indiqué ci-dessus doit toujours être utilisé pour donner accès à l'œuvre. Toute autre utilisation non mentionnée ci-dessus nécessite l'autorisation de l'auteur de l'œuvre ou de l'ayant droit.

----- **English Version** -----

This Ph.D. thesis has been digitized by Université libre de Bruxelles. The author who would disagree on its online availability in DI-fusion is invited to contact the University (di-fusion@ulb.be).

**If a native electronic version of the thesis exists, the University can guarantee neither that the present digitized version is identical to the native electronic version, nor that it is the definitive official version of the thesis.**

DI-fusion is the Institutional Repository of Université libre de Bruxelles; it collects the research output of the University, available on open access as much as possible. The works included in DI-fusion are protected by the Belgian legislation relating to authors' rights and neighbouring rights. Any user may, without prior permission from the authors or copyright owners, for private usage or for educational or scientific research purposes, to the extent justified by the non-profit activity, read, download or reproduce on paper or on any other media, the articles or fragments of other works, available in DI-fusion, provided:

- The authors, title and full bibliographic details are credited in any copy;
- The unique identifier (permalink) for the original metadata page in DI-fusion is indicated;
- The content is not changed in any way.

It is not permitted to store the work in another database in order to provide access to it; the unique identifier (permalink) indicated above must always be used to provide access to the work. Any other use not mentioned above requires the authors' or copyright owners' permission.

---

D 02737

LIBRE DE BRUXELLES

Faculté des Sciences  
de Chimie Physique

*Probabilistic and thermodynamic aspects  
of dynamical systems*

Thèse présentée en vue de l'obtention  
du grade de Docteur en Sciences

*David Daems*

Mars 1998

UNIVERSITE LIBRE DE BRUXELLES

Faculté des Sciences  
Service de Chimie Physique

*Probabilistic and thermodynamic aspects  
of dynamical systems*

Thèse présentée en vue de l'obtention  
du grade de Docteur en Sciences

*David Daems*

Mars 1998

## Acknowledgements

*I wish to express my deepest gratitude to Grégoire Nicolis who supervised this thesis. Through his suggestions, advices and criticisms he enabled me to perform this work while minimizing my entropy production.*

*Alexandre L. Baranovsky and Itamar Procaccia have offered a wonderful hospitality and taught me a lot during my stay in Tomsk State University and the Weizmann Institute of Science.*

*I owe much to Pierre Gaspard and John W. Turner for enlightening conversations and to Dean J. Driebe, Jérôme Losson, Thomas Gilbert and Dónal MacKernan with whom I had many exciting discussions.*

*I am indebted to Georges Destree for helping me so many times with computers and to José Halloy and Mamad Malek Mansour who often volunteered even when they were forced.*

*I have also benefited from insightful conversations with I. Antoniou, F. Bonetto, F. Bosco, , J. Bricmont, E. G. D. Cohen, C. I. Christov, A. L. Fairhall, B. Fernandez, S. V. Gonchenko, G. Keller, L. M. Lerman, V. S. L'vov, J. Piasecki, A. I. Rakhmanov, L. Rondoni, A. L. Shil'nikov, L. P. Shil'nikov, I. Sushko, S. Tasaki, T. Tél, D. V. Turaev, D. Vandembrouc, J. Vollmer, J. Weimar, J. A. Yorke and R. Zeitak.*

*It is my pleasure to mention those, from the department or met abroad, who have contributed to make these years so profitable in many ways: Adi, Adrienne, Alberto, Amer, Arkady, Arnaud, Astero, Barak, Benny, Benoit, Bernold, Bruno, Charlot, Damien, David, Daniel, Debra, Dima, Drisse, Dónal, Eli, Felipe, Gianluca, Hans, Hicham, Irène, Isabella, Jacques, Jean-Christophe, Jer, Jérôme, Jésus, José, Julia, Julian, Kristina, Laetitia, Laurent, Marcop, M'Feddal, Mike, Misha, Mustafa, Nadia, Ole, Olivier, Paul, Phil, Reuven, Sergei, Stam, Stéphane, Thierre, Tomo, Vassilis, Yves.*

*My thanks go to Pierre Kinet, Irène Saverino and Sonia Wellens for their kind assistance.*

*I acknowledge the financial support of the Belgian Fonds National de la Recherche Scientifique from October 1993 to September 1997 and of the Belgian Fondation David & Alice Van Buuren from October 1997 to March 1998.*

## Résumé

Il est bien établi que des larges classes de systèmes dynamiques présentent lorsqu'ils sont soumis à des contraintes de non-équilibre appropriées des comportements complexes associés à des bifurcations culminant en chaos déterministe. De par la sensibilité aux conditions initiales une description probabiliste constitue l'approche naturelle des systèmes chaotiques. Le point de départ est une équation analogue à celle de Liouville, appelée équation de Perron-Frobenius pour les systèmes à temps discret, qui fait évoluer les densités de probabilité.

Le formalisme de l'équation maîtresse généralisée nous permet d'obtenir une décomposition spectrale généralisée de l'opérateur de Perron-Frobenius en présence de blocs de Jordan. Une correspondance entre la non-diagonalisabilité de l'opérateur de Perron-Frobenius et les transitions entre modes de décroissance des fonctions d'auto-corrélation temporelle est établie. Nous étudions les propriétés statistiques d'une classe importante de systèmes dynamiques donnant lieu à du chaos homocline, observé notamment dans la réaction de Belousov-Zhabotinski, et montrons que les fonctions d'auto-corrélation temporelle fournissent une caractérisation des différents types d'attracteurs homoclines.

Le problème inverse qui consiste à construire des systèmes dynamiques ayant des propriétés probabilistes données est considéré. Nous sommes en mesure de construire des applications chaotiques unidimensionnelles ayant une densité de probabilité invariante et une fonction d'auto-corrélation à une échelle de temps prescrites.

Un modèle simplifié de systèmes étendus dans l'espace connu sous le nom d'applications couplées et donnant lieu à du chaos spatio-temporel est étudié. Le cas de deux applications couplées de manière diffusive est résolu exactement pour des valeurs finies de la constante de couplage. Nous proposons un réseau d'applications couplées à plus proches voisins et déterminons la projection unidimensionnelle de la densité de probabilité invariante du système pour une large classe de fonctions.

Enfin, nous apportons de nouvelles perspectives à un vieux problème de la mécanique statistique en développant une thermodynamique de non-équilibre pour les systèmes dynamiques amenable à une description en terme d'une équation de Fokker-Planck. Des termes de flux et de production d'entropie dépendant des caractéristiques de la dynamique dans l'espace des phases, en particulier le taux de contraction de volume, sont identifiés et leur connexion avec la thermodynamique des processus irréversibles est étudiée.

## Summary

It is by now well-established that large classes of dynamical systems exhibit under appropriate nonequilibrium constraints complex behaviors associated to bifurcations culminating eventually to deterministic chaos. Owing to the property of sensitivity to initial conditions a probabilistic description constitutes the natural and most fruitful approach to chaotic systems. The starting point is a Liouville-like equation describing the evolution of probability densities which for discrete time systems is known as the Perron-Frobenius equation.

The formalism of the generalized master equation allows us to obtain a generalized spectral decomposition of the Perron-Frobenius operator involving Jordan blocks. A correspondence between the non-diagonalizability of the Perron-Frobenius operator and transitions between decay modes of the time autocorrelation functions is established. We investigate the statistical properties of an important class of dynamical systems giving rise to homoclinic chaos, observed for instance in the Belousov-Zhabotinski reaction, and show that the time autocorrelation functions provide a characterization of the different types of homoclinic chaotic attractors.

The inverse problem of designing dynamical systems with prescribed statistical properties is addressed. We are able to construct one-dimensional chaotic maps with arbitrary invariant probability density and correlation function involving one time scale.

A simplified model of spatially extended systems known as coupled map lattice and giving rise to spatio-temporal chaos is studied. The case of two diffusively coupled piecewise linear maps is solved exactly for finite values of the coupling constant. We propose a coupled map lattice with constant nearest-neighbour coupling and compute the invariant one-dimensional projection of the full probability density for a large class of maps.

Finally, attempting to bring new perspectives to an old problem of statistical mechanics, we develop a nonequilibrium thermodynamics for the class of dynamical systems amenable to a Fokker-Planck type of description based on the balance equation for the information entropy. Entropy flux and entropy production-like terms depending on the characteristics of the dynamics in phase space, particularly the rate of phase space volume contraction, are identified and their connection with irreversible thermodynamics is explored.



# Contents

Acknowledgements	i
Résumé	ii
Summary	iii
<b>1 Introduction</b>	<b>1</b>
1.1 General formulation . . . . .	2
1.2 Probabilistic aspects of bifurcation . . . . .	6
1.3 Probabilistic aspects of deterministic chaos . . . . .	9
1.4 Thermodynamic fluctuations and external noise . . . . .	13
1.5 Thermodynamic characterization of nonequilibrium states . . . . .	14
<b>2 Probabilistic description of one-dimensional chaotic maps:</b>	
<b>Jordan blocks - homoclinic chaos.</b>	<b>21</b>
2.1 Introduction . . . . .	21
2.2 Generalized master equation . . . . .	23
2.3 Time autocorrelation function. . . . .	29
2.4 Jordan blocks and transitions between decay modes . . . . .	30
2.4.1 Incomplete map . . . . .	31
2.4.2 Full map . . . . .	33
2.4.3 Conclusions . . . . .	35
2.5 Probabilistic approach to homoclinic chaos . . . . .	36
2.5.1 The Shil'nikov map and its 1-d contraction . . . . .	36
2.5.2 Spiral-type attractor . . . . .	39
2.5.3 Screw-type attractor . . . . .	41
2.5.4 Conclusions . . . . .	45

<b>3</b>	<b>Inverse problem: designing one-dimensional chaotic maps with prescribed statistical properties.</b>	<b>47</b>
3.1	Introduction . . . . .	47
3.2	Statistical properties of piecewise linear full maps . . . . .	48
3.3	Statistical properties of a class of piecewise linear non-Markov maps . . . . .	53
3.4	Analytic construction of maps with prescribed invariant measure . . . . .	59
3.5	Analytic construction of maps with prescribed invariant measure and correlation function . . . . .	64
3.6	Conclusions . . . . .	69
<b>4</b>	<b>Statistical properties of coupled map lattices: exact results</b>	<b>71</b>
4.1	Introduction . . . . .	71
4.2	Two diffusively coupled piecewise linear maps . . . . .	74
4.2.1	Generalized master equation for the coupled system . . . . .	75
4.2.2	Two 1-d mappings for the coupled system . . . . .	77
4.2.3	2-d Markov partitions for coupled dyadic maps . . . . .	81
4.2.4	Bernoulli and anti-Bernoulli maps for $\epsilon = \frac{1}{4}$ . . . . .	84
4.3	Coupled map lattices . . . . .	92
4.3.1	Reduced probability densities and BBGKY hierarchy . . . . .	93
4.3.2	Invariant 1-d marginal for piecewise linear full maps . . . . .	95
4.4	Conclusions . . . . .	98
<b>5</b>	<b>Nonequilibrium thermodynamics of dynamical systems: entropy production and phase space volume contraction</b>	<b>101</b>
5.1	Introduction . . . . .	101
5.2	Setting . . . . .	103
5.3	The information entropy and its balance . . . . .	105
5.4	Thermostatted systems . . . . .	108
5.5	Mesoscopic systems . . . . .	112
5.6	Conclusions . . . . .	115
<b>6</b>	<b>Conclusions and perspectives</b>	<b>117</b>

# Chapter 1

## Introduction

It is by now well-established that under appropriate nonequilibrium constraints large classes of dynamical systems exhibit complex behaviors associated to bifurcations culminating eventually to deterministic chaos. Owing to the property of sensitivity to initial conditions chaotic systems are to be described statistically. In this thesis we shall be concerned with the probabilistic description of large classes of chaotic systems as well as of a simplified model of spatially extended systems known as coupled map lattices which exhibits spatio-temporal chaos. On the other hand we develop a nonequilibrium thermodynamics of dynamical systems. In particular we shall inquire whether one can relate quantitatively the thermodynamic properties of a system at the macroscopic level to the characteristics of phase space dynamics at the microscopic level, accepting at the outset full validity of the basic laws governing this dynamics.

In this Introduction we focus on the foundations of the probabilistic description, a necessary step toward understanding statistical mechanics, as opposed to the traditional deterministic description in terms of phase space trajectories. We sort out the conditions under which probabilistic description becomes necessary and then inquire on the ways one can map, in a systematic manner, the underlying deterministic dynamics into such a description.

Our main thesis is the close link between the complexity of the system at hand and the need for a probabilistic approach. Far from being merely identified to the practical "complications" arising, for instance, when dealing with a large number of elements, "complexity" is viewed here as an intrinsic phenomenon generated by the nonlinearity inherent in the evolution laws. Two of its principal manifestations with which we will be concerned are the bifurcation of multiple solutions and the onset

of chaotic dynamics.

## 1.1 General formulation

It is at the macroscopic level that the most common evidence of irreversibility and complexity is to be found, from the well-known transport and relaxation phenomena to the collective behavior in multi-unit systems giving rise to new, emergent properties absent at the level of the constituting units such as bistability, oscillations, chaos, pattern formation and turbulence.

It is remarkable that in many instances macroscopic-level phenomena are described by a closed system of evolution equations of the form

$$\frac{\partial \mathbf{x}}{\partial t} = \mathbf{F}(\mathbf{x}, \lambda) \quad (1.1)$$

where  $\mathbf{x} = (x_1, \dots, x_n)$  is the state vector of the observables (concentrations, temperature, bulk velocity etc.) and  $\lambda$  a set of control parameters such as the distance from thermodynamic equilibrium, describing the ways the system can be affected by the external world. The evolution operator  $\mathbf{F} = (F_1, \dots, F_n)$  is typically nonlinear, owing to the cooperativity inherent in the interactions. It is also a dissipative operator in the following sense: when embedding the evolution equations (1.1) into the phase space spanned by the full set of the variables one has, on average, a contraction of a volume element each point of which follows the evolution laws. One can show that this very important property is equivalent to [Ni95]

$$\overline{\text{div } \mathbf{F}^t} \equiv \frac{1}{t} \int_0^t d\tau \text{div } \mathbf{F}(\mathbf{x}(\tau), \lambda) < 0, \quad t \geq t_0. \quad (1.2)$$

As a result, time going on, the trajectories eventually wind toward an invariant set - the attractor [Ni95] - whose dimensionality is strictly less than the phase space dimensionality. In other words, in macroscopic-level dynamics irreversibility is incorporated at the outset in the description. Notice that, in the infinite time limit,

$$\overline{\text{div } \mathbf{F}^\infty} = \sum_i \sigma_i \quad (1.3)$$

where  $\sigma_i$  are the Lyapunov exponents.

A fundamental mechanism at the origin of the complexity of a system at a macroscopic level is bifurcation: an initially prevailing regime loses its stability and

is replaced by new, generally multiple stable regimes. Now, it is a fundamental property of nature that experiment - the process by which we communicate with a system - is subject to finite precision. Consider, then, a swarm of macroscopically indiscernible systems below bifurcation, in the sense that they are submitted to the same constraints but differ in their initial conditions by a distance less than or equal to the experimental accuracy. As the "uncertainty ball" containing this swarm is moved across the bifurcation point, it will split into two sub populations each of which will follow entirely different paths. We are, clearly, in the presence of a pronounced sensitivity to both the parameters and the initial conditions entailing the loss of uniqueness and hence of unlimited predictability. Probabilistic description is one natural way to cope with this fundamental limitation.

Bifurcation is far from being a unique event. Typically, one witnesses a whole sequence of transition phenomena often culminating in the regime of deterministic chaos where we are witnessing an even more unexpected form of sensitivity to initial conditions: for given parameter value a typical pair of initially nearby states will diverge, in the mean, exponentially in time. The rate of this divergence is an intrinsic property of the dynamics, referred as the maximum Lyapunov exponent. Once again two macroscopically indiscernible systems submitted to the same constraints will follow entirely different paths, a property that will entail for the observer the loss of predictability beyond a time horizon of the order of the inverse of the Lyapunov exponent. Here also probabilistic description, the only one to account naturally for the delocalization of the system in phase space, becomes an indispensable tool.

At the basis of the probabilistic description is the Liouville equation giving the time evolution of the probability density  $\rho(\mathbf{x}, t)$  (a non-negative normalized function), to which one must resort in order to account for the fact that the system at hand can be projected by its dynamics into widely different parts of phase space. The explicit form of this equation is

$$\frac{\partial \rho}{\partial t} = -\text{div } \mathbf{F} \rho = \mathcal{L} \rho \quad (1.4)$$

where  $\mathcal{L}$  is the Liouville operator.

The Liouville equation can also take an alternative integral form which turns out to be very useful in applications. Indeed, let us write the formal solution of (1.1) as

$$\mathbf{x}_t = \mathbf{f}^t(\mathbf{x}_0, \lambda) \quad (1.5)$$

where  $\mathbf{x}_0$  is the initial condition. One obtains then straightforwardly,

$$\rho(\mathbf{x}, t) = \int d\mathbf{x}_0 \delta(\mathbf{x} - \mathbf{f}^t(\mathbf{x}_0, \lambda)) \rho_0(\mathbf{x}_0) \quad (1.6)$$

or

$$\rho(\mathbf{x}, t) = \rho_0(\mathbf{f}^{-t}(\mathbf{x}, \lambda)) \left| \frac{\partial \mathbf{f}^{-t}(\mathbf{x}, \lambda)}{\partial \mathbf{x}} \right| \quad (1.7)$$

where  $\rho_0$  is the initial probability density and the bars denote the Jacobian determinant. The advantage of eq. (1.6) on eq. (1.4) is to apply to discrete time dynamical systems (mappings), which are widely used in the literature to understand the onset of complex behavior. In particular, for the iterative mapping

$$\mathbf{x}_{n+1} = \mathbf{f}(\mathbf{x}_n, \lambda) \quad (1.8)$$

one has

$$\rho_{n+1}(\mathbf{x}) = \int d\mathbf{x}_0 \delta(\mathbf{x} - \mathbf{f}(\mathbf{x}_0, \lambda)) \rho_n(\mathbf{x}_0) \equiv (\mathcal{P}\rho_n)(\mathbf{x}) \quad (1.9)$$

where  $\mathcal{P}$  is referred to as the Perron-Frobenius operator [LaMa85, Ni95]. The basic difference is that  $\mathbf{f}$  is generally not one-to-one for discrete time. Hence eq. (1.9) becomes

$$\rho_{n+1}(\mathbf{x}) = \sum_{\alpha} \rho_n(\mathbf{f}_{\alpha}^{-1}(\mathbf{x}, \lambda)) \left| \frac{\partial \mathbf{f}_{\alpha}^{-1}(\mathbf{x}, \lambda)}{\partial \mathbf{x}} \right| \chi_{C_{\alpha}(\mathbf{x}, \lambda)}(\mathbf{x}) \quad (1.10)$$

where  $\mathbf{f}_{\alpha}$  denotes the  $\alpha$ -th monotone branch of  $\mathbf{f}$ ,  $C_{\alpha}$  its support and  $\chi_A(x)$  the characteristic function of the set  $A$ .

There is ample awareness that complexity also appears at the microscopic level [Pr80]. In the classical mechanical setting the observables are now the coordinates  $\mathbf{q}_i$  and the momenta  $\mathbf{p}_i$ ,  $i = 1, \dots, N$  of the  $N$  particles constituting the system. Contrary to the macroscopic level description their dynamics, still described formally by evolution equations of the form of (1.1) or (1.4), is both time-reversible and conservative as long as the system is isolated,

$$\text{div } \mathbf{F} = 0. \quad (1.11)$$

It also generates various forms of deterministic chaos which lives now in a phase space of much higher dimensions than the dissipative chaos associated to the evolution of macroscopic observables, of the order of the Avogadro number.

Until recently the use of probabilistic description and Liouville-like equations was limited to the strict realm of statistical mechanics and hence to systems with a

number of degrees of freedom comparable to the Avogadro number. Our discussion shows that probabilistic concepts now pervade the much larger class of dynamical systems showing complex behavior such as bifurcations or chaos, even though these systems may involve a small number of variables. What is more, the relative tractability of these systems allows one to obtain the full solution of problems motivated by statistical mechanics but which could never be tackled for a many-body system. This new field of statistical mechanics of dynamical systems is nowadays a unique laboratory in which ideas, conjectures and methods can be tested.

In addition to its intrinsic interest microscopic-level analysis allows to elucidate the status of the macroscopic description and, whenever necessary, to provide relevant improvements. The advent of super computers has made it possible to execute this program in a novel way, in which the equations of motion of the constituent particles are numerically solved through the microscopic simulation techniques of molecular dynamics and Monte Carlo and macroscopic observables are subsequently constructed by appropriate averaging. This has provided new insight on how macroscopic order can be generated out of microscopic disorder in, among others, hydrodynamic or chemical instabilities leading to macroscopic patterns or to rhythmic phenomena [MaHo92].

Notice that systems in contact with an energy or matter reservoir and maintained in a nonequilibrium steady state have recently been modeled successfully by evolution laws which, in addition to a conservative part, contain a dissipative contribution accounting both for the nonequilibrium constraint and for the "thermostatting" action of the reservoir [EvMo90, PoHo97]. This description is, in certain ways, intermediate between the microscopic and the macroscopic ones. We come back to this interesting point in Section 1.4.

A variety of systems of growing importance (nano-structures, micelles) operate also on an intermediate scale between the macroscopic and the microscopic ones. This happens also to be the scale of many phenomena of fundamental biological relevance. Such mesoscopic systems also exhibit a rich variety of complex behaviors like anomalous kinetics and self-assembly. Mesoscopic level analysis provides a useful, pragmatic alternative to the microscopic description by incorporating the effect of fluctuations in the dynamics of the macroscopic observables. This is achieved by augmenting eqs. (1.1) through the addition of random forces

$$\frac{dx_i}{dt} = F_i(\{x_j\}, \lambda) + R_i(t) . \quad (1.12)$$

In many instances  $R_i(t)$  can be assimilated to a multi-Gaussian white noise,

$$\begin{aligned}\langle R_i(t) \rangle &= 0 \\ \langle R_i(t)R_j(t') \rangle &= Q_{ij}\delta(t-t')\end{aligned}\quad (1.13)$$

where the brackets indicate averaging over the various realizations of  $R_i$  and the covariance matrix  $\{Q_{ij}\}$  is positive definite. When  $R_i$  are taken to emulate the effect of microscopic dynamics  $Q_{ij}$  are linked to the evolution laws  $F_i$  by relationships provided by the fluctuation-dissipation theorem [DeMa62]. Alternatively,  $R_i$  may describe the action of external random disturbances in which case  $Q_{ij}$  are assigned from the outside.

The presence of noise in (1.12) makes the need for a probabilistic description even more obvious than before. Under the conditions of (1.13) this description is afforded by the Fokker-Planck equation descriptive of a Markov process of the diffusion type [Va81]

$$\begin{aligned}\frac{\partial \rho}{\partial t} &= -\text{div } \mathbf{F}\rho + \frac{1}{2} \sum_{ij} Q_{ij} \frac{\partial^2 \rho}{\partial x_i \partial x_j} \\ &= \mathcal{L}\rho + \frac{1}{2} \sum_{ij} Q_{ij} \frac{\partial^2 \rho}{\partial x_i \partial x_j}.\end{aligned}\quad (1.14)$$

We stress that the assimilation of fluctuations to "noise" is nothing but a shortcut to high-dimensional deterministic chaos. In this "thermodynamic" limit new properties are born, which are better accounted for by a low-dimensional Liouville equation augmented by a diffusion term, rather than by a high-dimensional Liouville equation.

An important feature of eqs. (1.4), (1.9) and (1.14), to be contrasted with eq. (1.1), is their linear character. As we see more amply in the following sections, this introduces substantial differences between deterministic and probabilistic descriptions. It also allows us to formulate the problem of the time evolution of the probability density in terms of the spectrum of the Liouville, Perron-Frobenius and Fokker-Planck operators.

## 1.2 Probabilistic aspects of bifurcation

In this section we take a closer look at the statistical properties of deterministic dynamical systems obeying a low-dimensional dissipative dynamics (eq.(1.1)) and giving rise to bifurcation. As pointed out already in Section 1.1, owing to the

contraction of phase space volumes such systems will reach in time a phase-space manifold, the attractor, whose dimensionality  $d$  is strictly less than the phase-space dimensionality  $n$ . As a result the invariant probability density  $\rho_s(\mathbf{x})$  describing the long-time dynamics on the attractor will necessarily be singular in phase space - essentially a delta function having the attractor as its support. Considerable effort has been devoted to the regularization of these singular probabilities. The two dominant approaches consist either in adding a small noise whose strength is eventually made to tend to zero, or in performing coarse-graining. They are discussed in Secs. 1.3 and 1.5.

To simplify the formalism as much as possible let us limit ourselves in the sequel to 0-d, point attractors describing steady-state behavior. In this setting we expect, then, bifurcation to be manifested in probability space by a transition from an invariant probability density  $\rho_s$  in the form of a unique delta peak to one in the form of (typically several) coexisting delta peaks. Our purpose here will be to understand how  $\rho_s$  is approached in the course of time, and what happens in the transition point. In doing so we will be greatly helped by the fundamental result that the dynamics of systems giving rise to a bifurcation at a simple eigenvalue can be cast in a universal normal form displaying a single variable, known as order parameter. This discussion follows [GaNiPrTa95]. In the particular case of supercritical pitchfork bifurcation the normal form equation becomes [Ni95]

$$\frac{dx}{dt} = \mu x - x^3 \quad (1.15)$$

where  $\mu$  denotes the bifurcation parameter. The Liouville operator, eq. (1.4), reduces then to

$$\mathcal{L} = -\frac{\partial}{\partial x}(\mu x - x^3) . \quad (1.16)$$

We want to construct the eigenvalues  $s_n$  as well as the right  $\{\tilde{\phi}_n\}$  eigenfunctions of this non self-adjoint operator. Let us write, formally,

$$\begin{aligned} \mathcal{L}\phi_n(x) &= s_n\phi_n(x) \\ \mathcal{L}^+\tilde{\phi}_n(x) &= s_n^*\tilde{\phi}_n(x) \end{aligned} \quad (1.17)$$

where  $\mathcal{L}^+$  is the adjoint of  $\mathcal{L}$ . Then, under mild conditions

$$\begin{aligned} (\tilde{\phi}_m, \phi_n) &= \delta_{mn} \\ \sum_{n=0}^{\infty} \phi_n(x) \tilde{\phi}_n(y) &= \delta(x - y) \end{aligned} \quad (1.18)$$

and one has, for non-degenerate eigenvalues, the spectral representation

$$\begin{aligned}\rho(x, t) &= \sum_n c_n(t) \phi_n(x) \\ &= \sum_n (\tilde{\phi}_n, \rho_0) e^{s_n t} \phi_n(x)\end{aligned}\quad (1.19)$$

where the parentheses denote scalar product, defined here as the integral of the quantities involved over the whole phase space. If the eigenvalues are degenerate an extension of eq. (1.19) involving Jordan blocks becomes necessary.

An alternative version of the spectral representation, applicable when dealing with the evolution of an observable  $A$  should also be mentioned. Using the definition of the average of  $A$  and of the adjoint of an operator one has

$$\begin{aligned}\langle A \rangle_t &= \int dx A(x) \rho(x, t) = (A, e^{t\mathcal{L}} \rho_0) \\ &= (e^{t\mathcal{L}^+} A, \rho_0) = \sum_n (A, \phi_n) e^{s_n t} (\tilde{\phi}_n, \rho_0).\end{aligned}\quad (1.20)$$

This representation is especially useful whenever  $\phi_n$  or  $\tilde{\phi}_n$  happen to be singular, as is usually the case for dissipative systems. One may then restrict the action of  $\mathcal{L}$  to the space of functions for which  $(A, \phi_n)$  and/or  $(\tilde{\phi}_n, \rho_0)$  are well-defined. The choice of this test function space will have important repercussions on the spectrum of the Liouville operator itself.

With this background in mind we now come to the spectrum of the operator in (1.16). We first observe that eq. (1.15) can be solved explicitly for  $t > 0$  to yield

$$x = f^t(x_0, \mu) = \begin{cases} x_0 \left( \frac{\mu}{x_0^2 + (\mu - x_0^2) e^{-2\mu t}} \right)^{\frac{1}{2}} & \mu \neq 0 \\ \frac{x_0}{\sqrt{1 + 2x_0^2 t}} & \mu = 0. \end{cases}\quad (1.21)$$

Using the first equality (1.20) along with the first part of eq. (1.6) one then has

$$\langle A \rangle_t = \int dx \rho_0(x) A(f^t(x, \mu)).\quad (1.22)$$

Depending on the value of  $\mu$  one can expand  $A$  in a way to exhibit exponentials in time with negative arguments. Upon identifying this expansion with (1.20)

one infers, then, the eigenvalues and the left and right eigenfunctions or, more appropriately, eigendistributions. The results are summarized in the following table [GaNiPrTa95].

	$\phi_n$	$\tilde{\phi}_n$	$s_n$
$\mu < 0$	lin. comb. of $\delta^{(n)}$	$\frac{1}{n!} \left( \frac{x}{\sqrt{x^2 +  \mu }} \right)^n$	$-n \mu $ non-degenerate
$\mu = 0$	lin. comb. of $\delta^{(n)}$	$\text{sgn}(x) \exp\left(\frac{s}{2x^2}\right)$	continuous in negative real axis doubly degenerate
$\mu > 0$	spectral representation involves Jordan blocks		

(1.23)

Two important conclusions emerge. First the spectrum is always in the negative real axis even when  $\mu > 0$ , guaranteeing the stability of the probabilistic description in the sense that as  $t \rightarrow \infty$   $\rho$  will irreversibly attain a unique final form  $\rho_s$ . This is to be contrasted with the instability prevailing at the level of the deterministic description, where for  $\mu > 0$  the solution  $x = 0$  becomes unstable and gives rise to two new stable branches at  $x_{\pm} = \pm \sqrt{\mu}$ . Second, at and beyond bifurcation the spectrum becomes degenerate. This reflects the symmetry-breaking concomitant to the pitchfork bifurcation. These results can be extended to other types of bifurcations, including the birth of periodic solutions by Hopf bifurcation.

### 1.3 Probabilistic aspects of deterministic chaos

There is a wide variety of chaotic behaviors [Ni95, Ma97]. The simplest one is generated by 1-d discrete time dynamical systems (necessarily dissipative) in which the iterative function  $f$ , eq. (1.8), is everywhere expanding in the sense  $|f'(x, \lambda)| > 1$ . The invariant manifold of such systems covers a measurable part of the real line, and the associated invariant probability density  $\rho_s$  is a smooth function. This property extends to certain "non-hyperbolic" 1-d discrete time systems which although not

everywhere expanding still possess nice invariant probabilities with at most integrable singularities. Typical examples of these two classes are, respectively:

- the tent map

$$x_{n+1} = \begin{cases} 2x & 0 \leq x \leq \frac{1}{2} \\ 2(1-x) & \frac{1}{2} \leq x \leq 1 \end{cases} \quad (1.24)$$

for which  $\rho_s = 1$

- the fully chaotic logistic map

$$x_{n+1} = rx_n(1-x_n) \quad 0 \leq x \leq 1 \quad (1.25)$$

for which, at  $r = 4$ ,

$$\rho_s = \frac{1}{\pi \sqrt{x(1-x)}},$$

- the cusp map describing intermittent behavior

$$x_{n+1} = 1 - 2|x_n|^{1/2} \quad -1 \leq x \leq 1 \quad (1.26)$$

for which

$$\rho_s = \frac{1-x}{2}.$$

A very different class of dissipative systems are those possessing strange attractors, that is to say, attractors formed by fractal or more typically multifractal sets. In 1-d discrete time systems this only happens for exceptional values of the control parameter, like e.g.  $r = 3.5699\dots$  in the logistic mapping (Feigenbaum attractor [Fe78, Fe79]), for which the dynamics loses the property of sensitivity to the initial conditions (zero Lyapunov exponent). On the other hand, continuous time dissipative systems typically possess attractors that are both multifractal and display non zero Lyapunov exponents. Their invariant distribution is thus by necessity singular. In the particular case of Axiom-A attractors, characterized by the coexistence of an attracting and an expanding direction in every point in phase space, the invariant distribution is of the Sinai-Bowen-Ruelle type [Ru76, EcRu85]. It is smooth in the expanding directions and singular in the contracting ones.

A particularly thoroughly studied class of conservative chaotic systems are Anosov flows. Here one has, again, the coexistence of an expanding and a contracting direction everywhere in phase space but, contrary to Axiom-A attractors, the invariant

set is now the entire phase space. This entails the existence of smooth (even constant) invariant distributions [ArAv68].

Despite the abundance of powerful qualitative results in this area there are relatively few quantitative and explicit results showing how an initial density is driven by the Liouville or Perron-Frobenius operator toward the invariant density. In the following we outline an approach to this problem based on the concept of coarse-graining [NiNi88].

The idea of coarse-graining stems from the observation made in Section 1.1, that in the presence of complex dynamics the monitoring of a phase space trajectory in a pointwise fashion loses much of its operational interest. We therefore partition the phase space into a finite number of non-overlapping cells  $C_i$ ,  $i = 1, \dots, N$  and monitor the successive cell-to-cell transitions of the phase space trajectory. One may look at the "states"  $C_1 \dots C_N$  as symbols of an  $N$ -letter alphabet. In this view, then, the initial dynamics induces on the partition a symbolic dynamics describing how the letters of the alphabet unfold in time.

We shall impose on the partition the condition that each element is mapped by the dynamics onto a union of cells. Furthermore, we shall restrict ourselves to "coarse-grained" initial probability densities having special properties on the partition such as being piecewise constant, piecewise linear or more generally piecewise analytic.

The chief difficulty in handling this type of systems is that, in the most general case, the action of the Liouville or Perron-Frobenius operators does not preserve coarse-graining. This is reminiscent of the problem of propagation of "molecular chaos" stipulated by Boltzmann in deriving his celebrated equation. An interesting class of systems for which this difficulty can be solved are 1-d dissipative piecewise linear discrete time mappings and 2-d Anosov diffeomorphisms [Ma97]. Introducing the projection operator  $E$  transforming the probability density  $\rho_n$  at time  $n$  to a discrete probability vector  $\mathbf{P}_n = (P_1^{(n)}, \dots, P_N^{(n)})$ ,

$$\mathbf{P}_n = E \rho_n \quad (1.27)$$

and applying  $E$  on both sides of the Perron-Frobenius equation (1.9) one obtains an equation of the form [NiNi88]

$$\mathbf{P}_{n+1} = \mathbf{W} \mathbf{P}_n \quad (1.28)$$

This equation maps the initial continuous dynamics into a discrete state process, in which transitions are mediated by the time-independent stochastic matrix  $\mathbf{W}$ .

Such processes are familiar in probability theory, the best known class being that of Markov chains. Eq. (1.28) is referred to in this context as the Chapman-Kolmogorov or the master equation. This mapping gives a concrete meaning to the statement made often in a rather loose way, that chaos is associated with a "random looking" evolution. There is no contradiction whatsoever between this result and the deterministic origin of chaos: in the probabilistic view afforded by eq. (1.28), we look at our system through a "window" (phase space cell), whereas in the deterministic view it is understood that we are exactly running on a trajectory. This is, clearly, an unrealistic assumption in view of our earlier comments.

As an illustration consider the tent map, eq. (1.24). We choose the 2-cell partition  $C_1 = [0, x_{11}]$ ,  $C_2 = [x_{11}, 1]$ ,  $x_{11} = \frac{2}{3}$  being the non-trivial fixed point of the map. Upon projection on this partition the Perron-Frobenius equation

$$\rho_{n+1}(x) = \frac{1}{2} \left[ \rho_n\left(\frac{x}{2}\right) + \rho_n\left(1 - \frac{x}{2}\right) \right] \quad (1.29)$$

is then mapped into

$$\begin{pmatrix} P_1^{(n+1)} \\ P_2^{(n+1)} \end{pmatrix} = \begin{pmatrix} \frac{1}{2} & 1 \\ \frac{1}{2} & 0 \end{pmatrix} \begin{pmatrix} P_1^{(n)} \\ P_2^{(n)} \end{pmatrix}. \quad (1.30)$$

The eigenvalues of the transition matrix are  $\lambda_1 = 1$ ,  $\lambda_2 = -\frac{1}{2}$ . The first corresponds to the discretized form of the invariant density

$$\rho_s = 1, \mathbf{u}_1 = \text{col} \left( \frac{2}{3}, \frac{1}{3} \right). \quad (1.31)$$

The second one, to which corresponds the eigenvector

$$\mathbf{u}_2 = \text{col} (-1, 1) \quad (1.32)$$

describes the irreversible relaxation toward the invariant state: the instability of the deterministic description is here replaced by a stable, predictable one. This highlights once again the merits of a probabilistic approach to complex systems.

In most real-world systems the exact mapping leading from Perron-Frobenius to eq. (1.28) is no longer applicable. A number of approximation schemes around Markov processes have been developed applicable, for instance, to non-hyperbolic systems of the logistic map family [AlMaGaNi96]. Generally speaking, for a system not belonging to these classes the process of transition between cells will be non-Markovian and would display long-term memory effects. An explicit example is provided by the cusp map, eq. (1.26). Choosing the two-cell partition

$C_1 = [-1, 0]$ ,  $C_2 = [-0, 1]$ , one can derive the explicit form of probability distributions of various types and establish the existence of long tails—a characteristic signature of non-Markovianity. One such distribution is the escape time distribution from cell 1, behaving as [BaNiNi97]

$$F(C_1, 0; C_2, n) \approx n^{-2}. \quad (1.33)$$

## 1.4 Thermodynamic fluctuations and external noise

As stressed in Section 1.1 an important class of systems for which probabilistic approach becomes the natural mode of description are dissipative systems driven by noise, representing the effect of thermodynamic fluctuations or of external random disturbances. In the white noise limit such systems are described by the Fokker-Planck equation (1.14), which differs from the Liouville equation by the addition of a diffusion term. A natural question to be raised is, then, to what extent this extra term modifies substantially the spectrum of the Liouville operator  $\mathcal{L}$  and hence the approach of the probability density to its invariant form  $\rho_s$ .

A full answer to this question can be given for dissipative dynamical systems operating around a pitchfork bifurcation, studied already in the absence of noise in Section 1.2. We briefly summarize the main results [GaNiPrTa95].

- (i) The eigenfunctions of  $\mathcal{L}$ , which are singular as we have seen in Section 1.2, are regularized by the presence of a diffusion term, however small  $Q_{ij}$  might be.
- (ii) The nonzero eigenvalues of  $\mathcal{L}$  are much more robust: they are just perturbed by diffusion, the correction being of  $O(|Q_{ij}|)$ .
- (iii) The zero eigenvalue  $s_0 = 0$  of  $\mathcal{L}$ , which was shown to be doubly degenerate, splits for  $\mu > 0$  under the effect of diffusion into a zero eigenvalue  $s_{00} = 0$  and a nonzero one  $s_{01}$  tending to zero exponentially with

$$|Q_{ij}|, \quad s_{01} \approx \exp\left(-\frac{1}{|Q_{ij}|}\right).$$

This eigenvalue describes the slow passage of probability mass across the "potential barrier" created by the presence of an unstable state.

- (iv) In the critical case  $\mu = 0$  the continuous spectrum of  $\mathcal{L}$  is transformed by the action of diffusion into a discrete one.

A very interesting question pertains to the role of fluctuations in the presence of chaotic dynamics. Since fluctuations continuously perturb the system and chaos amplifies small initial disturbances, one may argue that fluctuations will eventually reach a macroscopic level and become comparable to the averages. This will signal, then, the breakdown of the macroscopic description.

The answer to this apparent paradox is that macroscopic behavior is associated to the most probable rather than the average value. When the dynamics is simple these two coincide, but otherwise they may be quite different. What matters, then, for the validity of the macroscopic description is that the attractor remains robust under the effect of the fluctuations. This has been verified explicitly on a wide variety of systems [GeNi93].

A class of dynamical systems attracting increasing interest are spatially extended systems. Owing to the presence of a large number of interacting modes such systems may generate complexity in space as well as in time in the form of propagating waves, regular patterns and spatio-temporal chaos, an extreme case of which is fully developed turbulence. The very existence of such states requires the maintenance of spatial coherence over a macroscopic scale. Yet one might argue that under the effect of inhomogeneous fluctuations coherence between adjacent spatial regions would be destroyed by destructive interference, thereby precluding the bifurcation to a regime encompassing the system as a whole.

As it turns out, the validity of this conjecture depends on both the type of bifurcation considered and the spatial dimensionality of the system. An interesting case study is provided by the onset of Hopf bifurcation in a 1-d spatially extended system. Specifically, beyond a critical size fluctuations destroy the coherent deterministic pattern by introducing space-time defects [Ba96]. Remarkably, this latter pattern looks very much like the spatio-temporal chaotic pattern arising when the periodic solution of the deterministic system loses its stability at a different parameter value (Benjamin-Feir instability).

## 1.5 Thermodynamic characterization of nonequilibrium states

In this section we explore further the connection between the deterministic and probabilistic aspects of dynamical systems. Our more specific objective is to identify quantities, to which we shall refer as state functionals, providing a concise charac-

terization of the principal properties of the system at hand, largely independent of the details of the ongoing processes.

It is well-known that in the state of thermodynamic equilibrium entropy (for isolated systems) and Helmholtz or Gibbs free energies (for systems at constant temperature) provide a universal description of exactly this sort. Away from equilibrium this universality is, in principle, lost and one must resort to descriptions taking dynamical effects into consideration. However, in the range of irreversible phenomena in which a local formulation of the evolution laws of macroscopic observables is still possible entropy production provides a partial substitute to thermodynamic state functionals since it reflects the way dissipation - a ubiquitous attribute of nonequilibrium states - is released within the system [Pr61].

The starting point of irreversible thermodynamics is the local equilibrium hypothesis: in a system subjected to constraints varying slowly in space and time the traditional equilibrium thermodynamic state functions can still be defined by the same relationships as in equilibrium, provided these relationships are applied locally. For instance, writing the total entropy as

$$S = \int d\mathbf{r} \rho s(\mathbf{r}, t) \quad (1.34)$$

where  $\rho$  is the mass density and  $s$  the specific entropy, one has

$$s(\mathbf{r}, t) = s(e(\mathbf{r}, t), v(\mathbf{r}, t), c_i(\mathbf{r}, t)) \quad (1.35)$$

$e$  being the specific internal energy,  $v$  the specific volume and  $c_i$  the concentrations of the constituents present. Since  $e$ ,  $v$  and  $c_i$  satisfy balance equations directly related to the fundamental conservation laws of mass, momentum and energy eq. (1.35), known as Gibbs' entropy postulate, can be used to obtain a balance equation for the specific entropy and hence, through (1.34), for the total entropy itself. The principal outcome of this analysis is as follows:

- (i)  $S$  satisfies the balance equation

$$\frac{dS}{dt} = \frac{d_e S}{dt} + P. \quad (1.36)$$

The first term in this relation is the entropy flux, reflecting the exchanges of energy, momentum and matter with the surroundings, whereas the second one is the entropy production, associated to the irreversible processes going on spontaneously within the system.

- (ii) While the entropy flux has no definite sign,  $P$  is a non-negative quantity vanishing in the state of equilibrium (second law of thermodynamics)

$$P \geq 0, \quad P_{eq} = 0. \quad (1.37)$$

Furthermore, it can be expressed as a bilinear form [Pr61, DeMa62]

$$P = \int d\mathbf{r} \sum_k J_k X_k \quad (1.38)$$

where  $J_k$  are the fluxes of the irreversible processes present and  $X_k$  the associated generalized forces.

Inequality (1.37) can be regarded as the very expression of irreversibility at the macroscopic level. Ever since the time of Boltzmann and Gibbs a major challenge in statistical mechanics has been to derive it, as well as eq. (1.38), from the time-reversible laws of microscopic physics. This requires, in turn, a definition of entropy in terms of microscopic quantities which in Gibbs' view is achieved by assuming that  $S$  becomes a functional of the phase space probability density  $\rho(\{\mathbf{q}_i\}, \{\mathbf{p}_i\}, t)$ ,  $\{\mathbf{q}_i\}$  and  $\{\mathbf{p}_i\}$  being the coordinates and momenta of the particles. Under the additional requirement that  $S$  must be extensive one then arrives at the Gibbs definition of entropy

$$S_G = -k_B \int \{d\mathbf{q}_i\} \{d\mathbf{p}_i\} \rho(\{\mathbf{q}_i\}, \{\mathbf{p}_i\}, t) \ln \rho(\{\mathbf{q}_i\}, \{\mathbf{p}_i\}, t) \quad (1.39)$$

$k_B$  being the Boltzmann constant. This definition reproduces the correct equilibrium properties of entropy but is unfortunately unable to provide information on irreversibility, since one can show trivially using the Liouville equation (eq. (1.4)) that in a conservative system ( $\text{div}\mathbf{F} = 0$ , see eq. (1.11))

$$\frac{dS_G}{dt} = 0. \quad (1.40)$$

This is contrary to common experience showing that if an isolated system not in equilibrium is left to itself it will evolve irreversibly toward equilibrium and in the course of this evolution energy will be dissipated.

Boltzmann proposed an alternative view based on the use of reduced probability densities, describing what is going on in the vicinity of a representative particle within the system. In particular, denoting the one-particle position-velocity probability density by  $f(\mathbf{r}, \mathbf{v}, t)$  he proposes to define entropy density by

$$\rho s(\mathbf{r}, t) = -k_B \int d\mathbf{v} f \ln f. \quad (1.41)$$

A balance equation for  $s$  can then be obtained by using the evolution equation for  $f$ . In a dilute gas  $f$  obeys to the celebrated Boltzmann equation. In the range of phenomena close to local equilibrium this leads, then, exactly to eqs. (1.35)-(1.38) thereby establishing a highly interesting link between microscopic and macroscopic levels [Pr49]. Unfortunately, notwithstanding the fact that the Boltzmann equation itself contains some heuristic assumptions there is so far no extension of this result to general, dense or strongly coupled systems. Furthermore, whereas microscopic dynamics is implicitly present through the equation for  $f$ , the explicit link between entropy production and the quantifiers of the dynamical complexity of phase space trajectory (Lyapunov exponents etc) has been lost.

In Chap. 5 we shall attempt to bridge, at least partially, this gap. The starting point is the probabilistic description and the coarse-graining procedure introduced in Secs. 1.1 and 1.3 whose interest is to involve directly the observables at the level of which irreversibility is the most apparent. Let  $P_i$  be the probability to be in cell  $i$  of the partition, which actually means that the phase space variables will then lie within certain limits (we stress that  $x$  may represent coordinates and momenta or macroscopic variables like temperature or concentration). We ask the following question: what is the information  $S_I$ , that is to say, the amount of data (normalized by some reference value) necessary to localize this state in phase space? The answer to this question turns out to be unique if one accepts a set of axioms to which we shall refer as the Shannon-Khinchin axioms [BeSc93]:

- (i)  $S_I$  depends entirely of  $P_i$
- (ii)  $S_I$  takes its maximum value for the uniform distribution  $P_i = \frac{1}{N}$
- (iii)  $S_I$  remains unchanged if the state space is enlarged by an event of zero probability
- (iv) The information on a composite system  $A + B$  equals the information on  $A$  plus the conditional information on  $B$  given the state of  $A$ .

Under these conditions one has the celebrated formula for the Shannon entropy

$$S_i = - \sum_i P_i \ln P_i \quad (1.42)$$

At this point it seems tempting to take the limit of infinite resolution and express  $S_I$  in terms of probability densities  $\rho$  as in eq. (1.39). There is, however, a subtlety

related to the fact that in this limit

$$P_i \approx \rho |\Delta\Gamma_i| , \quad (1.43)$$

$\Delta\Gamma_i$  being the phase space cell corresponding to state  $i$ . As  $|\Delta\Gamma_i| \rightarrow 0$  eq. (1.42) develops, then, a logarithmic singularity. Since however the corresponding term is constant (state-independent) we shall in the sequel adopt it as a reference value and use the continuous version of eq. (1.42)

$$S_I(t) = - \int dx \rho(x, t) \ln \rho(x, t) . \quad (1.44)$$

This expression looks very much like the Gibbs definition, eq. (1.39), which actually can also be reformulated in information theoretic terms. There are, however, two important differences. First, it applies most naturally to the mesoscopic level of description introduced in Sec. 1.1, where the state variables  $x$  are the macroscopic observables driven by the deterministic evolution laws augmented by random forces (eqs. (1.12) - (1.14)). Second, at the microscopic level, as stressed recently by several authors [HoHoPo87, EvMo90, PoHo97], systems maintained in nonequilibrium steady states by external constraints may be modeled as dissipative dynamical systems, where the dissipation accounts for the action of the constraint and for the thermostating ensured by the reservoirs. As such dissipative interactions inevitably involve a reduced description of the reservoir, they need to be complemented by explicit consideration of the fluctuations. Under these conditions  $S_I$  is not a constant of motion. The limitations pointed out in connection with Gibbs' definition of entropy, eq. (1.39), are no longer applicable and  $S_I$  can be used as a valid alternative. In this respect another alternative is proposed in [Ga97a, Ga97b].

Be it as it may, the point is that  $S_I$  evolves in time through  $\rho(x, t)$ . One is therefore tempted to derive, in the spirit of irreversible thermodynamics, a balance equation for  $S_I$  [NiDa96, VoTeBr97a], explore the possibility to identify entropy production-like terms bearing in one way or the other some relationship with the quantifiers of the dynamics in phase space, and finally compare them with the entropy production or irreversible thermodynamics.

The thesis is organized as follows. In Chapter 2 we outline the generalized coarse-graining procedure which allows to solve the Perron-Frobenius equation for a large class of one-dimensional dynamical systems. A generalized spectral decomposition

of the Perron-Frobenius operator involving Jordan blocks is derived. We establish a correspondence between the non-diagonalizability of the Perron-Frobenius operator and transitions between decay modes of the time autocorrelation functions. The formalism of the generalized master equation is then used to investigate the statistical properties of an important class of dynamical systems giving rise to homoclinic chaos. We show that the time autocorrelation functions provide a useful characterization of the different types of homoclinic chaotic attractors. In Chapter 3 we address the inverse problem of designing dynamical systems with required statistical properties. We are able to construct one-dimensional chaotic maps with prescribed invariant probability density and correlation function. We turn to higher dimensional systems in Chapter 4 where a simplified model of spatially extended systems known as coupled map lattice and giving rise to spatio-temporal chaos is studied. The case of two diffusively coupled piecewise linear maps is solved exactly for finite values of the coupling constant. We then propose a coupled map lattice with constant nearest-neighbour coupling and compute the invariant one-dimensional projection of the full probability density for a large class of maps. In Chapter 5 we develop a nonequilibrium thermodynamics for the class of dynamical systems amenable to a Fokker-Planck type of description. In particular we relate entropy production and phase space volume contraction. The main conclusions and perspectives are given in Chapter 6.



## Chapter 2

# Probabilistic description of one-dimensional chaotic maps: Jordan blocks - homoclinic chaos.

### 2.1 Introduction

As we stressed in Sec. 1.1 the starting point of the probabilistic description is a Liouville-like equation describing the evolution of the probability density, which for discrete time is known as the Perron-Frobenius equation and takes the form

$$\rho_{n+1}(x) \equiv \mathcal{P}\rho_n(x) = \int_I dy \delta(x - f(y, \mu)) \rho_n(y) . \quad (2.1)$$

Here  $\rho_n(x)$  is the probability density for the system to be in  $x$  at time  $n$ ,  $I$  the 1-d phase space region available to the system and  $f(x, \mu)$  the deterministic evolution law

$$x_{n+1} = f(x_n, \mu) , \quad (2.2)$$

$\mu$  being the control parameter.

Traditionally, the statistical description of dynamical systems is limited to their ergodic properties. In recent years progress has been achieved in extending these studies to the time-dependent properties [GrTh77, MoSoOs81, NiNi88, ArAuCv90, BaKe90, Ma91, KeNo92, Ga92, HaSa92, TaAn94, MaNi94, AlMaGaNi96, Ma97]. Still, the knowledge remains fragmentary and, although one is able to obtain some formal results on more general systems for systems as simple as piecewise linear maps many features still remain poorly understood.

Of particular interest is the time autocorrelation function

$$C(n) = \frac{1}{\sigma^2} \lim_{N \rightarrow \infty} \frac{1}{N} \sum_{m=0}^{N-1} (x_m - \bar{x})(x_{m+n} - \bar{x}) \quad (2.3)$$

where  $\bar{x}$  and  $\sigma^2$  are the mean value and the variance of  $x$  respectively. This object which is accessible experimentally gives qualitative as well as quantitative informations on the dynamics of the system. By Birkhoff's theorem [LaMa85] eq. (2.3) can be given an alternative form for ergodic transformations. Roughly speaking a transformation  $f$  of  $I$  to itself is ergodic if all invariant sets under  $f$ , i.e. all sets  $A$  such that

$$f^{-1}(A) = A \quad (2.4)$$

are trivial subsets of  $I$ , in other words pointlike or  $I$  itself. Birkhoff's theorem then states the equality of time and ensemble averages (for almost all initial conditions). Hence for an ergodic map the time autocorrelation function can be written as

$$C(n) = \frac{1}{\sigma^2} \int dx \rho(x) (x - \bar{x})(f^n(x) - \bar{x}) \quad (2.5)$$

where  $\rho(x)$  is the invariant density.

In this chapter we derive for piecewise linear Markov maps an explicit expression for time autocorrelation functions of various observables on the basis of the so-called generalized master equation [MaNi94]. This equation to which the Perron-Frobenius equation can be mapped reduces the statistical description to a problem of linear algebra. In particular, the eigenvalues of the corresponding transition probability matrix are decay rates of the system.

We shall then be interested in i) showing the existence of Jordan blocks in 1-d maps, ii) computing the time autocorrelation function in that case and iii) understanding the particular feature leading to Jordan blocks. The two first points are also addressed by Driebe in [Dr97, Dr98] where a 1-d map which admits Jordan blocks is identified and the correlation function of quadratic observables is shown to be not purely exponential.

On the other hand, we will consider an important class of dynamical systems giving rise to deterministic chaos: homoclinic systems [Ga82, Ga87, Ni95], which possess for a particular combination of parameter values a structurally unstable trajectory biasymptotic to a fixed point. If the latter is of the saddle-focus type and the eigenvalues of the linearized equations around it satisfy a certain inequality known as

the Shil'nikov condition, then it can be established [Sh65, Sh70] that near homoclinicity the system possesses trajectories which are in one-to-one correspondence with a shift automorphism with an infinite number of symbols. For 3-variable systems the existence of a homoclinic orbit allows one to construct a 2-d map which captures all these properties. More significantly for the purposes of this investigation, in many instances, this map can be further reduced to a 1-d map [GaKaNi84, ArArRi90] in the form of distinct branches whose number tends to infinity as the distance to homoclinicity goes to zero. Near homoclinicity these branches can be assimilated to straight line segments, an idealization that seems in particular to fit reasonably well experimental data and model studies of the Belousov-Zhabotinski reaction [Ri87, ArArRi90]. One therefore disposes, in this sense, of examples of realistic continuous time dynamical systems that underly the particular class of the above described 1-d piecewise linear mappings.

The formalism of the generalized master equation is outlined in Sec. 2.2. It is then used in Sec. 2.3 to compute the time autocorrelation function of general observables. The case of Jordan blocks is considered in Sec. 2.4. Sec. 2.5 is devoted to the probabilistic description of homoclinic systems. Conclusions are drawn at the end of Secs. 2.4 and 2.5.

## 2.2 Generalized master equation

Consider a 1-d map  $f$  of the interval  $I$  to itself,

$$f: I \rightarrow I. \quad (2.6)$$

We shall be interested in maps  $f$  which are piecewise linear,

$$f|_{C_i} \equiv f_i: x \mapsto \Lambda_i x + \Delta_i \quad i = 1, \dots, M \quad (2.7)$$

where  $\Lambda_i, \Delta_i$  are constants and  $\{C_i\}_{i=1}^M$  is a partition of  $I$  into  $M$  non-overlapping cells,

$$\cup_{i=1}^M C_i = I \quad (2.8)$$

$$C_i \cap C_j = \emptyset \quad i \neq j.$$

Requiring the map to be everywhere expanding,  $|f'(x)| > 1 \quad \forall x \in I$ , it is chaotic in the sense that it displays a positive lyapunov exponent

$$\lambda \equiv \lim_{N \rightarrow \infty} \frac{1}{N} \sum_{m=0}^{N-1} \ln |f'(x_m)| > 0. \quad (2.9)$$

In addition, we assume the map  $f$  to be Markov, i.e. such that there exists a partition  $\{C_i\}_{i=1}^M$  of  $I$  into  $M$  non-overlapping cells which has the property that each of its elements is mapped by the transformation  $f$  onto a union of its elements. This property is expressed as

$$\chi_{f(C_j)} = \sum_{i=1}^M a_{ji} \chi_{C_i} \quad j = 1, \dots, M \quad (2.10)$$

where  $\chi_{C_i}(x)$  is the characteristic function of the cell  $C_i$ , and the elements  $a_{ji}$  of the topological transition matrix are 1 or 0 depending on whether  $C_i$  belongs or not to  $f(C_j)$ . Notice that the partitions  $\{C_i\}_{i=1}^M$  and  $\{C_i\}_{i=1}^M$  need not be identical. Hence there can be several branches of  $f$  on a given  $C_j$ . Let us define the set  $\alpha(j)$  as

$$\alpha(j) = \{\alpha : C_\alpha \cap C_j \neq \emptyset\}. \quad (2.11)$$

We then require each of the branches  $f_\alpha$ ,  $\alpha \in \alpha(j)$ , to map the intersection of its support with  $C_j$  onto the same union of intervals,

$$\chi_{f_\alpha(C_\alpha \cap C_j)} = \chi_{f(C_j)} \quad \forall \alpha \in \alpha(j), \quad j = 1, \dots, M. \quad (2.12)$$

MacKernan and Nicolis [MaNi94] have shown that for expanding piecewise linear Markov maps a piecewise polynomial density of order  $N$  remains under the Perron-Frobenius operator piecewise on the same partition and polynomial of the same or lower order. The action of the Perron-Frobenius operator on such functions is thus equivalent to that of a finite dimensional matrix on the vector of coefficients of the different monomials. More explicitly, let us consider a piecewise polynomial initial probability density

$$\rho_0(x) = \sum_{j=1}^M \sum_{l=0}^N c_{j+lM}^{(0)} x^l \chi_{C_j}(x). \quad (2.13)$$

The probability  $P_j^{(0)}$  to find the system in cell  $C_j$  at time 0 is thus

$$P_j^{(0)} \equiv \int_{C_j} dx \rho_0(x) = \sum_{l=0}^N c_{j+lM}^{(0)} \mu_{j+lM} \quad (2.14)$$

where

$$\mu_{j+lM} \equiv \int_{C_j} dx x^l. \quad (2.15)$$

One has the normalization condition

$$\sum_{j=1}^M P_j^{(0)} = \sum_{j=1}^M \sum_{l=0}^N c_{j+lM}^{(0)} \mu_{j+lM} = 1. \quad (2.16)$$

The Perron-Frobenius operator  $\mathcal{P}$  writes (cf eq. (1.10))

$$\mathcal{P}\rho_n(x) = \sum_{\alpha=1}^M \frac{1}{|f'(f_\alpha^{-1}(x))|} \rho_n(f_\alpha^{-1}(x)) \chi_{f(C_\alpha)}(x). \quad (2.17)$$

The action of  $\mathcal{P}$  on a coarse-grained  $\rho_0(x)$  in the sense of eq. (2.13) yields

$$\rho_1(x) = \sum_{\alpha=1}^M \sum_{j=1}^M \sum_{l=0}^N \frac{1}{|f'(f_\alpha^{-1}(x))|} c_{j+lM}^{(0)} [f_\alpha^{-1}(x)]^l \chi_{C_j}(f_\alpha^{-1}(x)) \chi_{f(C_\alpha)}(x). \quad (2.18)$$

Note that a point  $x$  has a preimage by the branch  $\alpha$ , i.e.  $f_\alpha^{-1}(x)$  exists, iff  $x \in f(C_\alpha)$ . The characteristic function  $\chi_{f(C_\alpha)}(x)$  in eq. (2.18) thus ensures that the contribution to  $\rho_1(x)$  is non-zero only when  $f_\alpha^{-1}(x)$  exists. Consider now the other characteristic function  $\chi_{C_j}(f_\alpha^{-1}(x))$ . Obviously  $f_\alpha^{-1}(x) \in C_\alpha$  so that  $f_\alpha^{-1}(x) \in C_j$  iff  $C_\alpha \cap C_j \neq \emptyset$ , i.e. iff  $\alpha \in \alpha(j)$ . The  $\alpha$ 's  $\in \alpha(j)$  are thus the only ones to contribute to the sum over  $\alpha$  in eq. (2.18) so that this latter rewrites

$$\rho_1(x) = \sum_{j=1}^M \sum_{\alpha \in \alpha(j)} \sum_{l=0}^N \frac{1}{|f'(f_\alpha^{-1}(x))|} c_{j+lM}^{(0)} [f_\alpha^{-1}(x)]^l \chi_{C_j}(f_\alpha^{-1}(x)) \chi_{f(C_\alpha)}(x). \quad (2.19)$$

Recalling eq. (2.12) we remark that the set of all the points  $x$  whose (existing) preimage by the branch  $\alpha \in \alpha(j)$  is contained in  $C_j$  is precisely  $f(C_j)$ ,

$$\chi_{C_j}(f_\alpha^{-1}(x)) \chi_{f(C_\alpha)}(x) = \chi_{f(C_j)}(x) \quad \forall \alpha \in \alpha(j). \quad (2.20)$$

Hence eq. (2.19) becomes

$$\rho_1(x) = \sum_{j=1}^M \sum_{\alpha \in \alpha(j)} \sum_{l=0}^N \frac{1}{|f'(f_\alpha^{-1}(x))|} c_{j+lM}^{(0)} [f_\alpha^{-1}(x)]^l \chi_{f(C_j)}(x). \quad (2.21)$$

Now eq. (2.7) yields

$$f_\alpha^{-1}(x) = \frac{x - \Delta_\alpha}{\Lambda_\alpha} \\ \frac{1}{|f'(f_\alpha^{-1}(x))|} = \frac{1}{|\Lambda_\alpha|}. \quad (2.22)$$

Using also the Markov property (2.10) gives

$$\rho_1(x) = \sum_{i=1}^M \sum_{l=0}^N \sum_{j=1}^M \sum_{\alpha \in \alpha(j)} \frac{a_{ji}}{|\Lambda_\alpha| |\Lambda_\alpha|^l} c_{j+lM}^{(0)} [x - \Delta_\alpha]^l \chi_{C_i}(x). \quad (2.23)$$

It follows that  $\rho_1(x)$  is again piecewise polynomial,

$$\rho_1(x) = \sum_{i=1}^{\mathcal{M}} \sum_{k=0}^N c_{i+k\mathcal{M}}^{(1)} x^k \chi_{c_i}(x). \quad (2.24)$$

One has

$$c_{i+k\mathcal{M}}^{(1)} = \sum_{j=1}^{\mathcal{M}} \sum_{l=k}^N w_{ij}^{(k,l)} c_{j+l\mathcal{M}}^{(0)} \quad i = 1, \dots, \mathcal{M}, \quad k = 0, \dots, N \quad (2.25)$$

where

$$w_{ij}^{(k,l)} = a_{ji} \sum_{\alpha \in \alpha(j)} \binom{l-k}{l} \frac{(-\Delta_\alpha)^{l-k}}{|\Lambda_\alpha| \Lambda_\alpha^l}. \quad (2.26)$$

It is convenient to define column vectors  $\mathbf{c}_n$ ,  $n = 0, 1, \dots$ , with components  $c_{i+k\mathcal{M}}^{(n)}$ ,  $i = 1, \dots, \mathcal{M}$ ,  $k = 0, \dots, N$  and a block upper triangular time-independent transition matrix  $\mathbf{W}$ ,

$$\mathbf{W} = \begin{pmatrix} \mathbf{W}^{(0,0)} & \dots & \mathbf{W}^{(0,N)} \\ \vdots & \ddots & \vdots \\ 0 & \dots & \mathbf{W}^{(N,N)} \end{pmatrix}, \quad (2.27)$$

the components of each block  $\mathbf{W}^{(k,l)}$  being given by eq. (2.26). Eq. (2.25) can then be rewritten as

$$\mathbf{c}_1 = \mathbf{W} \mathbf{c}_0. \quad (2.28)$$

Having in mind that the components of  $\mathbf{c}_n$  are the coefficients  $c_{i+k\mathcal{M}}^{(n)}$  of the piecewise monomials  $x^k \chi_{c_i}(x)$  at time  $n$  (cf eq. (2.13)), we define a row vector  $\mathbf{m}$  whose components are precisely these piecewise monomials,

$$m_{i+k\mathcal{M}} = x^k \chi_{c_i}(x) \quad i = 1, \dots, \mathcal{M}, \quad k = 0, \dots, N. \quad (2.29)$$

Hence

$$\rho_0(x) = \mathbf{c}_0 \cdot \mathbf{m} \quad (2.30)$$

where the dot denotes the scalar product, and

$$\rho_1(x) = \mathbf{c}_1 \cdot \mathbf{m}. \quad (2.31)$$

After  $n$  iterations, the density  $\rho_n(x) = \mathcal{P}^n \rho_0(x)$  is thus of the form

$$\rho_n(x) = \mathbf{c}_n \cdot \mathbf{m} \quad (2.32)$$

with

$$\mathbf{c}_n = \mathbf{W}^n \mathbf{c}_0 . \quad (2.33)$$

We refer to this equation as the generalized master equation [MaNi94]. In the case where piecewise constant densities are considered it reduces using eq. (2.14) to the master equation (1.28) discussed in Sec. 1.3. Let us point out two particular cases.

i) If the two partitions considered above (cf eqs. (2.7) and (2.10)) are identical

$$\{C_i\}_{i=1}^{\mathcal{M}} = \{C_i\}_{i=1}^M , \quad \mathcal{M} = M \quad (2.34)$$

then eq. (2.11) gives

$$\alpha(j) = \{j\} . \quad (2.35)$$

Hence eq. (2.26) becomes

$$w_{ij}^{(k,l)} = \binom{l-k}{l} \frac{a_{ji} (-\Delta_j)^{l-k}}{|\Lambda_j| \Lambda_j^l} . \quad (2.36)$$

ii) Suppose that each branch of  $f$  maps its support on the whole interval  $I$ ,

$$a_{ij} = 1 \quad i, j = 1, \dots, \mathcal{M} . \quad (2.37)$$

One can then choose the Markov partition as in i). Alternatively we may take the interval  $I$  itself as a Markov partition,

$$\{C_i\}_{i=1}^{\mathcal{M}} = \{I\} , \quad \mathcal{M} = 1 . \quad (2.38)$$

In the case of eq. (2.37), this latter choice constitutes the minimal Markov partition, i.e. the Markov partition with the smallest number of elements. Eq. (2.11) now gives

$$\alpha(j) = \alpha(1) = \{1, \dots, M\} , \quad (2.39)$$

and eq. (2.26)

$$w_{ij}^{(k,l)} = w_{11}^{(k,l)} = \sum_{\alpha=1}^M \binom{l-k}{l} \frac{(-\Delta_\alpha)^{l-k}}{|\Lambda_\alpha| \Lambda_\alpha^l} . \quad (2.40)$$

Each block  $\mathbf{W}^{(k,l)}$  appearing in eq. (2.27) contains thus only one element,  $w_{11}^{(k,l)}$ . Hence the matrix  $\mathbf{W}$  is upper triangular and the elements on the diagonal,

$$w_{11}^{(k,k)} = \sum_{\alpha=1}^M \frac{1}{|\Lambda_{\alpha}| \Lambda_{\alpha}^k}, \quad (2.41)$$

are its eigenvalues.

We are now in the position to obtain a generalized spectral decomposition for the Perron-Frobenius operator acting on piecewise polynomial functions. The eigenvalues of  $\mathbf{W}$  determine the decay rates of the system. To make them appear explicitly in the generalized master equation (2.28) one needs to decompose  $\mathbf{c}_0$  in the basis of the eigenvectors of  $\mathbf{W}$ , or, in the case where the set of all the eigenvectors is not sufficient to span the whole functional space of interest, in the basis formed by the generalized eigenvectors. These are also referred to as root vectors of rank  $k$  associated with the eigenvalue  $\lambda_s$  and can be obtained as [GoKr69]

$$\mathbf{W} \phi_{s,k} = \lambda_s \phi_{s,k} + \phi_{s,k-1} \quad k = 1, \dots, d_s \quad (2.42)$$

where  $d_s$  is the dimension of the root space of  $\lambda_s$  and  $\phi_{s,0} = 0$ . Note that the usual eigenvectors are root vectors of rank one. By successive iterations of  $\mathbf{W}$  on  $\phi_{s,k}$ , the root vectors of rank less than  $k$  appear, modulated by a polynomial in time,

$$\mathbf{W}^n \phi_{s,k} = \sum_{i=0}^n p_i(n) \lambda_s^{n-i} \phi_{s,k-i} \quad k = 1, \dots, d_s. \quad (2.43)$$

In this expression,  $p_i(n)$  is a polynomial of order  $i$  in  $n$  which turns out to be equal to the combinatorial factor  $\binom{n}{i}$ . It is understood that  $\phi_{s,l} = 0$  for  $l \leq 0$ .

Let  $g$  be the number of linearly independent eigenvectors of  $\mathbf{W}$ . We may write  $\mathbf{c}_0$  as

$$\mathbf{c}_0 = \sum_{s=1}^g \sum_{j=1}^{d_s} w_{s,j} \phi_{s,j} = \mathbf{B} \mathbf{w}. \quad (2.44)$$

Here  $\mathbf{B}$  is the matrix of column root vectors and  $\mathbf{w}$  is a column vector whose components are the weights  $w_{s,j}$

$$\mathbf{w} = \text{col} (w_{1,1}, \dots, w_{1,d_1}, w_{2,1}, \dots, w_{1,d_2}, \dots, w_{g,d_g}). \quad (2.45)$$

By the generalized master equation (2.33) and eq. (2.43), we then get for the class of expanding piecewise linear Markov maps the generalized spectral decomposition of the Perron-Frobenius operator acting on piecewise polynomial densities as [Da96]

$$\mathbf{c}_n = \sum_{s=1}^g \sum_{j=1}^{d_s} w_{s,j} \sum_{i=0}^n \binom{n}{i} \lambda_s^{n-i} \phi_{s,j-i}. \quad (2.46)$$

The weights  $w_{s,j}$  are determined by inversion of eq. (2.44), namely

$$\mathbf{w} = \mathbf{B}^{-1} \mathbf{c}_0. \quad (2.47)$$

### 2.3 Time autocorrelation function.

The generalized spectral decomposition (2.46) derived in the previous section enables one to compute the statistical properties of the above defined dynamical systems. Of particular interest is the time autocorrelation function of a general observable  $\theta(x)$  of the form

$$\theta(x) = \sum_{i=1}^{\mathcal{M}} \sum_{k=0}^N a_i^{(k)} x^k \chi_{c_i}(x). \quad (2.48)$$

This includes as a particular case the state variable  $x$  itself and piecewise constant observables  $\theta(x) = \sum_{j=1}^{\mathcal{M}} s_j \chi_{c_j}(x)$ , which are relevant in the case of homoclinic chaos for instance as we shall see later. The time autocorrelation function is defined as

$$C_\theta(n) = \frac{1}{\sigma_\theta^2} \lim_{N \rightarrow \infty} \frac{1}{N} \sum_{m=0}^{N-1} (\theta(x_m) - \bar{\theta})(\theta(x_{m+n}) - \bar{\theta}) \quad (2.49)$$

where  $\bar{\theta}$  and  $\sigma_\theta^2$  are respectively the mean value and the variance of  $\theta(x)$ . For ergodic transformations this expression can also be written as

$$C_\theta(n) = \frac{1}{\sigma_\theta^2} \int_I dx (\theta(x) - \bar{\theta}) \mathcal{P}^n(\theta(x) - \bar{\theta}) \rho(x) \quad (2.50)$$

where  $\rho(x)$  is the invariant density. Proceeding as in the previous section we therefore write the function  $(\theta(x) - \bar{\theta})\rho(x)$ , which we regard as an initial nonequilibrium density, as

$$(\theta(x) - \bar{\theta}) \rho(x) = \mathbf{c}_0 \cdot \mathbf{m}. \quad (2.51)$$

For expanding piecewise linear Markov maps the invariant density is piecewise constant,

$$\rho(x) = \sum_{i=1}^{\mathcal{M}} \phi_{1,1}(i) \chi_{c_i}(x) \quad (2.52)$$

where  $\phi_{1,1}$  is the eigenvector corresponding to the eigenvalue  $\lambda_1 = 1$ . Hence the function on the left handside of eq. (2.51) is piecewise polynomial of the same order  $N$  as the observable  $\theta(x)$ . Accordingly we may restrict the space on which the Perron-Frobenius operator acts to piecewise polynomial functions of order  $N$ . From eqs. (2.48),(2.51),(2.52) we deduce that

$$\begin{cases} c_i^{(0)} = (a_i^{(0)} - \bar{\theta}) \phi_{1,1}(i) & i = 1, \dots, \mathcal{M} \\ c_{i+k\mathcal{M}}^{(0)} = a_i^{(k)} \phi_{1,1}(i) & k = 1, \dots, N. \end{cases} \quad (2.53)$$

It follows that

$$\mathcal{P}^n[(\theta(x) - \bar{\theta}) \rho(x)] = \mathbf{c}_n \cdot \mathbf{m}. \quad (2.54)$$

Substituting eq. (2.54) into eq. (2.50) and performing the integration over  $x$  one gets

$$C_\theta(n) = \frac{1}{\sigma_\theta^2} \mathbf{c}_n \cdot \boldsymbol{\mu} \quad (2.55)$$

where the vector  $\boldsymbol{\mu}$  is related to the vector of monomials  $\mathbf{m}$  through

$$\mu_q = \int_I dx \theta(x) m_q \quad q = 1, \dots, (N+1)\mathcal{M}. \quad (2.56)$$

Using eq. (2.46) for  $\mathbf{c}_n$ ,  $C_\theta(n)$  becomes

$$C_\theta(n) = \frac{1}{\sigma_\theta^2} \sum_{s=1}^g \sum_{j=1}^{d_s} w_{s,j} \sum_{i=0}^n \binom{n}{i} \lambda_s^{n-i} \phi_{s,j-i} \cdot \boldsymbol{\mu} \quad (2.57)$$

where  $w_{s,j}$  and  $\boldsymbol{\mu}$  depend on  $\theta$ , which provides for any expanding piecewise linear Markov map an explicit expression for the time autocorrelation function of the observable  $\theta$ .

## 2.4 Jordan blocks and transitions between decay modes

In this section we are interested in i) showing the existence of Jordan blocks in 1-d maps, ii) computing the time autocorrelation function in that case and iii)

understanding the particular feature leading to Jordan blocks. We mainly focus on the time autocorrelation function of the observable  $x$ , so that as discussed in the previous section, we can restrict the Perron-Frobenius operator to piecewise linear functions, which amounts to taking  $N = 1$  in eq. (2.29). We shall establish a correspondence between the non-diagonalizability of the Perron-Frobenius operator and transitions between decay modes of the time autocorrelation function. On the basis of eq. (2.10) one can make a distinction between the maps such that each cell  $C_i$  is sent by the transformation on the whole interval  $I$  (all  $a_{ij} = 1$ , full map) and those for which at least one cell  $C_i$  is not mapped on the whole interval (some  $a_{ij} = 0$ , incomplete map). From now on we will always take (unless explicitly specified) the partition on which the map is defined (eq. (2.7)) and the Markov partition (eq. (2.10)) to be identical. Hence, as discussed below eq. (2.33) the components  $w_{ij}^{(k,l)}$  are given by eq. (2.36).

### 2.4.1 Incomplete map

Consider the map

$$f(x) = \begin{cases} \frac{1-r}{r}x + r & x \in C_1 = [0, r[ \\ -\frac{1}{1-r}x + \frac{1}{1-r} & x \in C_2 = [r, 1[ \end{cases} \quad r \in ]0, \frac{1}{2}[ , \quad (2.58)$$

which is such that

$$\begin{aligned} f(C_1) &= C_2 \\ f(C_2) &= C_1 \cup C_2 . \end{aligned} \quad (2.59)$$

The corresponding transition matrix  $\mathbf{W}$ , eq. (2.27), reads

$$\mathbf{W} = \begin{pmatrix} 0 & 1-r & 0 & 1-r \\ \frac{r}{1-r} & 1-r & -\frac{r^2}{(1-r)^2} & 1-r \\ 0 & 0 & 0 & -(1-r)^2 \\ 0 & 0 & \frac{r^2}{(1-r)^2} & -(1-r)^2 \end{pmatrix} . \quad (2.60)$$

For  $r = 2 - \sqrt{3}$ , its eigenvalues and the dimensions of the associated root spaces are

$$\begin{aligned} \lambda_1 &= 1 & d_1 &= 1 \\ \lambda_2 &= -r & d_2 &= 3 , \end{aligned} \quad (2.61)$$

so that there is a 3-d Jordan block associated to the eigenvalue  $-r$ . Computing the root vectors according to eq. (2.42) yields

$$\phi_{1,1} = \begin{pmatrix} \frac{1}{1+r} \\ \frac{1}{1-r^2} \\ 0 \\ 0 \end{pmatrix}, \phi_{2,1} = \begin{pmatrix} -\frac{1-r}{r} \\ 1 \\ 0 \\ 0 \end{pmatrix}, \phi_{2,2} = \begin{pmatrix} \frac{1}{2-r} \\ \frac{2-r}{r(1-r)} \\ \frac{2}{r^2} \\ -\frac{1}{r^2} \end{pmatrix}, \phi_{2,3} = \begin{pmatrix} 0 \\ 1 \\ \frac{2}{r(1-r)} \\ -\frac{2}{r^3} \\ 0 \end{pmatrix}. \quad (2.62)$$

By eq. (2.57) the time autocorrelation function of the observable  $x$  is then

$$C_x(n) = (-r)^n + \alpha n (-r)^{n-1} + \beta n(n-1) (-r)^{n-2} \quad (2.63)$$

where

$$\alpha = \frac{1(1+r)(5r-2)}{7r}, \quad \beta = \frac{1}{7}(1-2r)^2. \quad (2.64)$$

The presence of a Jordan block leads thus to a non purely exponential decay of the  $x$  autocorrelation, namely to a polynomial growth of the correlation modulated by a decaying exponential which ensures the final decay of correlations, ubiquitous in mixing dynamical systems. This function is displayed in fig. 2.1 together with the numerical data obtained by computing the correlation function from the trajectory of the dynamical system according to eq. (2.49). To emphasize the importance of the non purely exponential terms, the exponential  $(-r)^n$  is also displayed.

Let us now regard the constant  $r$  of this example as a control parameter  $r \in (0, \frac{1}{2})$ . In the vicinity of  $r^* = 2 - \sqrt{3}$  we can write  $r$  as

$$r = r^* + \varepsilon \quad |\varepsilon| \ll 1. \quad (2.65)$$

To the dominant order in  $\varepsilon$ , the eigenvalues of the matrix  $\mathbf{W}$  become

$$1, -r^* - \varepsilon, -r^* \pm \sqrt{-\varepsilon}. \quad (2.66)$$

Accordingly, there is a transition from distinct real eigenvalues to complex ones which occurs precisely at  $r = r^*$  when the Perron-Frobenius operator acting on piecewise linear functions is not diagonalizable. The presence of complex conjugate eigenvalues  $r e^{\pm i\varphi}$  is responsible for a decaying contribution in  $\cos(n\varphi) r^n$  in the

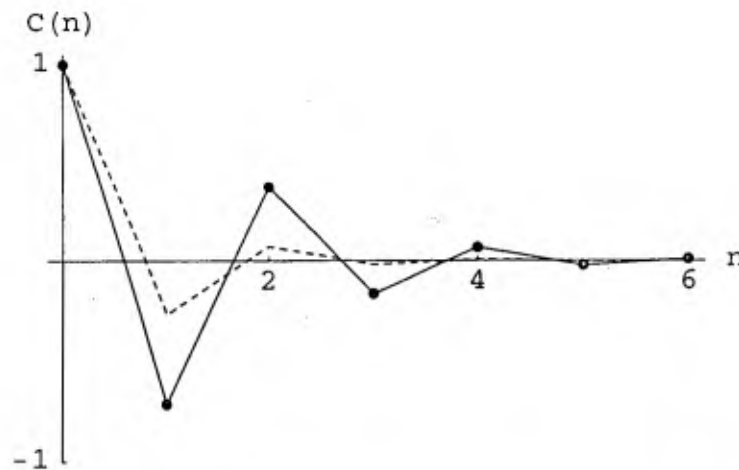


Figure 2.1: Comparison of the analytical expression of the time autocorrelation function of the observable  $x$  (solid line), the numerical data obtained by computing this function from the trajectory of eq. (2.58) for  $r = 2 - \sqrt{3}$  (dots) and the pure exponential  $(-r)^n$  (dashed line).

time autocorrelation function  $C_x(n)$  while the decay is monotone or oscillatory with period 2 if the eigenvalue is respectively a positive or a negative real number. A positive leading eigenvalue (apart from 1) arises from the fact that on the average consecutive iterates of the map lie on one side of the mean value  $\bar{x}$  while the iterates oscillate around the mean value with period 2 if this eigenvalue is negative or with a more complicated period given by the trigonometric representation if it is complex. A transition in the decay mode corresponds therefore to a significant qualitative change in the dynamics.

### 2.4.2 Full map

As an example of full map consider the tent map

$$f(x) = \begin{cases} 2x & x \in C_1 = [0, \frac{1}{2}[ \\ 2(1-x) & x \in C_2 = [\frac{1}{2}, 1[ \end{cases} \quad (2.67)$$

In this case, the Perron-Frobenius operator restricted to piecewise linear densities defined by eq. (2.29) admits a 2-dimensional Jordan block associated to a zero

eigenvalue:

$$\begin{aligned} \lambda_1 &= 1 & d_1 &= 1 \\ \lambda_2 &= 0 & d_2 &= 1 \\ \lambda_3 &= 0 & d_3 &= 2 \end{aligned} \quad (2.68)$$

The root vectors of the transition matrix  $W$  are

$$\phi_{1,1} = \begin{pmatrix} 1 \\ 1 \\ 0 \\ 0 \end{pmatrix}, \phi_{2,1} = \begin{pmatrix} 1 \\ -1 \\ 0 \\ 0 \end{pmatrix}, \phi_{3,1} = \begin{pmatrix} -\frac{1}{2} \\ \frac{1}{2} \\ -\frac{1}{2} \\ 1 \\ 1 \end{pmatrix}, \phi_{3,2} = \begin{pmatrix} -\frac{1}{2} \\ \frac{1}{2} \\ -\frac{1}{2} \\ 4 \\ 0 \end{pmatrix}. \quad (2.69)$$

Using eq. (2.57) for the time autocorrelation function of the observable  $x$  one recovers the well-known result that the tent map is delta correlated

$$C_x(n) = \delta_{n,0}. \quad (2.70)$$

Here the presence of a Jordan block does not lead to a non purely exponential decay of the correlation, the reason being that the function  $\rho(x)(x - \bar{x})$  is entirely spanned by the single eigenvector  $\phi_{3,1}$  of zero eigenvalue, so that the single contribution to the correlation function is purely exponential (with an infinite decay rate). As a corollary, the correlation function of any linear observable other than  $x$  is no longer purely exponential. An example is provided by the observable

$$\theta(x) = x \chi_{C_1}(x) \quad (2.71)$$

for which the autocorrelation function, displayed in fig. 2.2, is

$$C_\theta(n) = \delta_{n,0} - \frac{1}{5} \delta_{n,1}. \quad (2.72)$$

As above, we may regard the nondifferentiable point of the tent map as a control parameter  $\tau = \frac{1}{2}(1 + \varepsilon)$ ,  $-1 < \varepsilon < 1$ . In doing so, we replace the tent map by a skew tent map whose correlation function of the observable  $x$  is<sup>1</sup>

$$C_x(n) = \varepsilon^n. \quad (2.73)$$

<sup>1</sup>The skew tent being a full map we can use eq. (2.41) which yields the eigenvalues 1 for  $k = 0$  and  $\sum_{i=1}^M \frac{1}{|\Lambda_i| \Lambda_i}$  for  $k = 1$ . For any full map the associated eigenvectors correspond respectively to the functions  $\chi_{[0,1]}(x)$  (uniform invariant density) and  $(x - \frac{1}{2}) \chi_{[0,1]}(x)$ . Hence for the observable  $\theta = x$  the function on the left hand side of eq. (2.51) is entirely spanned by the second eigenvector (cf eq. (2.44)). Eq. (2.57) reduces thus to  $C_x(n) = \left[ \sum_{i=1}^M \frac{1}{|\Lambda_i| \Lambda_i} \right]^n$ .

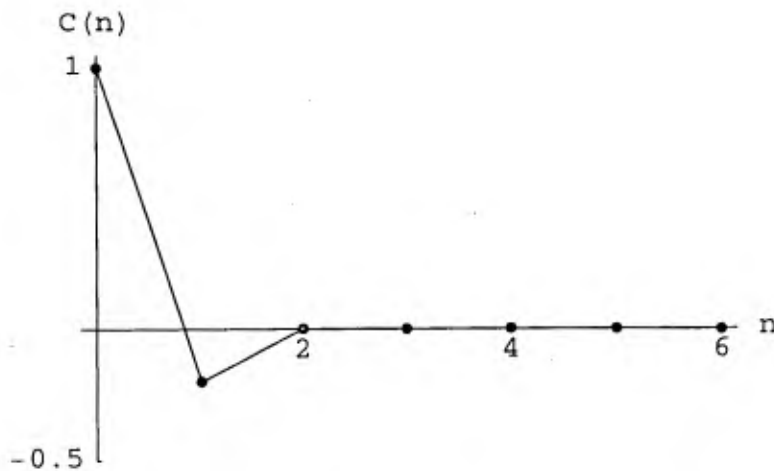


Figure 2.2: Time autocorrelation function of the observable  $x \chi_{C_1}(x)$  for the tent map. The solid line represents eq. (2.72) and the dots the numerical data.

The Perron-Frobenius operator acting on piecewise linear functions is thus nondiagonalizable with respect to a zero eigenvalue at the transition between a monotone and an oscillatory decay of the  $x$ -autocorrelation function.

### 2.4.3 Conclusions

As the above two examples illustrate, the Perron-Frobenius operator associated to piecewise linear Markov maps may admit Jordan blocks when it acts on piecewise linear functions. This leads generally, i.e. as soon as the function  $(\theta(x) - \bar{\theta})\rho(x)$  cannot be spanned by the set of eigenvectors, to a polynomial growth of the correlations modulated by a decaying exponential.

Furthermore, for mixing piecewise linear Markov maps with 2 branches ( $M = 2$ ) and a corresponding 2-cell partition, there is a one-to-one correspondence between the existence of Jordan blocks for the Perron-Frobenius operator acting on piecewise linear functions and the transition between decay modes of the time autocorrelation function of the observable  $x$ . We conjecture that this conclusion extends to mixing piecewise linear Markov maps with more branches ( $M > 2$ ).

To conclude, it is worth mentioning that if the Perron-Frobenius operator is not restricted to piecewise linear functions but acts on piecewise polynomial functions of order  $N$ , for the class of full maps such that for each branch of  $f$  there is a

branch of opposite slope the difference in algebraic and geometric multiplicities of the zero eigenvalue is proportional to  $N$ , irrespective of  $M$ . Since this latter is nothing but the total number of root vectors of rank greater than 1 associated to the zero eigenvalue, this entails that as  $N \rightarrow \infty$  there is an infinite order Jordan block or an infinite number of Jordan blocks of finite order.

## 2.5 Probabilistic approach to homoclinic chaos

The objective of this section is to investigate 3-d systems possessing a homoclinic orbit associated to a saddle-focus and giving rise to homoclinic chaos when the Shil'nikov condition is satisfied. The derivation of the 2-d Poincaré map and its 1-d contractions capturing the essential features of the flow is outlined. At homoclinicity, these 1-d maps are found to be piecewise linear with an infinite number of branches. Near homoclinicity these branches can be assimilated to straight line segments, an idealization that seems to fit reasonably well experimental data and model studies of the Belousov-Zhabotinski reaction. This property allows one to reduce the Perron-Frobenius equation to a generalized master equation and to work out the probabilistic properties of the spiral- and screw-type of homoclinic chaotic attractors.

### 2.5.1 The Shil'nikov map and its 1-d contraction

Consider the 3-variable continuous time dynamical system

$$\begin{cases} \dot{x} = \rho_\mu x - \omega_\mu y + P_\mu(x, y, z) \\ \dot{y} = \omega_\mu x + \rho_\mu y + Q_\mu(x, y, z) \\ \dot{z} = -\lambda_\mu z + R_\mu(x, y, z) \end{cases} \quad (2.74)$$

where  $\mu$  is a control parameter and  $P_\mu, Q_\mu, R_\mu$  are analytic functions in  $x, y, z$  and  $\mu$ , vanishing together with their first derivatives in  $(0, 0, 0)$ . We suppose that the origin behaves as a saddle-focus ( $\lambda_\mu > 0, \rho_\mu > 0$ ), that there exists for  $\mu = 0$  a homoclinic orbit  $\Gamma_0$  biasymptotic to the origin, and that the inequality  $\rho_0 < \lambda_0$  is satisfied. Under these conditions Shil'nikov's theorem [Sh65, Sh70] asserts that the flow contains a subset of chaotic trajectories in the sense specified in the introduction.

Although a homoclinic orbit is structurally unstable, for parameter values near those characterizing the homoclinic situation a general pattern of reinjection of trajectories near the saddle focus should subsist. This property allows one to construct

a 2-d mapping capturing the essential features of the flow. To this end, we assume that it is possible to carry out a  $C^3$  coordinate transformation which linearizes eqs. (2.74) near the origin. In a neighborhood  $V$  of this point, the equations in new coordinates (denoted for simplicity as the old ones) take the form

$$\begin{cases} \dot{x} = \rho_\mu x - \omega_\mu y \\ \dot{y} = \omega_\mu x + \rho_\mu y \\ \dot{z} = -\lambda_\mu z . \end{cases} \quad (2.75)$$

The local unstable manifold of the saddle-focus is now the  $x - y$  plane, whereas the stable one is the  $z$  axis. The Poincaré map in a plane transverse to the local stable manifold is then obtained as the composition of two transformations. The first one, which accounts for the behavior near the saddle-focus, is obtained by straightforward integration of the linear eqs. (2.75), whereas the second one, which is responsible for the reinjection of the dynamics in the vicinity of the fixed point is assumed to be an isometric transport. One arrives thus at the 2-d mapping [ArArRi90, Ri87]

$$\begin{cases} x' = (\sqrt{x^2 + y^2} \xi_\mu^\kappa - x^*) \cos \varphi - h \xi_\mu^{-\frac{\lambda_\mu}{\rho_\mu} \kappa} \sin \varphi + \hat{x}_\mu \\ y' = (\sqrt{x^2 + y^2} \xi_\mu^\kappa - x^*) \sin \varphi + h \xi_\mu^{-\frac{\lambda_\mu}{\rho_\mu} \kappa} \cos \varphi + \hat{y}_\mu \end{cases} \quad x, y \in \mathcal{D} \quad (2.76)$$

where  $\xi_\mu = e^{-\frac{\pi \rho_\mu}{\omega_\mu}}$ ,  $\kappa = \kappa(x, y) = \frac{[1 - \text{sgn}(x)]}{2} - 2k + \frac{1}{\pi} \arctan \frac{y}{x}$ .  $\mathcal{D}$  is the inner domain delimited by the arc of spiral  $r = \tilde{x} \xi_\mu^{2 - \frac{\theta}{\pi}}$ ,  $0 \leq \theta < 2\pi$  and the segment joining its extremities. In this expression,  $x^*$  and  $h$  define the points  $(x^*, 0, 0)$  and  $(0, 0, h)$  where the homoclinic orbit respectively leaves and enters the neighborhood  $V$ ;  $\tilde{x}$  is such that  $\tilde{x} \xi_\mu^2 \leq x^* \leq \tilde{x}$ ;  $\hat{x}_\mu$  and  $\hat{y}_\mu$  describe the distance from homoclinicity ( $\hat{x}_0 = 0, \hat{y}_0 = 0$ );  $\varphi$  accounts for a rotation during the rigid transport and  $k$  is an integer which corresponds to the number of turns the trajectory completes around the saddle-focus between two successive intersections of the Poincaré plane. In the infinite area contraction limit ( $\frac{h}{x^*} \rightarrow 0$ ) and choosing for simplicity  $\varphi = 0$ , eq. (2.76) reduces to the 1-d map

$$x' = \sqrt{x^2 + \hat{y}^2} \xi^\kappa + \hat{x} - 1 \quad \tilde{x} \xi^2 + \hat{x} - 1 < x \leq \tilde{x} + \hat{x} - 1 . \quad (2.77)$$

Here  $x, \tilde{x}, \hat{x}$  and  $\hat{y}$  denote respectively a new variable and new control parameters, equal to the old ones divided by  $x^*$ . A detailed analysis of this globally highly nonlinear law reveals two qualitative different types of maps:

(i) A map in the form of non overlapping increasing or decreasing linear branches whose number tends to infinity as the distance to homoclinicity, or more precisely, the new parameter  $\hat{x}$  tends to zero

$$f_s(x) = |x| \xi^{\frac{1-\text{sgn}(x)}{2} - 2k} + \hat{x} - 1 \quad \hat{x} + (\xi^2 - 1) \frac{1-\text{sgn}(x)}{2} \leq x < \hat{x} + (\frac{1}{\xi^2} - 1) \frac{1+\text{sgn}(x)}{2} \quad (2.78)$$

Since each branch corresponds to a given even or odd number of half-turns of the trajectory around the origin between two crossings of the Poincaré surface, this type of map describes a spiral-type attractor<sup>2</sup>.

(ii) A map which at homoclinicity exhibits two infinite sequences of decreasing and increasing branches. At finite distance from homoclinicity, these two family of branches are finite and separated by a quadratic well which becomes deeper as the system evolves to homoclinicity.

$$f_v(x) = |x| \xi^{\frac{1-\text{sgn}(x)}{2} - 2k + \frac{1}{\pi} \arctan \frac{\hat{y}}{x}} \sqrt{1 + \frac{\hat{y}^2}{x^2}} - 1 \quad \tilde{x} \xi^2 - 1 < x \leq \tilde{x} - 1 \quad (2.79)$$

As this map allows for reinjection on both sides of the origin, it describes a screw type attractor.

Notice that at homoclinicity both maps turn out to be piecewise linear. In the sequel the statistical properties of the two types of attractors generated by the dynamical system (2.77) will be explored by adopting the simplification that the piecewise linear character of the maps extends in a certain vicinity of homoclinicity as well.

As shown in Sec. 2.2, in addition to the requirement of piecewise linear maps, the reduction of the Perron-Frobenius equation to a generalized master equation relies on the property that the phase space partition be Markov, i.e. such that each of its elements is transformed by the deterministic dynamics into a union of its elements. In this section we build models of spiral and screw-type attractors compatible with these properties and derive subsequently the generalized master equation and the behavior of the time autocorrelation function of two classes of observables: the observable  $x$  and a piecewise constant observable  $\theta(x) = \sum_{j=1}^M s_j \chi_{c_j}(x)$  where the

<sup>2</sup>At homoclinicity, the reinjections of the dynamics in the  $x - y$  plane are made along a line passing by the origin. By definition, for the spiral-type attractor the reinjections occur on one side of the origin, whereas for the screw-type they occur on both sides.

symbol  $s_j$  corresponds to the number of half-turns that the trajectory performs around the origin. Hereafter, we consider separately the cases of spiral and screw-type attractors.

## 2.5.2 Spiral-type attractor

Let us consider the map (2.78) when limited to three branches corresponding to 1, 3 and 5 half-turns of the trajectory around the origin ( $k = 1, 2, 3$ ). The 1-d map  $f_s$  reads then

$$f_s(x) = -\frac{x}{\xi^{2i-1}} + \hat{x} - 1 \quad b_{i-1} < x \leq b_i \quad i = 1, 2, 3. \quad (2.80)$$

We choose

$$\begin{aligned} f_s(C_1) &= C_1 \cup C_2 \\ f_s(C_2) &= C_1 \cup C_2 \cup C_3 \\ f_s(C_3) &= C_2 \cup C_3 \end{aligned} \quad (2.81)$$

where the partition considered is the one defined by the points of discontinuity,  $C_i = ]b_{i-1}, b_i]$ . One can easily check that these relations imply

$$\begin{aligned} \xi &\simeq 0.67546 \\ \hat{x} &= 1 - \xi^2(1 + \xi)(1 + \xi^2) \\ b_0 &= \xi^2 + \hat{x} - 1 \\ b_1 &= -\xi^3 \\ b_2 &= -\xi^5 \\ b_3 &= \hat{x}. \end{aligned} \quad (2.82)$$

Using eq. (2.36) the block  $\mathbf{W}^{(k,k)}$  of the transition matrix  $\mathbf{W}$  writes

$$\mathbf{W} = \begin{pmatrix} (-1)^k \xi^{k+1} & (-1)^k \xi^{3(k+1)} & 0 \\ (-1)^k \xi^{k+1} & (-1)^k \xi^{3(k+1)} & (-1)^k \xi^{5(k+1)} \\ 0 & (-1)^k \xi^{3(k+1)} & (-1)^k \xi^{5(k+1)} \end{pmatrix}. \quad (2.83)$$

The eigenvalues  $\lambda_i^{(k)}$  of  $\mathbf{W}^{(k,k)}$  and thus of  $\mathbf{W}$  are, for  $k = 0, 1$ , all real,

$$\begin{aligned} \lambda_1^{(0)} &= 1 & \lambda_1^{(1)} &= -0.552 \\ \lambda_2^{(0)} &= 0.244 & \lambda_2^{(1)} &= -0.050 \\ \lambda_3^{(0)} &= -0.120 & \lambda_3^{(1)} &= 0.031. \end{aligned} \quad (2.84)$$

The eigenvector of  $\mathbf{W}$  associated to the eigenvalue unity yields for the stationary density

$$\rho_s(x) = 1.87 \chi_{C_1}(x) + 1.97 \chi_{C_2}(x) + 0.70 \chi_{C_3}(x) \quad (2.85)$$

which enables one to compute the average value of various quantities and deduce for instance that the 1-d map (2.80) displays sensitivity to initial conditions with a Lyapunov exponent equal to 0.681. The other eigenvectors of  $\mathbf{W}$  allow us as discussed in Sec. 2.3 to compute time-dependent properties such as the time autocorrelation functions which we consider now.

**The observable  $\theta(x) = x$**

From eq. (2.57) we deduce that the time autocorrelation function of the observable  $x$  decays as

$$C(n) = \sum_{j=1}^3 \sum_{k=0}^1 c_j^{(k)} \lambda_j^{(k)n} \quad (2.86)$$

where

$$\begin{aligned} c_1^{(0)} &= 0 & c_1^{(1)} &= 0.927 \\ c_2^{(0)} &= 0.180 & c_2^{(1)} &= 0.024 \\ c_3^{(0)} &= -0.128 & c_3^{(1)} &= -0.003 . \end{aligned} \quad (2.87)$$

In fig. 2.3 the comparison is made between the analytical expression of eq. (2.86) and the numerical data obtained by computing the time autocorrelation function from the trajectory according to eq. (2.49).

**The observable  $\theta(x) = \sum_{j=1}^M s_j \chi_{C_j}(x)$**

A discrete observable of interest in the context of homoclinic systems is the number of half-turns the trajectory completes in the vicinity of the saddle-focus between two successive intersections of the Poincaré plane. For the map  $f_s$ , this observable is expressed as

$$\theta(x) = 1 \chi_{C_1}(x) + 3 \chi_{C_2}(x) + 5 \chi_{C_3}(x) . \quad (2.88)$$

Its time autocorrelation function, which is given by eq. (2.57), is found to decay as

$$C(n) = \sum_{j=1}^3 c_j^{(0)} \lambda_j^{(0)n} \quad (2.89)$$

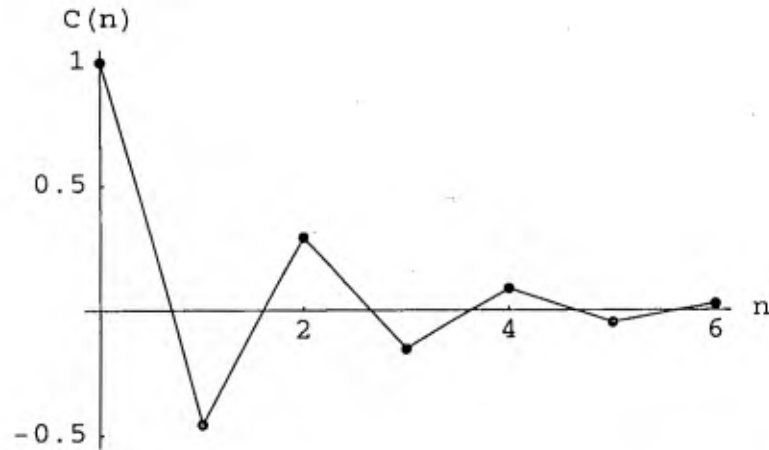


Figure 2.3: Comparison between the analytical expression of the time autocorrelation function of the observable  $x$  (solid line) and the numerical data obtained by computing this function from the trajectory (dots) for the spiral-type attractor (2.80).

where

$$\begin{aligned} c_1^{(0)} &= 0 \\ c_2^{(0)} &= 0.768 \\ c_3^{(0)} &= 0.232 . \end{aligned} \quad (2.90)$$

In fig. 2.4 the comparison is made between the analytical expression of eq. (2.89) and the numerical data obtained from eq. (2.49).

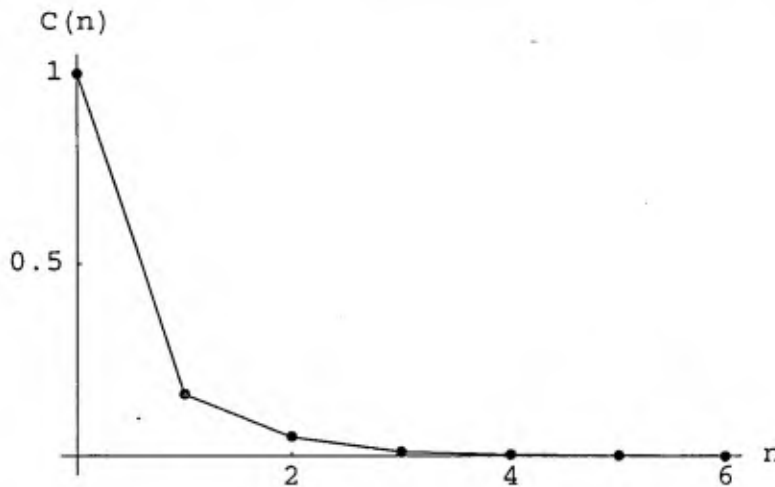
### 2.5.3 Screw-type attractor

Let us restrict the 1-d map  $f_v$  given by eq. (2.79) to two branches  $k = 1$  and one well  $k = 2$ . We also choose

$$\begin{aligned} \bar{f}_v(C_1) &= C_1 \cup C_2 \cup C_3 \cup C_4 \\ \bar{f}_v(C_2) &= C_4 \\ \bar{f}_v(C_3) &= C_4 \\ \bar{f}_v(C_4) &= C_1 \cup C_2 \cup C_3 \cup C_4 \end{aligned} \quad (2.91)$$

where  $\bar{f}_v$  denotes the piecewise linear map obtained by neglecting the terms in  $\frac{y^2}{x^2}$  in the two branches of  $f_v$  and by replacing the well by two segments of straight line

Figure 2.4: Comparison between the analytical expression of the time autocorrelation function of the piecewise constant observable (2.88) (solid line) and the numerical data obtained by computing this function from the trajectory (dots) for the spiral type-attractor (2.80).



going through its minimum. As above, the partition is determined by the points of discontinuity,  $C_i = ] b_{i-1}, b_i ]$ . The map  $\bar{f}_v(x)$  reads then

$$\bar{f}_v(x) = \begin{cases} -2x - 1 & b_0 < x \leq b_1 \\ \frac{1}{\beta-1} x + \frac{2\beta-1}{6(\beta-1)} & b_1 < x \leq b_2 \\ \frac{1}{\beta} x + \frac{4\beta-1}{12\beta} & b_2 < x \leq b_3 \\ 4x - 1 & b_3 < x \leq b_4 \end{cases} \quad (2.92)$$

where

$$\begin{aligned} b_0 &= -\frac{2}{3} & b_3 &= \frac{1}{12} \\ b_1 &= -\frac{1}{6} & b_4 &= \frac{1}{3} \\ b_2 &= \frac{13 \ln 2}{192\pi (1+(\frac{\ln 2}{\pi})^2)^{\frac{1}{2}} 2^{\frac{1}{\pi}} \arctan \frac{\pi}{\ln 2}} & \beta &= \frac{1}{3} - 4b_2. \end{aligned} \quad (2.93)$$

By construction this map is Markov so that densities evolve according to the generalized master equation (2.33). Taking into account eqs. (2.91) to (2.93), the block

$W^{(k,k)}$ ,  $k = 0, 1$ , of the transition matrix  $W$  is

$$W = \begin{pmatrix} \frac{(-1)^k}{2^{k+1}} & 0 & 0 & \frac{1}{4^{k+1}} \\ \frac{(-1)^k}{2^{k+1}} & 0 & 0 & \frac{1}{4^{k+1}} \\ \frac{(-1)^k}{2^{k+1}} & 0 & 0 & \frac{1}{4^{k+1}} \\ \frac{(-1)^k}{2^{k+1}} & (-1)^k(1-\beta)^{k+1} & \beta^{k+1} & \frac{1}{4^{k+1}} \end{pmatrix} \quad (2.94)$$

The transition matrix  $W$  admits now one pair of complex eigenvalues,

$$\begin{aligned} \lambda_1^{(0)} &= 1 & \lambda_1^{(1)} &= -0.09375 + 0.1321 i \\ \lambda_2^{(0)} &= -\frac{1}{4} & \lambda_2^{(1)} &= -0.09375 - 0.1321 i \\ \lambda_3^{(0)} &= 0 & \lambda_3^{(1)} &= 0 \\ \lambda_4^{(0)} &= 0 & \lambda_4^{(1)} &= 0 \end{aligned} \quad (2.95)$$

The stationary density is

$$\rho_s(x) = \frac{4}{5} [\chi_{C_1}(x) + \chi_{C_2}(x) + \chi_{C_3}(x) + 2\chi_{C_4}(x)] \quad (2.96)$$

which gives a Lyapunov exponent of 0.952. Turning to the time autocorrelation functions we consider two observables as above.

**The observable  $\theta(x) = x$**

From eq. (2.57) we deduce that the autocorrelation function of the observable  $x$  is

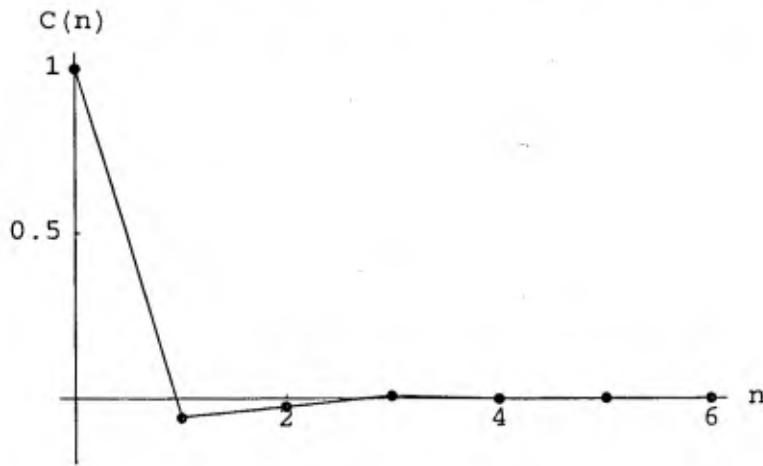
$$C(n) = \sum_{j=1}^4 \sum_{k=0}^1 c_j^{(k)} \lambda_j^{(k)n} \quad (2.97)$$

where

$$\begin{aligned} c_1^{(0)} &= 0 & c_1^{(1)} &= 0.608 - 0.016 i \\ c_2^{(0)} &= -0.216 & c_2^{(1)} &= 0.608 + 0.016 i \\ c_3^{(0)} &= 0 & c_3^{(1)} &= 0 \\ c_4^{(0)} &= 0 & c_4^{(1)} &= 0 \end{aligned} \quad (2.98)$$

In fig. 2.5 the comparison is made between the analytical expression of eq. (2.97) and the numerical data obtained from the trajectory according to eq. (2.49).

Figure 2.5: As in fig. 2.3, but for the screw-type attractor (2.92).



The observable  $\theta(x) = \sum_{j=1}^M s_j \chi_{C_j}(x)$

Let us consider the observable that gives the number of half-turns the trajectory completes around the origin between two intersections of the Poincaré plane, or explicitly in the case of map (2.92)

$$\theta(x) = 4 \chi_{C_1}(x) + 2 \chi_{C_2}(x) + 2 \chi_{C_3}(x) + 4 \chi_{C_4}(x) \quad (2.99)$$

For such an observable, the time autocorrelation function given by eq. (2.57) is

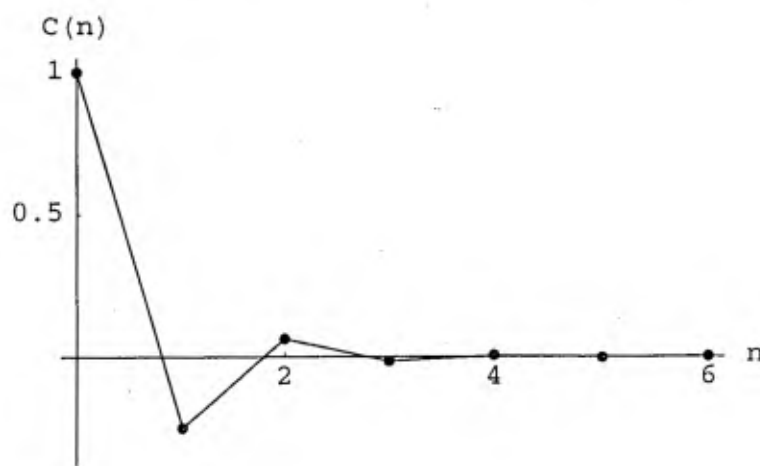
$$C(n) = \sum_{j=1}^4 c_j^{(0)} \lambda_j^{(0)n} \quad (2.100)$$

where

$$\begin{aligned} c_1^{(0)} &= 0 \\ c_2^{(0)} &= 1 \\ c_3^{(0)} &= 0 \\ c_4^{(0)} &= 0 \end{aligned} \quad (2.101)$$

In fig. 2.6 the comparison is made between the analytical expression of eq. (2.100) and the numerical data obtained from eq. (2.49).

Figure 2.6: As in fig. 2.4, but for the screw-type attractor (2.92) and the observable (2.99).



#### 2.5.4 Conclusions

In this section a probabilistic description of homoclinic systems has been carried out. In particular, the time autocorrelation functions of observables such as the state variable  $x$  have been derived for models of the spiral and screw-type attractors associated to homoclinic chaos. In addition to giving quantitative information on the way the dynamics loses its memory, the decay modes of the time autocorrelation function of the  $x$ -observable provide a useful characterization of spiral-type versus screw-type attractor. For the spiral-type attractor, the leading decay rate of the time autocorrelation of the  $x$ -observable is determined by a negative eigenvalue. This means that the point of reinjection of the flow on the Poincaré plane oscillates around the mean value  $\bar{x}$  with period two. For the screw-type attractor, there is also a negative leading eigenvalue, so that the point of reinjection of the flow still oscillates around the mean value  $\bar{x}$  with period two. But, in addition, there exist complex eigenvalues. The point of reinjection oscillates then, in the average, from one side to the other with a more complicated period obtained from the trigonometric representation of the complex eigenvalues. Furthermore, for the examples considered here, the decay modes of the screw type of attractor interfere in a destructive way whereas for the spiral type they reinforce the oscillation of the leading one. This trend is confirmed by the study of further examples involving

higher number of branches. It turns out that several negative eigenvalues of about the same amplitude may exist for both types of attractors. But, in the case of the spiral-type, their effect seems to reinforce that of the leading eigenvalue whereas for the screw-type these negative eigenvalues, eventually together with complex ones, seem to cancel the effect of the leading one. We believe this is due to the coexistence of increasing and decreasing branches which occurs in the 1-d map of the screw but not in that of the spiral type of attractor and so finally to the topology of the attractor itself. Furthermore, when every branch is mapped on the whole interval the correlation function is determined by a single non-trivial eigenvalue:  $\sum_i 1/|\Lambda_i|$ , the magnitude of which is then smaller in the case of the screw-type attractor. This property would extend to the leading eigenvalue when every branch is not mapped onto the interval. Owing to the destructive interference between the decay modes of the screw-type attractor, the time autocorrelation functions of these attractors appear less organized. As a consequence the power spectra of screw-type attractors have a more pronounced broad band component than those of the spiral-type where characteristic frequencies emerge. This is corroborated by power spectrum computation of continuous time dynamical systems generating as the parameters vary spiral and screw chaos [FaCrFrPaSh80].

## Chapter 3

# Inverse problem: designing one-dimensional chaotic maps with prescribed statistical properties.

### 3.1 Introduction

In the previous chapter we have been concerned with the statistical properties of given dynamical systems in the form of piecewise linear Markov maps. The aim of this chapter is to address the inverse problem of tailoring dynamical systems with prescribed probabilistic properties, namely invariant density and correlation function. In this sense, we deal here with the general problem of the control of chaos, that finds applications in various fields. On the other hand, we will have access to more general dynamical systems like non-Markov piecewise linear maps and smooth maps. The basic idea is to use a class of piecewise linear Markov maps for which all statistical properties are known as a system of reference and transform these maps by conjugacy or some other transformations to be defined below into maps with the prescribed statistical properties, which are typically non-Markov and smooth maps.

In Sec. 3.2, we consider the class of 1-d piecewise linear full maps and compile their statistical properties. We then address the inverse problem of designing a map with a prescribed correlation function. In Sec. 3.3, we define a transformation from this class into a larger one including non-Markov maps and compile the statistical properties of these maps. Secs. 3.4 and 3.5 are devoted to the design of 1-d maps with prescribed invariant measure and correlation function. Conclusions are drawn

in Sec. 3.6.

### 3.2 Statistical properties of piecewise linear full maps

Let  $K(\phi)$  be the class of 1-d piecewise linear maps  $\phi : X \rightarrow X$  given by

$$\phi|_{C_i} = \phi_i : x \mapsto a_i x + b_i \quad (3.1)$$

where  $\{C_i = ]c_{i-1}, c_i]\}_{i=1}^m$  is a partition of the closed interval  $X = [-1, 1]$

$$\begin{aligned} \cup_{i=1}^m C_i &= X \\ C_i \cap C_j &= \emptyset \quad \forall i \neq j. \end{aligned} \quad (3.2)$$

It is assumed that each element of the partition is mapped by the transformation  $\phi$  on the whole interval  $X$

$$\phi_i : C_i \rightarrow X \quad \forall i \quad (3.3)$$

implying

$$a_i = \pm \frac{2}{c_i - c_{i-1}} \quad b_i = \pm \frac{c_{i-1} + c_i}{c_{i-1} - c_i}. \quad (3.4)$$

For  $m \geq 2$  the maps  $\phi$  are everywhere expanding

$$\left| \frac{d\phi}{dx}(x) \right| > 1 \quad \forall x \in X \quad (3.5)$$

and therefore [LaMa85] there is a function  $\rho(x)$  such that

$$(i) \quad \rho(x) \geq 0$$

$$(ii) \quad \int_X \rho(x) dx = 1$$

$$(iii) \quad \rho(x) = \frac{d}{dx} \int_{\phi^{-1}(\text{inf}_X, x)} \rho(x') dx' \quad \text{where } \phi^{-1}(x) \text{ is the preimage of } X.$$

One can readily check that this function - the invariant density of the Perron-Frobenius operator - is equal to  $\frac{1}{2}$ , that is, the sequence  $\{x_n\}$  generated by the 1-d dynamical system

$$x_n = \phi(x_{n-1}) \quad (3.6)$$

is uniformly distributed on  $X$ . The invariant density  $\rho$  determines the  $\phi$ -Lebesgue measure  $\mu(A)$  of any measurable set  $A \subset X$

$$\mu(A) \equiv \int_A dx \rho(x) \quad (3.7)$$

which is invariant under  $\phi$ . As maps  $\phi$  are everywhere expanding and ergodic, they display sensitivity to initial conditions with a Lyapunov exponent given by

$$0 < \lambda_\phi = - \sum_{i=1}^m \mu(C_i) \ln \mu(C_i) < \ln m . \quad (3.8)$$

In order to study the chaotic dynamics of the maps  $\phi$  we consider their time autocorrelation function

$$C_\phi(n) = \frac{1}{\sigma^2} \lim_{N \rightarrow \infty} \frac{1}{N} \sum_{i=0}^{N-1} (x_i - \bar{x}) (x_{i+n} - \bar{x}) \quad (3.9)$$

where  $\bar{x}$  and  $\sigma^2$  are respectively the mean value and the variance of  $x$ . Using Birkhoff's ergodic theorem, this expression is rewritten as

$$C_\phi(n) = \frac{1}{\sigma^2} \left[ \int_X \mu(dx) x \phi^n(x) - \bar{x}^2 \right] . \quad (3.10)$$

Taking into account the piecewise character of  $\phi$  together with  $\mu(dx) = \frac{1}{2} dx$  and  $\bar{x} = 0$ , we get

$$C_\phi(n) = \frac{1}{2\sigma^2} \sum_{i=1}^m \int_{C_i} dx x \phi^{n-1}(\phi_i(x)) \quad (3.11)$$

or with the change of variable  $\phi(x) = z$

$$C_\phi(n) = \frac{1}{2\sigma^2} \sum_{i=1}^m \frac{1}{|a_i| a_i} \left[ \int_{-1}^{+1} dz z \phi^{n-1}(z) - b_i \int_{-1}^{+1} dz \phi^{n-1}(z) \right] \quad (3.12)$$

where we used eq. (3.1). Note that the last term vanishes as it is proportional to  $\bar{x}$ . For  $n = 1$ , the remaining term in eq. (3.12) becomes

$$C_\phi(1) = \sum_{i=1}^m \frac{1}{|a_i| a_i} = \sum_{i=1}^m \text{sgn}(a_i) \cdot \mu^2(C_i) . \quad (3.13)$$

Thus, eq. (3.12) can be rewritten in the recursive form

$$C_\phi(n) = C_\phi(n-1) C_\phi(1) \quad (3.14)$$

or, repeating the procedure

$$C_\phi(n) = [C_\phi(1)]^n . \quad (3.15)$$

Note that the following inequalities hold

$$|C_\phi(1)| \leq \sum_{i=1}^m \mu^2(C_i) < [\sum_{i=1}^m \mu(C_i)]^2 = 1 \quad (3.16)$$

so that the maps  $\phi$  are mixing.

Depending on the sign and value of  $C_\phi(1)$  one may now distinguish three types of correlation functions

- exponential ( $0 < C_\phi(1) < 1$ )

$$C_\phi(n) = e^{n \ln C_\phi(1)} \quad (3.17)$$

- delta-type ( $C_\phi(1) = 0$ )

$$C_\phi(n) = \delta_{n0}^{Kr} \quad (3.18)$$

- periodically modulated exponential ( $-1 < C_\phi(1) < 0$ )

$$C_\phi(n) = \cos n\pi e^{n \ln |C_\phi(1)|} . \quad (3.19)$$

Given any  $\phi \in K(\phi)$  only one of these behaviors will be realized. Alternatively, if one of these types of correlation function is to be obtained, a map  $\phi$  yielding exactly the required correlation function can be constructed using eq. (3.13). For example, one way to get the first type of correlation function is to consider a map with a uniform phase space partition,  $\mu(C_i) = \mu(C_j) \quad \forall i, j$  and only positive slopes,  $a_i > 0 \quad \forall i$ . From eq. (3.13) we then obtain

$$C_\phi(n) = \left(\frac{1}{m}\right)^n = e^{-n \ln m} . \quad (3.20)$$

Note from eqs. (3.8) and (3.13) that for given  $m$ , i.e. given number of branches, this realization corresponds to a maximal exponential decay of correlation together with a maximal Lyapunov exponent. The second type of correlation function, corresponding to  $\delta$ -correlated process occurs according to eq. (3.13) whenever

$$\sum_{i=1}^m \text{sgn}(a_i) \mu^2(C_i) = 0 . \quad (3.21)$$

This condition is satisfied if to every branch there corresponds a branch, defined on a segment of equal measure, whose slope has the same absolute value but the opposite sign. However, it is important to note that this "symmetry" is not necessary to have a  $\delta$ -correlated process. Regarding the third type of correlation function, one way to obtain it is to consider, as for the first case, a uniform partition but with all slopes negative,  $a_i < 0 \quad \forall i$ . The correlation function reads then

$$C_\phi(n) = \left(-\frac{1}{m}\right)^n = \cos n\pi e^{-n \ln m} . \quad (3.22)$$

Having at our disposal the analytic expression for the correlation function of any map  $\phi \in K(\phi)$  we can compute its power spectrum, defined by

$$S_\phi(\omega) = \frac{1}{2\pi} \left(1 + 2 \sum_{r=1}^{\infty} C_\phi(r) \cos r\omega\right) \quad (3.23)$$

Using eq. (3.15) we obtain

$$S_\phi(\omega) = \frac{1}{2\pi} \frac{1 - C_\phi^2(1)}{1 - 2C_\phi(1) \cos \omega + C_\phi^2(1)} . \quad (3.24)$$

By varying  $C_\phi(1)$  in the range  $] -1, 1[$  eq. (3.24) spans the class of reproducible spectral densities. Fig. 3.1 shows the evolution of the power spectrum of  $\phi$  for different values of  $C_\phi(1)$ .

### Example

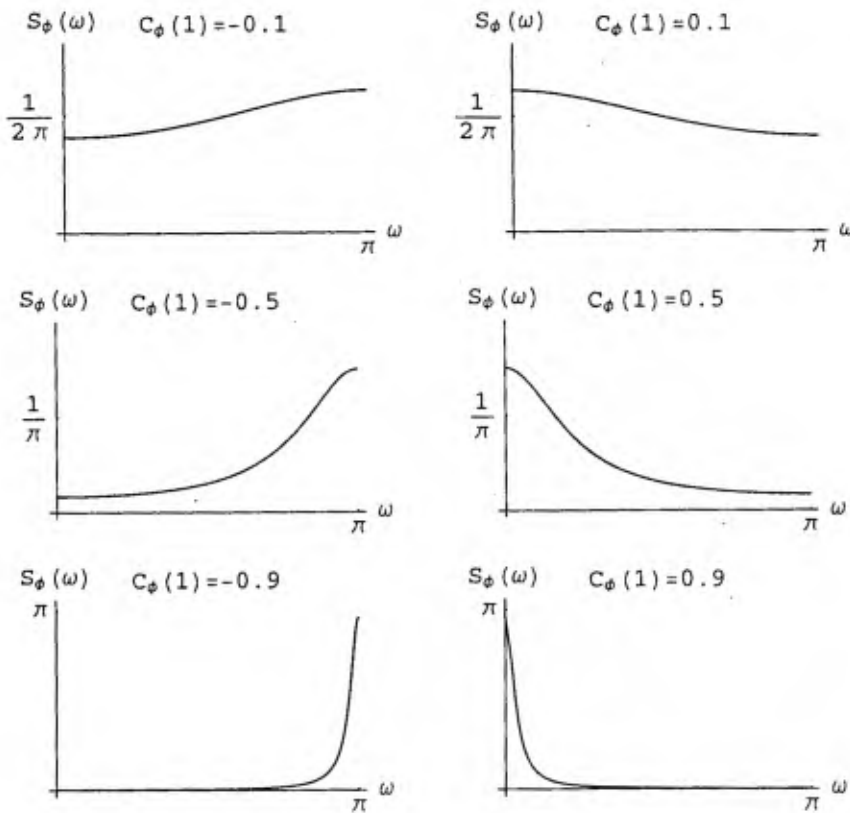
Let us design a map  $\phi$  such that

$$C_\phi(1) = 1 - 2\delta \quad 0 < \delta \ll 1 . \quad (3.25)$$

The motivation is that the corresponding power spectrum behaves in the low frequencies region according to a power law

$$S_\phi(\omega) \approx \frac{2}{\pi} \frac{\delta(1 - \delta)}{\omega^2(1 - 2\delta) + 4\delta^2} \quad (3.26)$$

where we have approximated  $\cos \omega$  by the first two terms of its Taylor expansion around  $\omega = 0$ . This behavior, which is typical of flicker noise, is observed in many physical situations. At the level of the map, it arises because long laminar regions

Figure 3.1: Power spectra of the maps  $\phi \in K(\phi)$  for different values of  $C_\phi(1)$ .

occur. Choosing a map with two branches ( $m = 2$ ), we have to determine  $c_1$  using eq. (3.13) which yields

$$C_\phi(1) = \frac{(1+c_1)^2}{4} - \frac{(1-c_1)^2}{4} = c_1 \quad (3.27)$$

from which we deduce the map  $\phi$

$$\phi(x) = \begin{cases} \frac{1}{1-\delta}x + \frac{\delta}{1-\delta} & -1 < x < 1-2\delta \\ -\frac{1}{\delta}x + \frac{1-\delta}{\delta} & 1-\delta < x < 1. \end{cases} \quad (3.28)$$

Actually, it is a skew tent map whose non-differentiable point is  $1 - 2\delta$ .

It is clear that the maps  $\phi \in K(\phi)$  do not reproduce all the known correlation functions of 1-d maps, as, for instance, correlation functions displaying several

competing decay modes or behaviors other than purely exponential as obtained in Chap. 2. In the next section, we introduce a class of maps yielding richer correlational properties.

### 3.3 Statistical properties of a class of piecewise linear non-Markov maps

Let us define a transformation of any map  $\phi \in K(\phi)$  such that  $\phi$  is shifted by the quantity  $\delta$  inside  $[-1, 1]$  and the part of the last branch exceeding 1 is reinjected from  $-1$ . This transformation  $\mathcal{S}$  is given by

$$\mathcal{S} : \phi \rightarrow v(x) = \begin{cases} v_1(x) = \phi_m(x - \delta + 2) & x \in Q_1 \\ v_{i+1}(x) = \phi_i(x - \delta) & x \in Q_{i+1} \quad i = 1, \dots, m \end{cases} \quad (3.29)$$

where  $Q_i = ]q_{i-1}, q_i]$ ,  $q_0 = -1$ ,  $q_i = c_{i-1} + \delta$ ,  $q_{m+1} = 1$  and  $\delta$  is a shift parameter such that  $0 \leq \delta \leq 1 - c_{m-1}$ . We shall denote by  $K(\phi, \mathcal{S})$  the set of all the maps  $v$  obtained by  $\mathcal{S}$ -transforming the maps  $\phi$  of  $K(\phi)$ . Obviously,  $K(\phi, \mathcal{S})$  includes  $K(\phi)$ .

The new map  $v$  has the same invariant measure and mean value as map  $\phi$ . It is also ergodic with respect to the Lebesgue measure, except when  $\phi$  is the tent or skew tent map. To show this we determine the conditions under which the map  $v = \mathcal{S} \circ \phi$  is not ergodic with respect to the Lebesgue measure, that is, the conditions to have non-trivial invariant subsets of  $X$

$$v^{-1}(I) = I \quad 0 < \mu(I) < 1. \quad (3.30)$$

First, we note that since  $\phi : C_i \rightarrow X \quad \forall i$ , there exist at most 2 such invariant sets

$$\begin{aligned} I_1 &= [-1, a] & a &\in Q_2 \\ I_2 &= [b, 1] & b &\in Q_m \end{aligned} \quad (3.31)$$

For the same reason, for these non-trivial invariant sets to exist, it is necessary that

$$\text{sgn}(a_1) = \text{sgn}(a_{m-1}) = -\text{sgn}(a_m) = 1. \quad (3.32)$$

As these sets may not have preimages outside themselves there cannot be any branch of  $v$  between them, so that  $m = 2$  and  $a = b$ . It follows that the nontrivial invariant

subsets  $I_1$  and  $I_2$  exist if and only if the corresponding map  $\phi$  is given by

$$\phi(x) = \begin{cases} 1 + \frac{2}{1+\alpha}(x-\alpha) & -1 \leq x < \alpha \\ 1 - \frac{2}{1-\alpha}(x-\alpha) & \alpha \leq x < 1 \end{cases} \quad -1 < \alpha < 1 \quad (3.33)$$

which is the tent or skew tent map. As a consequence, for all  $\phi \in K(\phi)$  except the skew tent map, the map  $\nu = \mathcal{S} \circ \phi$  is ergodic with respect to the Lebesgue measure.

We now turn to the correlation function of the map  $\phi$  which is given by

$$C_\nu(n) = \frac{1}{2\sigma^2} \int_X dx x \nu^n(x) . \quad (3.34)$$

As  $\nu$  is piecewise linear, for  $n \geq 1$  eq. (3.34) can be written

$$C_\nu(n) = \frac{1}{2\sigma^2} \sum_{k=1}^{m+1} \mathcal{L}_k(n) \quad (3.35)$$

where

$$\mathcal{L}_k(n) \equiv \int_{q_{k-1}}^{q_k} dx x \nu^{n-1}(\nu_k(x)) . \quad (3.36)$$

Let us carry the change of variable  $z = \nu_k(x)$  in  $\mathcal{L}_k$ . Then using eq. (3.29) for  $\nu_k(x)$  we obtain

- $k = 1$

$$\mathcal{L}_1(n) = \frac{1}{a_m^2} \left[ \int_\beta^s dz z \nu^{n-1}(z) + ((\delta - 2) a_m - b_m) \int_\beta^s dz \nu^{n-1}(z) \right] \quad (3.37)$$

- $k = 2, \dots, m$

$$\mathcal{L}_k(n) = \frac{1}{|a_{k-1}| |a_{k-1}|} \left[ \int_{-1}^{+1} dz z \nu^{n-1}(z) + (\delta a_{k-1} - b_{k-1}) \int_{-1}^{+1} dz \nu^{n-1}(z) \right] \quad (3.38)$$

- $k = m + 1$

$$\mathcal{L}_{m+1}(n) = \frac{1}{a_m^2} \left[ \int_{-s}^\beta dz z \nu^{n-1}(z) + (\delta a_m - b_m) \int_{-s}^\beta dz \nu^{n-1}(z) \right] \quad (3.39)$$

where  $\beta \equiv v_1(-1) = s - \delta a_m$  and  $s \equiv \text{sgn}(a_m)$ . Let us define the quantity  $\mathcal{I}_{n-1}(\beta)$  by

$$\mathcal{I}_{n-1}(\beta) \equiv \int_{-1}^{\beta} dz v^{n-1}(z) = - \int_{\beta}^1 dz v^{n-1}(z) \quad (3.40)$$

where the second equality holds because of  $\int_{-1}^{+1} dz v^{n-1}(z) = 0$ . Then, using eqs. (3.37) and (3.39), it follows that

$$\frac{1}{2\sigma^2} [\mathcal{L}_1(n) + \mathcal{L}_{m+1}(n)] = \frac{1}{a_m |a_m|} C_v(n-1) + \frac{1}{\sigma^2 a_m} \mathcal{I}_{n-1}(\beta) . \quad (3.41)$$

As the second term of the right hand side of eq. (3.38) for  $\mathcal{L}_k$  vanishes, it follows that for  $k = 2, \dots, m$

$$\frac{1}{2\sigma^2} \mathcal{L}_k(n) = \frac{1}{|a_{k-1}| a_{k-1}} C_v(n-1) . \quad (3.42)$$

Therefore, eq. (3.35) for  $C_v(n)$  becomes

$$C_v(n) = C_\phi(1) C_v(n-1) + \frac{1}{\sigma^2 a_m} \mathcal{I}_{n-1}(\beta) \quad (3.43)$$

To evaluate  $\mathcal{I}_{n-1}(\beta)$  one has to know to what cell  $\beta$  belongs. Actually, there are two cases to consider.

- $\beta \in Q_1$

Then

$$\mathcal{I}_{n-1}(\beta) = \int_{-1}^{\beta} dz v^{n-2}(v_1(z)) \quad (3.44)$$

or through the change of variable  $x = v_1(z)$

$$\mathcal{I}_{n-1}(\beta) = -\frac{1}{a_m} \int_{-1}^{\beta} dx v^{n-2}(x) + \frac{1}{a_m} \int_{-1}^{v_1(\beta)} dx v^{n-2}(x) \quad (3.45)$$

where we have decomposed the integral from  $\beta$  to  $v_1(\beta)$  into two integrals. From eq. (3.40) it follows that

$$\mathcal{I}_{n-1}(\beta) = -\frac{1}{a_m} \mathcal{I}_{n-2}(\beta) + \frac{1}{a_m} \mathcal{I}_{n-2}(v_1(\beta)) . \quad (3.46)$$

- $\beta \in Q_{i+1}$ ,  $i = 1, \dots, m$

Then

$$\mathcal{I}_{n-1}(\beta) = \int_{-1}^{q_1} dz v^{n-2}(v_1(z)) + \sum_{k=1}^{i-1} \int_{q_k}^{q_{k+1}} dz v^{n-2}(v_{k+1}(z)) + \int_{q_i}^{\beta} dz v^{n-2}(v_{i+1}(z)) . \quad (3.47)$$

As every contribution to the sum over  $k$  vanishes, one is left with only two terms. Carrying the change of variable  $x = v_1(z)$  and  $x = v_{i+1}(z)$  in the first and second term respectively, we obtain

$$\mathcal{I}_{n-1}(\beta) = \frac{1}{a_m} \int_{\beta}^{\infty} dx v^{n-2}(x) + \frac{1}{a_i} \int_{-\text{sgn}(a_i)}^{v_{i+1}(\beta)} dx v^{n-2}(x) \quad (3.48)$$

or, taking into account eq. (3.40)

$$\mathcal{I}_{n-1}(\beta) = -\frac{1}{a_m} \mathcal{I}_{n-2}(\beta) + \frac{1}{a_i} \mathcal{I}_{n-2}(v(\beta)) . \quad (3.49)$$

The general equation for  $\mathcal{I}_{n-1}(\beta)$  takes then the recursive form

$$\mathcal{I}_{n-1}(\beta) = -\frac{1}{a_m} \mathcal{I}_{n-2}(\beta) + \frac{1}{a_i} \mathcal{I}_{n-2}(v(\beta)) \quad \beta \in Q_{i+1} \quad (3.50)$$

$$i = 0, \dots, m$$

where  $a_0 = a_m$  and, from eq. (3.40),  $\mathcal{I}_0(\beta) = \frac{1}{2}(\beta^2 - 1)$ . It follows that eq. (3.43) enables one to compute analytically the correlation function of any map  $v$ . This equation calls for some comments. Indeed, substituting eq. (3.50) into eq. (3.43) one sees that due to the term in  $\mathcal{I}_{n-1}(\beta)$  the correlation function  $C_v(n)$  is a function of the 0 to  $(n-1)$ -th iterates of  $\beta$ . If the map  $v$  is Markov the iterates of  $\beta$  are finite in number and the knowledge of this limited set, say 0 to  $k$ , is sufficient to compute exactly the correlation function for any  $n$ . But, if  $v$  is not Markov, which is typically the case, to obtain the exact correlation function from 0 to  $n$  we need to know the full set of  $(n-1)$  first iterates of  $\beta$ . Alternatively, one can truncate this set and define an approximate Markov partition which then leads to a rapidly convergent approximation [Ma92]. However we emphasize that our result here is exact. As demonstrated by the following example, non-Markov maps typically display richer correlational properties.

### Example

Let us consider the map

$$\phi(x) = \begin{cases} -2x - 1 & -1 < x \leq 0 \\ 2x - 1 & 0 < x \leq 1. \end{cases} \quad (3.51)$$

Transforming it as described above yields the new map

$$v(x) = \begin{cases} 2(x - \delta) + 3 & -1 < x \leq \delta - 1 \\ -2(x - \delta) - 1 & \delta - 1 < x \leq \delta \\ 2(x - \delta) - 1 & \delta < x \leq 1 \end{cases} \quad 0 \leq \delta \leq 1. \quad (3.52)$$

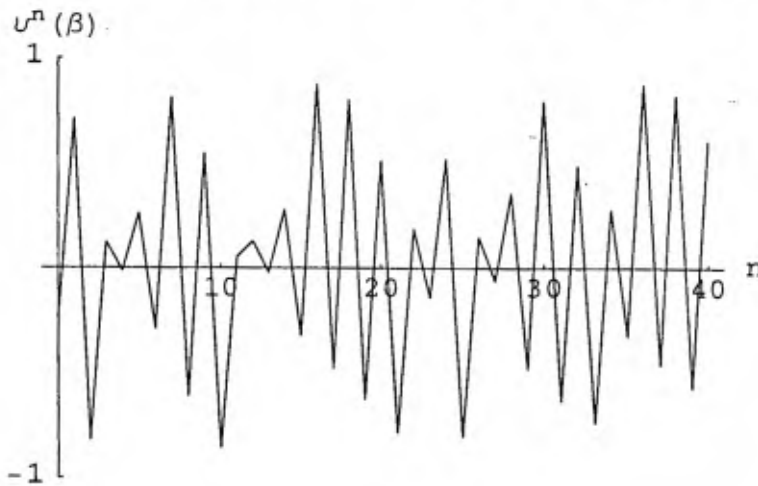
As the branch reinjected from  $-1$  has a positive slope,  $\beta = v_1(-1)$  may belong to any of the cells  $Q_i$ ,  $i = 1, 2, 3$ , depending on  $\delta$ . We choose  $\delta = \frac{\sqrt{5}-1}{2}$  so that  $\beta \in Q_2$ . With a few lines of symbolic computing one can obtain its exact iterates and check that they do not fall on each other up to any given time. The first few are displayed in fig. 3.2 and write explicitly

$$\begin{aligned} \beta &= 2 - \sqrt{5} && \in Q_2 \\ v(\beta) &= 3\sqrt{5} - 6 && \in Q_3 \\ v^2(\beta) &= 5\sqrt{5} - 12 && \in Q_1 \\ v^3(\beta) &= 9\sqrt{5} - 20 && \in Q_2 \\ v^4(\beta) &= 38 - 17\sqrt{5} && \in Q_2 \\ v^5(\beta) &= 35\sqrt{5} - 78 && \in Q_2 \\ v^6(\beta) &= 154 - 69\sqrt{5} && \in Q_2 \\ v^7(\beta) &= 139\sqrt{5} - 310 && \in Q_3 \\ v^8(\beta) &= 277\sqrt{5} - 620 && \in Q_1 \\ v^9(\beta) &= 553\sqrt{5} - 1236 && \in Q_2 \\ v^{10}(\beta) &= 2470 - 1105\sqrt{5} && \in Q_1. \end{aligned} \quad (3.53)$$

The correlation function of this non-Markov map is given by eq. (3.43) where from eq. (3.13)  $C_\phi(1)$  vanishes

$$C_v(n) = \frac{3}{2} \mathcal{I}_{n-1}(\beta). \quad (3.54)$$

Figure 3.2: Exact iterates of  $\beta$  by the map  $\nu$  of eq. (3.52) for  $\delta = \frac{\sqrt{5}-1}{2}$ .

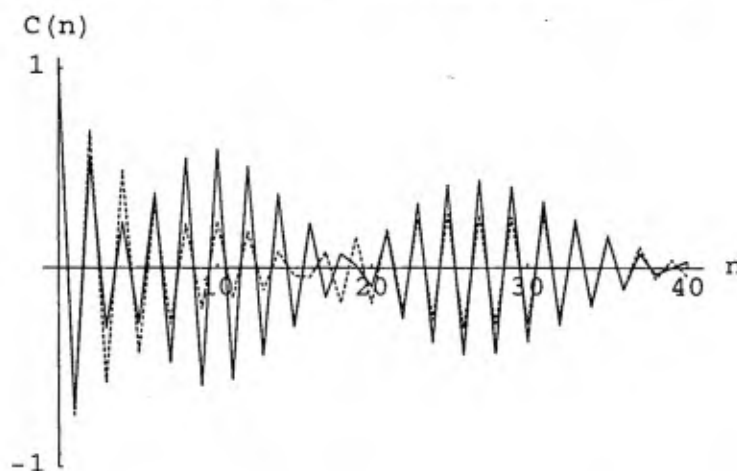


The quantities  $\mathcal{I}_{n-1}(\beta)$  are deduced from the recursion of eq. (3.50). The first few are

$$\begin{aligned}
 \mathcal{I}_0(\beta) &= 4 - 2\sqrt{5} \\
 \mathcal{I}_1(\beta) &= 10\sqrt{5} - 22 \\
 \mathcal{I}_2(\beta) &= \frac{11}{2}\sqrt{5} - \frac{25}{2} \\
 \mathcal{I}_3(\beta) &= 7\sqrt{5} - \frac{31}{2} \\
 \mathcal{I}_4(\beta) &= \frac{603}{4} - \frac{135}{2}\sqrt{5} \\
 \mathcal{I}_5(\beta) &= \frac{1813}{8}\sqrt{5} - \frac{1013}{2} \\
 \mathcal{I}_6(\beta) &= \frac{44159}{32} - \frac{19753}{32}\sqrt{5} \\
 \mathcal{I}_7(\beta) &= \frac{50645}{32}\sqrt{5} - \frac{56617}{16} \\
 \mathcal{I}_8(\beta) &= \frac{757031}{128} - \frac{338577}{128}\sqrt{5} \\
 \mathcal{I}_9(\beta) &= \frac{505043}{128}\sqrt{5} - \frac{282315}{32} \\
 \mathcal{I}_{10}(\beta) &= \frac{2817703}{128} - \frac{2520273}{256}\sqrt{5}.
 \end{aligned} \tag{3.55}$$

The theoretical correlation function is shown in fig. 3.3. It consists essentially of pseudo-period 2 oscillations modulated by a slowly decaying oscillating envelope. The numerical correlation function computed from the trajectory of eq. (3.52) is also displayed in fig. 3.3. Notice the poor agreement which is due to the perturbation of

Figure 3.3: Comparison between the analytical correlation function of the map  $v$  given by eq. (3.52) for  $\delta = \frac{\sqrt{5}-1}{2}$  (solid line) and the numerical data obtained by computing this function from the trajectory (dashed line).



the original system required to prevent the numerical trajectory from being trapped because of the slope 2. As a result the recurrences of the numerical correlation function are diminished. The main features of the theoretical correlation function are nevertheless observed numerically.

### 3.4 Analytic construction of maps with prescribed invariant measure

We begin by recalling the notion of topological equivalence of maps [ShMaRo84]. The maps  $\psi : Y \rightarrow Y$  and  $\varphi : Z \rightarrow Z$  are topologically equivalent if there is a homeomorphism  $h : Z \rightarrow Y$  such that

$$h \circ \varphi = \psi \circ h . \quad (3.56)$$

In other words, the iterates of the 1-d dynamical systems

$$\begin{aligned} y_n &= \psi(y_{n-1}) & y_n &\in Y \\ z_n &= \varphi(z_{n-1}) & z_n &\in Z \end{aligned} \quad (3.57)$$

are related for all  $n$  through

$$y_n = h(z_n) . \quad (3.58)$$

We assume that map  $\varphi$  possesses a uniform probability measure on a single interval  $Z = [0, 1]$ , i.e.  $\mu_\varphi(A) = \int_A dz \quad \forall A \subset Z$ , entailing that the iterates  $z_n = \varphi^n(z_0)$  are uniformly distributed on  $Z$ . It follows that the variable  $F^{-1}(z_n)$  has a cumulative probability distribution function given by  $F$ . Therefore, taking the function  $F^{-1}$  as the homeomorphism  $h$ , the composition

$$F^{-1} \circ \varphi \circ F = \psi \quad (3.59)$$

produces a map  $\psi$  with probability measure  $\mu_\psi(B) = \int_B dF(y) \quad \forall B \subset Y$ . Alternatively, the iterates  $y_n = \psi^n(y_0)$  are characterized by the probability distribution function  $F(y)$ . To construct a map  $\psi$  with a prescribed probability measure  $\mu_\psi$  it suffices therefore to introduce in the functional composition eq. (3.59) any map  $\varphi$  with uniform density on  $Z$ . It is convenient to choose this map  $\varphi$  in the class  $K(\phi, S)$  introduced in Sec. 3.3 because of the relatively simple structure of these maps and the possibility to control their statistical properties.

Obviously, the map  $\varphi$  conjugate to the map  $\psi$  with known probability measure  $\mu_\psi$  is not necessarily piecewise linear. For example, the map  $\varphi$  conjugate to the cusp map  $\psi$

$$\psi(y) = 1 - 2\sqrt{|y|} \quad -1 < y < 1 \quad (3.60)$$

is piecewise smooth. The invariant measure  $\mu_\psi$  of the cusp map is linear:  $\mu_\psi(dy) = \frac{1}{2}(1-y)dy$ . The cumulative distribution function is therefore given by

$$F(y) = \int_{-1}^y \mu_\psi(dy) = \frac{1}{4}(1+y)(3-y) \quad (3.61)$$

and its inverse by

$$F^{-1}(z) = 1 - 2\sqrt{1-z} \quad 0 < z < 1. \quad (3.62)$$

Using the functional composition eq. (3.59) to find the map with uniform probabilistic measure  $\mu_\psi$  we obtain the piecewise smooth map  $\varphi$

$$\varphi(z) = \begin{cases} 2(1 - \sqrt{1-z}) & 0 < z < \frac{3}{4} \\ 2\sqrt{1-z} & \frac{3}{4} < z < 1. \end{cases} \quad (3.63)$$

Generally, the synthesized map  $\psi$  is also piecewise smooth. Let us compile some of its characteristic properties

- The Lebesgue measure  $\mu_\psi$  is invariant under  $\psi$

$$\mu_\psi(B) = \mu_\psi(\psi^{-1}(B)) \quad \forall B \subset Y. \quad (3.64)$$

- The map  $\psi$  is ergodic with respect to  $\mu_\psi$

$$\forall g \in \mathcal{L}_1(Y, \mu_\psi) \quad \lim_{N \rightarrow \infty} \frac{1}{N} \sum_{i=1}^N g(\psi^{(i)}(y_0)) = \int_Y \mu_\psi(dy) g(y) \quad (3.65)$$

The ergodicity of  $\psi$  with respect to  $\mu_\psi$  results from the ergodicity of  $\varphi$  with respect to  $\mu_\varphi$ . The map  $\varphi$  satisfies all conditions of a lemma by Kosyakin and Sandler [KoSa72] about ergodicity with respect to the Lebesgue measure of piecewise smooth transformations of an interval to itself, namely

1.  $\varphi$  is regionally transitive as for any nonempty sets  $Z_i$  and  $Z_j \in Z$

$$\varphi(Z_i) \cap Z_j \neq \emptyset.$$

2.  $\varphi(z)$  is twice smooth differentiable on intervals  $Z_i = (\alpha_{i-1}, \alpha_i)$  and there are one-sided first derivatives at points  $\alpha_i$ .
3. There exists constants  $K, d$  and  $c$  such that

$$K \geq \left| \frac{d\varphi}{dz}(z) \right| = |d_i| \geq d > 1, \quad c \geq \left| \frac{d^2\varphi}{dz^2}(z) \right| = 0 \quad \forall z \in Z_i, i = 1, \dots, m.$$

4.  $0 \leq \varphi(z) \leq 1 \quad \forall z \in Z$

Therefore  $\forall f \in \mathcal{L}_1(Z, \mu_\varphi)$  the equality

$$\lim_{N \rightarrow \infty} \frac{1}{N} \sum_{i=1}^N f(\varphi^i(z_0)) = \int_Z \mu_\varphi(dz) f(z) \quad (3.66)$$

holds almost everywhere. As  $F(y)$  is a smooth distribution function, according to (3.59),  $\varphi$  is conjugate with  $\psi$  by smooth one-to-one invertible homeomorphism  $F^{-1} : Z \rightarrow Y$ . It is clear that  $F^{-1} \in \mathcal{L}_1(Z, \mu_\varphi)$ . If  $g \in \mathcal{L}_1(Y, \mu_\psi)$  then  $g(F^{-1}(z)) \in \mathcal{L}_1(Z, \mu_\varphi)$ . Let us take this function as function  $f$  of (3.66). Substituting into (3.66) and taking into account  $F^{-1}(\varphi^i(z)) = \psi^i(y)$  we have

$$\lim_{N \rightarrow \infty} \frac{1}{N} \sum_{i=1}^N g(\psi^i(y_0)) = \int_Z \mu_\varphi(dz) g(F^{-1}(z)). \quad (3.67)$$

As  $F^{-1} : Z \rightarrow Y$ , the change of variable  $F^{-1}(z) = y$  yields

$$\lim_{N \rightarrow \infty} \frac{1}{N} \sum_{i=1}^N g(\psi^i(y_0)) = \int_Y \mu_\psi(dy) g(y) \quad (3.68)$$

which proves the statement.

- The Lyapunov exponents of  $\psi$  and  $\varphi$  are equal

$$\lambda_\psi = \lambda_\varphi.$$

To show this we first calculate the first derivative of  $\psi$  using the chain rule for the derivative of implicit functions

$$\frac{d}{dy} \psi(y) = \frac{\frac{d\varphi}{dF}(F(y)) \cdot \frac{dF}{dy}(y)}{\frac{dF}{dy}(F^{-1}(\psi(y)))}. \quad (3.69)$$

The Lyapunov exponent of  $\psi$  becomes

$$\begin{aligned} \lambda_\psi &\equiv \int_Y dF(y) \ln \left| \frac{d\psi}{dy}(y) \right| \\ &= \int_Y dF(y) \left[ \ln \frac{dF(y)}{dy} - \ln \frac{dF(\psi(y))}{dy} + \ln \left| \frac{d\varphi}{dF}(F(y)) \right| \right]. \end{aligned} \quad (3.70)$$

Because of the previous property, the first two terms in the right handside cancel each other, so that with the change of variable  $F(y) = z$ , we obtain

$$\lambda_\psi = \int_Z dz \ln \left| \frac{d\varphi}{dz}(z) \right| \quad (3.71)$$

which is the Lyapunov exponent of the map  $\varphi$ .

- If a map  $\gamma$  is conjugate to  $\varphi$  then  $\gamma$  and  $\psi$  are topologically equivalent and the previous properties hold.

Let us give some examples of construction of maps with required probability measure, choosing  $\varphi$  to be the tent map

$$\varphi(z) = \begin{cases} 2z & 0 < z < \frac{1}{2} \\ 2(1-z) & \frac{1}{2} < z < 1. \end{cases} \quad (3.72)$$

### Example 1

Let us require that the iterates  $y_n$  are distributed on  $[0, 1]$  according to Simpson's law, i.e.

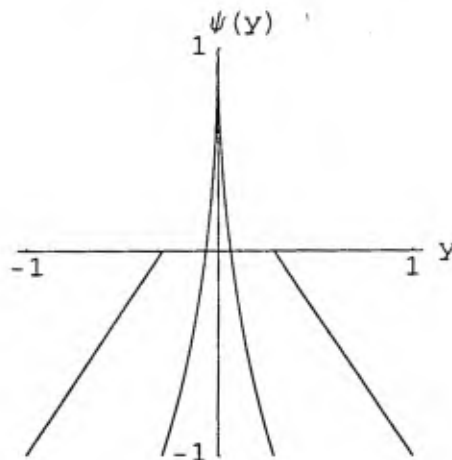
$$F(y) = -\frac{y^2}{2} \operatorname{sgn}(y) + y + \frac{1}{2} \quad 0 \leq y \leq 1. \quad (3.73)$$

Then according to eq. (3.59) we get

$$\psi(y) = \begin{cases} 1 - 2\sqrt{-2(y^2 - 2|y|)} & |y| < a \\ -1 + 2\sqrt{\frac{1}{2}y^2 - |y| + \frac{1}{2}} & a < |y| < 1 \end{cases} \quad (3.74)$$

where  $a = 1 - \frac{\sqrt{2}}{2}$ . This map is shown in fig. 3.4.

Figure 3.4: Map  $\psi$  of eq. (3.74) for which the iterates are distributed according to Simpson's law.



### Example 2

Let the invariant density of the 1-d system eq. (3.57) be

$$\rho(y) = \frac{3}{8}(1 + y^2) \quad -1 < y < 1 \quad (3.75)$$

modelling molecular scattering of photons in the atmosphere [ErMi82]. Then  $F(y)$  will be

$$F(y) = \frac{1}{8}y^3 + \frac{3}{8}y + \frac{1}{2} \quad -1 < y < 1. \quad (3.76)$$

Let us calculate its inverse by solving the cubic equation  $F(y) - z = 0$

$$F^{-1}(z) = \sqrt[3]{4z - 2 + a} + \sqrt[3]{4z - 2 - a} \quad 0 < z < 1 \quad (3.77)$$

where

$$a = \sqrt{16z^2 - 16z + 5}. \quad (3.78)$$

Taking the composition (3.59) of the obtained functions we have

$$\psi(y) = \sqrt[3]{-|y|y^2 - 3|y| + 2 + b} + \sqrt[3]{-|y|y^2 - 3|y| + 2 - b} \quad (3.79)$$

where

$$b = \sqrt{5 + y(1+y)(y^4 - y^3 + 7y^2 - 3y + 12)}. \quad (3.80)$$

### Example 3

Let

$$\rho(y) = \frac{1}{\pi} \frac{1}{\sqrt{y(1-y)}}. \quad (3.81)$$

Using eq. (3.59) we obtain, as expected, the well-known logistic map

$$\psi(y) = 4y(1-y) \quad 0 < y < 1. \quad (3.82)$$

## 3.5 Analytic construction of maps with prescribed invariant measure and correlation function

As we have seen in Sec. 3.4, the construction of a map  $\psi$ , having a given probability measure, requires the use of an arbitrary map  $\varphi$  with uniform invariant density. We have already emphasized the reasons to take the latter in the class  $K(\phi, S)$ . Let us write the general expression of  $\varphi$  as

$$\varphi(x) = \varphi_i(x) = \alpha_i x + \beta_i \quad x \in \Gamma_i = [\gamma_{i-1}, \gamma_i] \quad i = 1, \dots, m \quad (3.83)$$

where  $\{\Gamma_i\}_{i=1}^m$  is a partition of the closed interval  $[0, 1]$ . As  $\varphi$  is arbitrary, we can choose it such as to provide other desired probabilistic properties, for instance, the time autocorrelation function.

The ergodicity of  $\psi$  implies that its correlation function can be written as

$$C_\psi(n) = \frac{1}{\sigma^2} \left[ \int_Y \mu_\psi(dy) y \psi^n(y) - \bar{y}^2 \right] \quad (3.84)$$

where  $\bar{y}$  and  $\sigma^2$  are respectively the mean value and the variance of  $y$ . In order to solve the problem of synthesis of a map  $\psi$  with the required invariant measure  $\mu_\psi(dy)$  and correlation function  $C_\psi(n)$  it is necessary to find a map  $\varphi$  as a solution of the integral equation eq. (3.84) in which  $\psi$  has been substituted from eq. (3.59). Setting  $F(y) = z$  one obtains

$$C_\psi(n) = \frac{1}{\sigma^2} \left[ \int_0^1 dz F^{-1}(z) F^{-1}(\varphi^n(z)) - \bar{y}^2 \right]. \quad (3.85)$$

In its general form, this equation is analytically unsolvable with respect to  $\varphi$ . Let us consider this problem at the level of a piecewise linear approximation of  $F^{-1}(z)$

$$\hat{F}^{-1}(z) = \hat{F}_i^{-1}(z) = h_i z + g_i \quad z \in \Gamma_i \quad i = 1, \dots, m, \quad (3.86)$$

where

$$\begin{aligned} h_i &= \frac{F^{-1}(\gamma_i) - F^{-1}(\gamma_{i-1})}{\gamma_i - \gamma_{i-1}} \\ g_i &= -\gamma_{i-1} h_i + F^{-1}(\gamma_i). \end{aligned} \quad (3.87)$$

This approximation is given on the same partition of  $[0, 1]$  as for  $\varphi$ . Therefore, let us choose the partition  $\{\Gamma_i\}_{i=1}^m$  so that

$$\text{dist}(F^{-1}, \hat{F}^{-1}) = \left( \int_0^1 dz |F^{-1}(z) - \hat{F}^{-1}(z)|^p \right)^{1/p} < \varepsilon. \quad (3.88)$$

Substituting eq. (3.86) into eq. (3.85) and denoting by  $\hat{\psi}$  the composition  $\hat{F}^{-1} \circ \varphi \circ \hat{F}$  we have

$$C_{\hat{\psi}}(n) = \frac{1}{\sigma^2} \left[ \sum_{i=1}^m \int_{\gamma_{i-1}}^{\gamma_i} dz \hat{F}_i^{-1}(z) \hat{F}_i^{-1}(\varphi^{n-1}(\varphi_i(z))) - \bar{y}^2 \right] \quad (3.89)$$

or through the change  $\varphi(z) = v$

$$C_{\hat{\psi}}(n) = \frac{1}{\sigma^2} \left[ \sum_{i=1}^m \int_{\varphi_i(\gamma_{i-1})}^{\varphi_i(\gamma_i)} d\varphi_i^{-1}(v) \hat{F}_i^{-1}(\varphi_i^{-1}(v)) \hat{F}_i^{-1}(\varphi^{n-1}(v)) - \bar{y}^2 \right]. \quad (3.90)$$

As  $\varphi_i^{-1}(v) = \frac{v-\beta_i}{\alpha_i}$ , eq. (3.90) becomes

$$C_{\hat{\psi}}(n) = \frac{1}{\sigma^2} \left[ \sum_{i=1}^m \frac{1}{|\alpha_i| \alpha_i} \left\{ h_i \int_0^1 dv v \hat{F}^{-1}(\varphi^{n-1}(v)) + (\alpha_i g_i - \beta_i h_i) \int_0^1 dv \hat{F}^{-1}(\varphi^{n-1}(v)) \right\} - \bar{y}^2 \right]. \quad (3.91)$$

We introduce the following notation for the quantity in the first term of eq. (3.91)

$$\mathcal{J}_{n-1} \equiv \int_0^1 dv v \hat{F}^{-1}(\varphi^{n-1}(v)). \quad (3.92)$$

Through the change of variable  $\varphi(v) = z$ ,  $\mathcal{J}_{n-1}$  becomes

$$\mathcal{J}_{n-1} = \sum_{j=1}^m \frac{1}{|\alpha_j| \alpha_j} \left[ \int_0^1 dz z \hat{F}^{-1}(\varphi^{n-2}(z)) - \beta_j \int_0^1 dz \hat{F}^{-1}(\varphi^{n-2}(z)) \right]. \quad (3.93)$$

Let  $\varphi$  be a map  $\phi$  from  $K(\phi)$  rescaled to  $[0, 1]$ . From Sec. 3.2 we know that  $\sum_{j=1}^m \frac{1}{|\alpha_j| \alpha_j} = C_\varphi(1)$ . It follows that

$$\mathcal{J}_{n-1} = C_\varphi(1) \mathcal{J}_{n-2} - \sum_{j=1}^m \frac{\beta_j}{|\alpha_j| \alpha_j} \bar{y}. \quad (3.94)$$

The second term of the right hand side of eq. (3.91) can be simplified using

$$\hat{F}^{-1} \circ \varphi^{n-1} = \hat{\psi} \circ \hat{F}^{-1} \circ \varphi^{n-2} = \dots = \hat{\psi}^{n-1} \circ \hat{F}^{-1}, \quad (3.95)$$

so that setting  $\hat{F}^{-1}(v) = y$  we have

$$\int_0^1 dv \hat{F}^{-1}(\varphi^{n-1}(v)) = \int_Y d\hat{F}^{-1}(y) \hat{\psi}^{n-1}(y) = \bar{y}. \quad (3.96)$$

For the sake of simplicity, let us assume  $\bar{y} = 0$ . Taking into account eqs. (3.94), (3.96), eq. (3.91) becomes

$$C_{\hat{\psi}}(n) = [C_\varphi(1)]^n. \quad (3.97)$$

Thus, if a piecewise linear map  $\varphi$  is given on a partition of  $[0, 1]$  such that

$$\text{dist}(F^{-1}, \hat{F}^{-1}) < \varepsilon,$$

the iterates of  $\psi$  are characterized by the correlation function of  $\varphi$ . Therefore, the problem of designing a map  $\psi$  with given invariant measure and correlation function

amounts in a first step to design a piecewise linear map  $\varphi$  with the required  $C_\varphi(1)$  and such that  $\text{dist}(F^{-1}, \hat{F}^{-1}) < \varepsilon$  and in a second step to use the homeomorphism  $F^{-1}$  to obtain by conjugacy the map  $\psi$  with the required invariant measure and correlation function.

### Example

Let us design a map  $\psi : [-\frac{2}{3}, \frac{1}{3}] \rightarrow [-\frac{2}{3}, \frac{1}{3}]$  such that its invariant measure

$$\mu_\psi(dy) = 2 \left( y + \frac{2}{3} \right) dy \quad (3.98)$$

and its correlation function

$$C_\psi(n) = \left( -\frac{1}{r} \right)^n \quad (3.99)$$

where  $r$  is the golden mean. The first step is to design a map  $\varphi : [0, 1] \rightarrow [0, 1]$  with uniform invariant measure and the same correlation function as  $\psi$ , at least in the sense of eq. (3.88). Let it be a map from  $K(\phi)$  rescaled to  $[0, 1]$ . We choose  $m = 4$  and without loss of generality  $\alpha_i < 0 \quad \forall i$ . Then according to eq. (3.13) we have

$$C_\varphi(1) = - \sum_{i=1}^4 \frac{1}{\alpha_i^2} = - \sum_{i=1}^4 (\gamma_i - \gamma_{i-1})^2 \quad (3.100)$$

where  $\gamma_0 = 0$ ,  $\gamma_4 = 1$  and  $\gamma_1, \gamma_2, \gamma_3$  are to be determined. It is clear that the solution of this problem is not unique. Let us use an algorithm yielding straightforwardly a particular solution. Considering this equation as a quadratic equation for  $\gamma_1$  we have

$$\gamma_1 = \frac{\gamma_2}{2} \pm \frac{1}{2} \sqrt{-3\gamma_2^2 - 4\gamma_3^2 + 4\gamma_2\gamma_3 + 4\gamma_3 - 2C_\varphi(1) - 2}. \quad (3.101)$$

The positivity of the radical implies the following limitations for  $\gamma_2$

$$\left| \gamma_2 - \frac{2}{3}\gamma_3 \right| \leq \frac{1}{3} \sqrt{2(-4\gamma_3^2 + 6\gamma_3 - 3C_\varphi(1) - 3)}, \quad (3.102)$$

which in turn imply limitations for  $\gamma_3$

$$\left| \gamma_3 - \frac{3}{4} \right| \leq \frac{1}{2} \sqrt{-3 \left( C_\varphi(1) + \frac{1}{4} \right)}. \quad (3.103)$$

Substituting  $C_\varphi(1)$  by its value - the golden mean - and taking the equality sign in eq. (3.103) we determine  $\gamma_3$ . Having taken the equality sign in eq. (3.103) implies

that the right hand side of eq. (3.102) vanishes. Taking also the equality sign in this equation we obtain  $\gamma_2 = \frac{2}{3}\gamma_3$  together with  $\gamma_1 = \frac{1}{2}\gamma_2$ . The map  $\varphi$  with  $C_\varphi(1) = r$  is then

$$\varphi(x) = \frac{x - \gamma_i}{\gamma_{i-1} - \gamma_i} \quad \gamma_{i-1} < x < \gamma_i \quad i = 1, \dots, 4 \quad (3.104)$$

where  $\gamma_0 = 0$ ,  $\gamma_1 = \frac{1}{4} - \frac{1}{2}\sqrt{-\frac{1}{3}(\frac{1}{4} - \frac{1}{r})}$ ,  $\gamma_2 = 2\gamma_1$ ,  $\gamma_3 = 3\gamma_1$ ,  $\gamma_4 = 1$ . The second step to obtain the map  $\psi$  with the given invariant measure and correlation function is to perform the functional composition  $F^{-1} \circ \varphi \circ F$  where

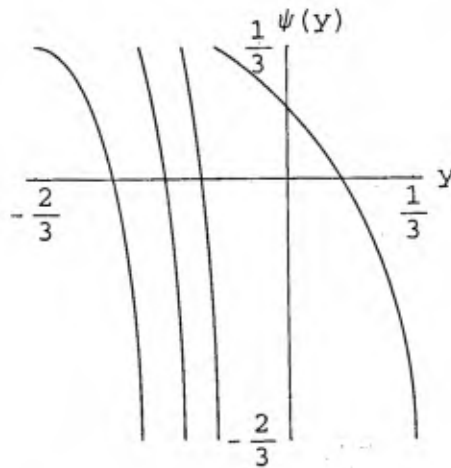
$$\begin{aligned} F(y) &= \int_{-\frac{2}{3}}^y \mu_\psi(dy) = \left(y + \frac{2}{3}\right)^2 & 0 < y < 1 \\ F^{-1}(z) &= \sqrt{z} - \frac{2}{3} & 0 < z < 1. \end{aligned} \quad (3.105)$$

Therefore, we obtain

$$\psi(x) = \sqrt{\frac{(y + \frac{2}{3})^2 - \gamma_i}{\gamma_{i-1} - \gamma_i}} - \frac{2}{3} \quad \sqrt{\gamma_{i-1}} - \frac{2}{3} < x < \sqrt{\gamma_i} - \frac{2}{3} \quad i = 1, \dots, 4. \quad (3.106)$$

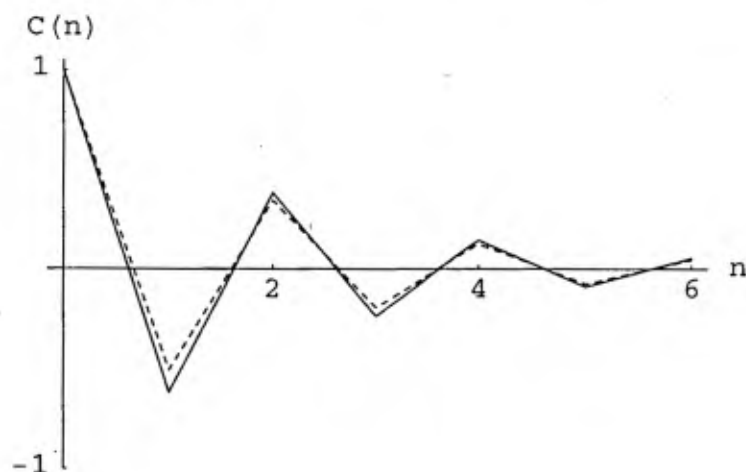
This map is shown in fig. 3.5. The prescribed and numerical correlation functions

Figure 3.5: Map  $\psi$  of eq. (3.106) with the prescribed invariant measure and correlation function.



are compared in fig. 3.6. Note that the agreement can be improved by increasing the number of branches  $m$ .

Figure 3.6: Comparison between the prescribed correlation function (dashed line) and the numerical data obtained by computing the correlation of the map  $\psi$  of fig. 3.5 from the trajectory (solid line).



### 3.6 Conclusions

In this chapter, the inverse problem of designing dynamical systems with prescribed statistical properties has been addressed. We have developed methods enabling one to design piecewise linear full maps with exponential, periodically modulated exponential or delta decay of correlations. More complicated behaviours were also obtained by introducing a transformation of piecewise linear full maps. These complex behaviours include for instance the coexistence of several competing decay modes or the presence of a slowly decaying oscillating envelope. The first possibility arises only for incomplete maps, in which at least one of the elements of the partition of the invariant interval is not mapped by the transformation on the whole interval, whereas the second one may occur when the map is non-Markov. Tackling the inverse problem for these maps is more involved because of their more complicated structure and will be the subject of further investigations.

We have also considered the design of maps with any prescribed invariant measure independently of, or together with a prescribed correlation function. Though the first task is achieved exactly, the second requires an approximation since the map obtained by conjugacy is generally smooth. As the conjugate map with uniform invariant measure is arbitrary, by a judicious choice, this approximation can

be improved up to any accuracy.

In addition to giving means to deal with applications, the results of this chapter enable one to identify in a given dynamical system the features that are responsible for a given correlation function or equivalently for a given law governing the loss of memory of the chaotic signal.

Recently, a great deal of interest has been devoted to the control of chaos through slight perturbations of the evolution law [OtGrYo90]. Our approach suggests a new way to look at this problem, in which emphasis is placed on the probabilistic properties of the dynamics rather than the detailed structure of the trajectories. Since the probabilistic viewpoint is natural in systems undergoing chaotic dynamics, it may be reasonably expected that this approach is worth exploring in the future.

# Chapter 4

## Statistical properties of coupled map lattices: exact results

### 4.1 Introduction

Spatially extended systems are described by partial differential equations. Owing to their difficulty, till recently the main rigorous results concerned the determination of simple solutions, their stability analysis or the estimation of attractors dimensions [Te88, Co96]. This has motivated the introduction at the beginning of the eighties of a simplified model of spatially extended systems known as coupled map lattices (CML's) [Ka84, WaKa84a, WaKa84b, De84].

CML's are dynamical systems with discrete time, discrete space and continuous or uncountable local phase space. The state of the system at time  $n$ ,  $n = 0, 1, \dots$ , can thus be represented as

$$\mathbf{x}^n = (x_s^n)_{s \in L} \quad (4.1)$$

where  $s$  is a site of a lattice  $L$  and  $x_s^n \in I_s$ , the local phase space. In the sequel we shall consider only 1-d lattice, finite with periodic boundary conditions or infinite. The global phase space is the direct product of the local phase spaces, which we denote  $\otimes_{s \in L} I_s$ . The state evolves according to

$$\mathbf{x}^{n+1} = \Phi \mathbf{x}^n \quad (4.2)$$

where  $\Phi$  is usually taken as the composition of two transformations

$$\Phi = A \circ F . \quad (4.3)$$

The transformation  $F$  evolves each site of the lattice independently,

$$(F\mathbf{x})_s = f_s(x_s) \quad (4.4)$$

where

$$f_s : I_s \rightarrow I_s ; \quad (4.5)$$

and  $A$  is a spatial interaction between the sites

$$(A\mathbf{x})_s = a_s(\mathbf{x}) \quad (4.6)$$

where

$$a_s : \otimes_{i \in L} I_i \rightarrow I_s . \quad (4.7)$$

The functions  $f_s$  and  $a_s$  are chosen depending on the problem one is interested in. For instance two phases in competition via a diffusive process can be modeled by bistable maps [Fe96, FeRa97] whereas spatio-temporal chaos is investigated with chaotic maps [Ka93]. In both cases one considers a spatial interaction which mimics diffusion

$$a_s(\mathbf{x}) = x_s + \frac{\varepsilon}{2}(x_{s-1} - 2x_s + x_{s+1}) \quad s \in L \quad (4.8)$$

where  $0 \leq \varepsilon \leq 1$  is the coupling parameter. This leads to the most popular and well-studied example of CML

$$(\Phi\mathbf{x}^n)_s = x_s^{n+1} = (1 - \varepsilon) f(x_s^n) + \frac{\varepsilon}{2} [f(x_{s-1}^n) + f(x_{s+1}^n)] \quad s \in L \quad (4.9)$$

where the maps are identical at each site. This CML is generally called diffusive as it is reminiscent of the Laplacian of a diffusion equation.

CML's are very convenient to implement numerically. As the control parameters are varied, they exhibit a variety of complex behaviors in time and space culminating in spatio-temporal chaos [Ka89a]. At the theoretical level, one of the goals is to show that the CML's generated by the weak spatial interactions of local dynamical systems with strongly chaotic dynamics such as eq. (4.9) have the property of space-time mixing

$$|\int g \circ \Phi^n h d\mu - \int g d\mu \int h d\mu| \leq \text{Cst} \|g\| \|h\| e^{-\gamma(n+d(B,D))} \quad \gamma > 0, \quad (4.10)$$

where, skipping the details,  $g$  and  $h$  are functions supported on the subset  $B$  and  $D$  of the lattice,  $\mu$  is the invariant measure and  $d(B, D)$  is the distance between  $B$  and  $D$ . This property, introduced by Bunimovich and Sinai in [BuSi88], means

that there is a decay of the correlations in time and space and is precisely what is understood by the terms spatio-temporal chaos. In eq. (4.10) this decay is exponential. One is also interested in constructing nontrivial solutions for these systems. Another direction of research is to explore the possibility of setting up a reduced type of description for these simple models of spatially extended systems. The first rigorous results were obtained by Bunimovich and Sinai [BuSi88] who have proven space-time mixing for expanding maps of the interval with a special type of coupling which is state-dependent. This special coupling is introduced to preserve the existence of Markov partitions that are otherwise destroyed by the spatial interaction. A clear presentation and some clarifications can be found in [Gi94]. Bricmont and Kupiainen [BrKu95, BrKu96, BrKu97] have proven the space-time mixing property for a more general class of spatial interactions in the case of circle maps if the coupling parameter  $\varepsilon$  is sufficiently small. The existence of so-called Sinai-Ruelle-Bowen measures for weak interactions of general type on a 1-d infinite lattice was proven by Keller and Künzle again for small  $\varepsilon$  [KeKu92, Ku93]. Some results on the existence of Sinai-Ruelle-Bowen measures for coupled maps on lattices of arbitrary finite dimension were obtained by Volevich [Vo93, Vo94]. Blank [Bl93, Bl97] has constructed examples of pathological behavior for coupled non-smooth maps with arbitrarily weak coupling. Losson and Mackey [LoMa94a, LoMa94b, Lo94, LoMiMa95] have highlighted the presence of coupling induced statistical cycling. Sensitivity to initial conditions in systems of large spatial extension giving rise to spatio-temporal chaos has been shown to obey a subexponential law by Nicolis, Nicolis and Wang [NiNiWa92]. Op de Beeck, Nicolis and Nicolis [Op94, NiOpNi97] have studied truncation schemes and proposed new ways to probe the dynamics of spatially extended systems using coarse-grained observables. Just [Ju98] has an interesting approach, although it does not apply to diffusive coupling, in which he fixes a Markov partition and then require the map to be linear on this partition.

The objective of this chapter is to study CML's in which themaps are coupled to their nearest neighbours with a finite coupling constant  $\varepsilon$ . In Sec. 4.2 we consider a system of two diffusively coupled piecewise linear maps. We show that under a simple condition a 2-d Markov partitions can be constructed on the basis of 1-d Markov partitions for two particular mappings defined below. A class of such partitions is obtained for dyadic coupled maps. The case of a Bernoulli and an anti-Bernoulli map coupled with  $\varepsilon = \frac{1}{4}$  is then studied in detail. In particular the 2-d probability density and its 1-d projection are obtained explicitly using a generalized master

equation for the coupled system. In Sec. 4.3 we propose a CML with constant nearest-neighbour coupling. For this system the invariant 1-d reduced probability density is computed for all  $\varepsilon$  when the maps belong the class of piecewise linear full maps. Conclusions are drawn in Sec. 4.4.

## 4.2 Two diffusively coupled piecewise linear maps

In this section we consider two maps

$$f : [0, 1] \rightarrow [0, 1], \quad g : [0, 1] \rightarrow [0, 1] \quad (4.11)$$

which are piecewise linear

$$\begin{aligned} f|_{C_i} &= f_i : x \mapsto \Lambda_i x + \Delta_i \\ g|_{\Gamma_i} &= g_i : y \mapsto \lambda_i y + \delta_i \end{aligned} \quad (4.12)$$

and expanding

$$|\Lambda_i| > 1, \quad |\lambda_i| > 1, \quad (4.13)$$

$\{C_i\}_{i=1}^M$  and  $\{\Gamma_i\}_{i=1}^M$  being partitions of  $[0, 1]$ . These maps are diffusively coupled according to eq. (4.9)

$$\begin{cases} x' = (1 - \varepsilon) f(x) + \varepsilon g(y) \\ y' = (1 - \varepsilon) g(y) + \varepsilon f(x) \end{cases} \quad 0 < \varepsilon < \frac{1}{2}. \quad (4.14)$$

The Perron-Frobenius operator  $\mathcal{P}$  of the coupled system is thus given by

$$\begin{aligned} \rho_{n+1}(x, y) &= \mathcal{P} \rho_n(x, y) \\ &= \int_I du \int_I dv \rho_n(u, v) \delta(x - [(1 - \varepsilon) f(u) + \varepsilon g(v)]) \delta(y - [(1 - \varepsilon) g(v) + \varepsilon f(u)]) . \end{aligned} \quad (4.15)$$

Hence one obtains

$$\begin{aligned} \rho_{n+1}(x, y) &= \sum_{\alpha, \beta=1}^M \frac{1}{(1 - 2\varepsilon) |\Lambda_\alpha| |\lambda_\beta|} \\ &\quad \rho_n \left( f_\alpha^{-1} \left( \frac{1 - \varepsilon}{1 - 2\varepsilon} x - \frac{\varepsilon}{1 - 2\varepsilon} y \right), g_\beta^{-1} \left( \frac{1 - \varepsilon}{1 - 2\varepsilon} y - \frac{\varepsilon}{1 - 2\varepsilon} x \right) \right) \chi_{\mathbb{P}(C_\alpha \otimes \Gamma_\beta)}(x, y), \end{aligned} \quad (4.16)$$

where  $\Phi(C_\alpha \otimes \Gamma_\beta)$  denotes the image of the direct product of the cells  $C_\alpha$  and  $\Gamma_\beta$  under the mapping  $\Phi$  of eq. (4.14).

In the next section we derive a generalized master equation for the coupled system  $\Phi$  assuming there exists a 2-d Markov partition. Explicit examples of Markov partitions will be constructed in the subsequent sections.

#### 4.2.1 Generalized master equation for the coupled system

Let  $\{S_i\}_{i=1}^{\mathcal{M}}$  be a partition of the unit square  $[0, 1] \otimes [0, 1]$  which is Markov in the sense that

$$\chi_{\Phi(S_j)} = \sum_{i=1}^{\mathcal{M}} a_{ji} \chi_{S_i} \quad j = 1, \dots, \mathcal{M}. \quad (4.17)$$

Here  $\Phi$  denotes the mapping of eq. (4.14) and the elements  $a_{ji}$  of the topological transition matrix are 1 or 0 depending on whether  $S_i$  belongs or not to  $\Phi(S_j)$ . We assume that on each element  $S_j$  of the partition there is only one branch of  $f$  and one branch of  $g$ , which we denote  $f_{\alpha_j}$  and  $g_{\beta_j}$ , respectively. This amounts to having

$$S_j \subset C_{\alpha_j} \otimes \Gamma_{\beta_j} \quad \forall j. \quad (4.18)$$

Consider now a 2-d piecewise polynomial density

$$\rho_n(x, y) = \sum_{j=1}^{\mathcal{M}} \sum_{k+l=0}^N c_{jkl}^{(n)} x^k y^l \chi_{S_j}(x, y). \quad (4.19)$$

By eq. (4.16), under the action of the Perron-Frobenius operator it becomes

$$\begin{aligned} \rho_{n+1}(x, y) &= \sum_{\alpha, \beta=1}^{\mathcal{M}} \frac{1}{(1-2\varepsilon) |\Lambda_\alpha| |\lambda_\beta|} \sum_{j=1}^{\mathcal{M}} \sum_{k+l=0}^N c_{jkl}^{(n)} \\ &\left[ f_\alpha^{-1} \left( \frac{1-\varepsilon}{1-2\varepsilon} x - \frac{\varepsilon}{1-2\varepsilon} y \right) \right]^k \left[ g_\beta^{-1} \left( \frac{1-\varepsilon}{1-2\varepsilon} y - \frac{\varepsilon}{1-2\varepsilon} x \right) \right]^l \\ &\chi_{S_j} \left( f_\alpha^{-1} \left( \frac{1-\varepsilon}{1-2\varepsilon} x - \frac{\varepsilon}{1-2\varepsilon} y \right), g_\beta^{-1} \left( \frac{1-\varepsilon}{1-2\varepsilon} y - \frac{\varepsilon}{1-2\varepsilon} x \right) \right) \chi_{\Phi(C_\alpha \otimes \Gamma_\beta)}(x, y). \end{aligned} \quad (4.20)$$

From eq. (4.18) the sums over  $\alpha$  and  $\beta$  reduce to the contribution with  $\alpha = \alpha_j$  and  $\beta = \beta_j$ . Notice also that  $\forall j$

$$\chi_{S_j} \left( f_{\alpha_j}^{-1} \left( \frac{1-\varepsilon}{1-2\varepsilon} x - \frac{\varepsilon}{1-2\varepsilon} y \right), g_{\beta_j}^{-1} \left( \frac{1-\varepsilon}{1-2\varepsilon} y - \frac{\varepsilon}{1-2\varepsilon} x \right) \right) \chi_{\Phi(C_{\alpha_j} \otimes \Gamma_{\beta_j})}(x, y) = \chi_{\Phi(S_j)}(x, y). \quad (4.21)$$

Eq. (4.20) becomes then

$$\rho_{n+1}(x, y) = \sum_{i,j=1}^M \sum_{k+l=0}^N \frac{1}{(1-2\varepsilon)^{1+k+l} \Lambda_{\alpha_j}^k |\Lambda_{\alpha_j} \lambda_{\beta_j}^l|} c_{jkl}^{(n)} [(1-\varepsilon)x - \varepsilon y - (1-2\varepsilon)\Delta_{\alpha_j}]^k [(1-\varepsilon)y - \varepsilon x - (1-2\varepsilon)\delta_{\beta_j}]^l a_{ji} \chi_{S_i}(x, y). \quad (4.22)$$

Hence, as in the 1-d case,  $\rho_{n+1}$  is again piecewise polynomial

$$\rho_{n+1}(x, y) = \sum_{i=1}^M \sum_{p+q=0}^N c_{ipq}^{(n+1)} x^p y^q \chi_{S_i}(x, y). \quad (4.23)$$

Arranging the elements  $c_{jkl}^{(n)}$  in a column vector  $\mathbf{c}_n$  rather than a tensor and defining a time-independent transition matrix  $\mathbf{W}$  one obtains the generalized master equation for the 2-d coupled system  $\Phi$

$$\mathbf{c}_{n+1} = \mathbf{W} \mathbf{c}_n. \quad (4.24)$$

The case  $N = 0$  yields

$$\mathbf{c}_n = \begin{pmatrix} c_{100}^{(n)} \\ \vdots \\ c_{M100}^{(n)} \end{pmatrix} \quad (4.25)$$

and

$$\mathbf{W} = \begin{pmatrix} \frac{1}{(1-2\varepsilon) |\Lambda_{\alpha_1} \lambda_{\beta_1}|} a_{11} & \cdots & \frac{1}{(1-2\varepsilon) |\Lambda_{\alpha_2} \lambda_{\beta_2}|} a_{21} \\ \vdots & \ddots & \vdots \\ \frac{1}{(1-2\varepsilon) |\Lambda_{\alpha_1} \lambda_{\beta_1}|} a_{12} & \cdots & \frac{1}{(1-2\varepsilon) |\Lambda_{\alpha_2} \lambda_{\beta_2}|} a_{22} \end{pmatrix}. \quad (4.26)$$

For  $N = 1$ , one has

$$\mathbf{c}_n = \begin{pmatrix} c_{i00}^{(n)} \\ c_{i10}^{(n)} \\ c_{i01}^{(n)} \end{pmatrix} \quad (4.27)$$

and

$$W = \begin{pmatrix} \frac{1}{(1-2\varepsilon) |\Lambda_{\alpha_j} \lambda_{\beta_j}|} a_{ji} & -\frac{\Delta_{\alpha_j}}{(1-2\varepsilon) \Lambda_{\alpha_j} |\Lambda_{\alpha_j} \lambda_{\beta_j}|} a_{ji} & -\frac{\delta_{\beta_j}}{(1-2\varepsilon) \lambda_{\beta_j} |\Lambda_{\alpha_j} \lambda_{\beta_j}|} a_{ji} \\ 0 & \frac{1-\varepsilon}{(1-2\varepsilon)^2 \Lambda_{\alpha_j} |\Lambda_{\alpha_j} \lambda_{\beta_j}|} a_{ji} & -\frac{\varepsilon}{(1-2\varepsilon)^2 \lambda_{\beta_j} |\Lambda_{\alpha_j} \lambda_{\beta_j}|} a_{ji} \\ 0 & -\frac{\varepsilon}{(1-2\varepsilon)^2 \Lambda_{\alpha_j} |\Lambda_{\alpha_j} \lambda_{\beta_j}|} a_{ji} & \frac{1-\varepsilon}{(1-2\varepsilon)^2 \lambda_{\beta_j} |\Lambda_{\alpha_j} \lambda_{\beta_j}|} a_{ji} \end{pmatrix} \quad (4.28)$$

where  $i, j = 1, \dots, M$ .

#### 4.2.2 Two 1-d mappings for the coupled system

We have seen in Chap. 2 that for individual piecewise linear maps of the form of eq. (4.12) the supports of the invariant density are determined by the iterates of the extremities of the support of each branch, i.e. by the iterates of the points  $c_i$ ;  $\gamma_i$  defined by

$$C_i = [c_{i-1}, c_i], \quad \Gamma_i = [\gamma_{i-1}, \gamma_i], \quad (4.29)$$

with  $c_0 = \gamma_0 = 0$  and  $c_M = \gamma_M = 1$ . For a system of coupled piecewise linear maps of the form of eq. (4.14) the supports of the invariant density are also expected, because of monotonicity to be determined by the iterates under  $\Phi$  of the boundaries of the support of the branches of the coupled system. These boundaries are now segments of straight lines whose parametric equations are

$$\begin{cases} x = \theta \\ y = \gamma_i \end{cases} \quad (4.30)$$

for those parallel to  $Ox$  and

$$\begin{cases} x = c_i \\ y = \theta \end{cases} \quad (4.31)$$

for those parallel to  $Oy$ ,  $\theta \in [0, 1]$  being the parameter.

This motivates us to consider explicitly the first iterates by  $\Phi$  of the segment

$$\begin{cases} x = \theta \\ y = q \end{cases} \quad (4.32)$$

where  $q \in [0, 1]$  is fixed and  $\theta$  is running through  $[0, 1]$ . The first iterate of eq. (4.32) is

$$\begin{cases} x' = (1 - \varepsilon) f(\theta) + \varepsilon g(q) \\ y' = (1 - \varepsilon) g(q) + \varepsilon f(\theta) \end{cases} \quad (4.33)$$

Eliminating  $\theta$  yields

$$y' = \frac{\varepsilon}{1 - \varepsilon} x' + \frac{1 - 2\varepsilon}{1 - \varepsilon} g(q) \quad (4.34)$$

Notice that eq. (4.34) holds for any  $f$  and  $g$ , not only piecewise linear maps. This straight line will be partially run through as many times as there are branches in  $f$ , i.e.  $M$  times. Indeed let  $\theta$  go through the support of the  $l$ -th branch,

$$\theta \in C_l = [c_{l-1}, c_l] \quad l = 1, \dots, M \quad (4.35)$$

Hence  $f(\theta)$  goes strictly monotonically from  $f_l(c_{l-1})$  to  $f_l(c_l)$  so that for each  $l$  as  $\theta$  increases the straight line (4.34) is run from

$$x'_{l-} \equiv (1 - \varepsilon) f_l(c_{l-1}) + \varepsilon g(q) \quad (4.36)$$

to

$$x'_{l+} \equiv (1 - \varepsilon) f_l(c_l) + \varepsilon g(q) \quad (4.37)$$

Notice that the straight line is run in the positive  $x$ -direction for  $\Lambda_l > 0$  and in the negative direction for  $\Lambda_l < 0$ . Let us rewrite eq. (4.34) in the form

$$\begin{cases} x' = \theta'_l \\ y' = \frac{\varepsilon}{1 - \varepsilon} \theta'_l + \frac{1 - 2\varepsilon}{1 - \varepsilon} g(q) \end{cases} \quad (4.38)$$

where  $\theta'_l$  belongs to the interval delimited by eqs. (4.36) and (4.37), namely

$$\theta'_l \in \begin{cases} [x'_{l-}, x'_{l+}] & \Lambda_l > 0 \\ [x'_{l+}, x'_{l-}] & \Lambda_l < 0 \end{cases} \quad (4.39)$$

Now the second iterate by  $\Phi$  of eq. (4.32) is

$$\begin{cases} x'' = (1 - \varepsilon) f(\theta'_l) + \varepsilon g \left( \frac{\varepsilon}{1 - \varepsilon} \theta'_l + \frac{1 - 2\varepsilon}{1 - \varepsilon} g(q) \right) \\ y'' = (1 - \varepsilon) g \left( \frac{\varepsilon}{1 - \varepsilon} \theta'_l + \frac{1 - 2\varepsilon}{1 - \varepsilon} g(q) \right) + \varepsilon f(\theta'_l) \end{cases} \quad (4.40)$$

We can have a more explicit form if we let

$$\theta'_i \in C_k \quad (4.41)$$

and

$$\frac{\varepsilon}{1-\varepsilon} \theta'_i + \frac{1-2\varepsilon}{1-\varepsilon} g(q) \in \Gamma_j . \quad (4.42)$$

Then using eq. (4.12), eq. (4.40) becomes

$$\begin{cases} x'' = \left( (1-\varepsilon) \Lambda_k + \frac{\varepsilon^2}{1-\varepsilon} \lambda_j \right) \theta'_i + (1-\varepsilon) \Delta_k + \varepsilon \delta_j + \varepsilon \frac{1-2\varepsilon}{1-\varepsilon} \lambda_j g(q) \\ y'' = \varepsilon (\Lambda_k + \lambda_j) \theta'_i + (1-2\varepsilon) \lambda_j g(q) + (1-\varepsilon) \delta_j + \varepsilon \Delta_k . \end{cases} \quad (4.43)$$

Eliminating  $\theta'_i$  one gets

$$\begin{aligned} y'' = \varepsilon (1-\varepsilon) (\Lambda_k + \lambda_j) & \frac{x''_1 - \varepsilon (1-\varepsilon) \Delta_k - \varepsilon \delta_j - \varepsilon \frac{1-2\varepsilon}{1-\varepsilon} \lambda_j g(q)}{(1-\varepsilon)^2 \Lambda_k + \varepsilon^2 \lambda_j} \\ & + (1-2\varepsilon) \lambda_j g(q) + (1-\varepsilon) \delta_j + \varepsilon \Delta_k . \end{aligned} \quad (4.44)$$

Now one notices that if the maps  $f$  and  $g$  are chosen such that

$$\lambda_j = -\Lambda_k = \lambda \quad \forall j, k \quad (4.45)$$

then eq. (4.44) reduces to

$$y'' = (1-2\varepsilon) \lambda g(q) + (1-\varepsilon) \delta_j + \varepsilon \Delta_k . \quad (4.46)$$

We recall that the indices  $k$  and  $j$  appearing in eq. (4.46) are determined from eqs. (4.41)-(4.42).

The condition (4.45) means that all the branches of  $f$  have the same slope  $\Lambda$  and those of  $g$  the same slope  $\lambda = -\Lambda$ . Under this condition the second iterate of a parallel to  $Ox$

$$y = q \quad q \in [0, 1], \quad (4.47)$$

is itself a parallel to  $Ox$ ,

$$y'' = ( [1-2\varepsilon] \lambda g(q) + [1-\varepsilon] \delta_j + \varepsilon \Delta_k ) |_{[0,1]} . \quad (4.48)$$

Here we have taken the restriction to  $[0, 1]$  which amounts to satisfy eqs. (4.41), (4.42) but has the advantage to be self-defined and thus true for any  $k$  and  $j$ . One can define a mapping

$$G : [0, 1] \rightarrow [0, 1] \quad (4.49)$$

taking the right handside of eq. (4.47) to that of eq. (4.48)

$$G : q \mapsto ( [1 - 2\varepsilon] \lambda g(q) + [1 - \varepsilon] \delta_j + \varepsilon \Delta_k ) |_{[0,1]} . \quad (4.50)$$

Notice that since  $k$  and  $j$  run from 1 to  $M$  and  $g$  itself has  $M$  branches, this mapping has up to  $M^3$  branches, which generally overlap each other, meaning that it is multivalued. The support of a given branch is the intersection of the interval which is mapped by this branch into  $[0, 1]$  with the supports of  $g$ . Remark that for  $\varepsilon \rightarrow 0$ ,  $G(q)$  reduces to  $g(g(q))$ . This mapping is displayed in fig. 4.1 for  $\varepsilon = \frac{1}{8}$  in the case where  $g$  is the Bernoulli map. Roughly speaking it is the superposition of two maps  $g(g(q))$  translated vertically by a distance  $\varepsilon$ .

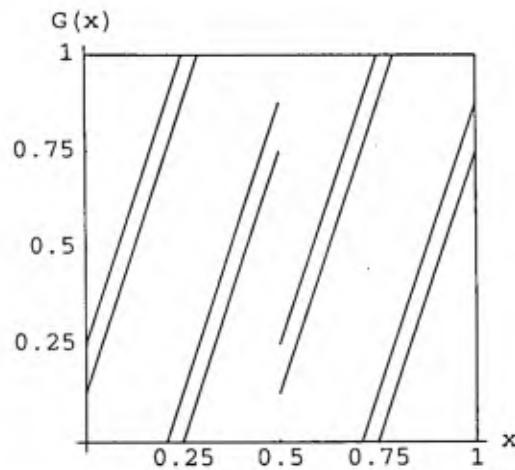


Figure 4.1: Mapping  $G$  of eq. (4.50) for  $\varepsilon = \frac{1}{8}$ ,  $g$  being the Bernoulli map.

Obviously one can reproduce this procedure for the segments of straight line parallel to  $Oy$ . The mapping

$$F : [0, 1] \rightarrow [0, 1] \quad (4.51)$$

taking the abscissa  $p \in [0, 1]$  of a parallel to  $Oy$  to the abscissa of the second iterate of this segment is

$$F : p \mapsto ( -[1 - 2\varepsilon] \lambda f(p) + [1 - \varepsilon] \Delta_j + \varepsilon \delta_k ) |_{[0,1]} . \quad (4.52)$$

Now suppose we can find a set of points which is invariant under the mapping  $G$  and another one, possibly the same, which is invariant under the mapping  $F$ . This corresponds to identifying a Markov partition for the mapping  $G$  or  $F$ . We emphasize that these mappings are not the usual type of mappings one is considering in dynamical systems theory since they are multivalued. Nevertheless it is a well-posed problem to look for a Markov partition. Such a partition then implies that there exists a set of segments parallel to one of the axis which is mapped to itself after two iterations of the coupled system  $\Phi$  of eq. (4.14). After just one iteration of  $\Phi$ , this set yields a new set of segments whose slope is  $\frac{\epsilon}{1-\epsilon}$  (or the inverse in the case of  $F$ ). This new set of segments is itself also invariant under two iterations of (4.14). As a consequence, the union of these two sets is invariant under  $\Phi$ . Since this is true in the direction  $x$  as well as in the direction  $y$ , we have a 2-d Markov partition for the coupled system  $\Phi$  of eq. (4.14). In the next sections we will construct explicitly such 2-d Markov partitions.

### 4.2.3 2-d Markov partitions for coupled dyadic maps

In this section we focus on piecewise linear maps with two branches ( $M = 2$  in eq. (4.12)). Our objective is to identify Markov partitions for the mapping  $G$  defined in eq. (4.50).

To start with, the condition (4.45) which is necessary for the mapping  $G$  to make sense has to be satisfied. Hence

$$\lambda_1 = \lambda_2 = -\Lambda_1 = -\Lambda_2 = \lambda > 0. \quad (4.53)$$

We want to remain with only one parameter,  $\lambda$ , for the maps  $f$  and  $g$ , so we require first that the supports of the branches of both  $f$  and  $g$  are of length  $\frac{1}{2}$  and second that each branch maps one extremity of its support to zero. Using eq. (4.12) one then obtains

$$f(x) = \begin{cases} -\lambda x + \frac{\lambda}{2} & 0 \leq x \leq \frac{1}{2} \\ -\lambda x + \lambda & \frac{1}{2} \leq x \leq 1 \end{cases} \quad (4.54)$$

$$g(x) = \begin{cases} \lambda x & 0 \leq x \leq \frac{1}{2} \\ \lambda x - \frac{\lambda}{2} & \frac{1}{2} \leq x \leq 1. \end{cases}$$

The parameter  $\lambda$  satisfies

$$1 < \lambda \leq 2. \quad (4.55)$$

The lower bound implies that the individual maps are chaotic and the upper one that no trajectory escapes  $[0, 1]$ . Notice that for  $\lambda = 2$ ,  $g$  is the Bernoulli map. The coupled system also displays another parameter, the coupling constant  $\varepsilon$

$$0 < \varepsilon < \frac{1}{2}. \quad (4.56)$$

The mapping  $G$ , eq. (4.50), writes here

$$G(q) = \begin{cases} G_1(q) = \lambda^2(1 - 2\varepsilon)q + \lambda\varepsilon & 0 \leq q < \frac{1 - \frac{\lambda}{2}\varepsilon}{\lambda^2(1 - 2\varepsilon)} \\ G_2(q) = \lambda^2(1 - 2\varepsilon)q + \frac{\lambda}{2}\varepsilon & 0 \leq q < \frac{1 - \lambda\varepsilon}{\lambda^2(1 - 2\varepsilon)} \\ G_3(q) = \lambda^2(1 - 2\varepsilon)q - \frac{\lambda}{2}(1 - 3\varepsilon) & \frac{1}{2\lambda} < q \leq \frac{1}{2} \\ G_4(q) = \lambda^2(1 - 2\varepsilon)q - \frac{\lambda}{2}(1 - 2\varepsilon) & \frac{1 - 3\varepsilon}{2\lambda(1 - 2\varepsilon)} < q \leq \frac{1}{2} \\ G\left(q - \frac{1}{2}\right) & \frac{1}{2} \leq q \leq 1. \end{cases} \quad (4.57)$$

We now show that there exists a set of points which is invariant under  $G$ , and delimits thus a Markov partition for this mapping. In particular the points of the form

$$q_k = \frac{k}{m} \quad k = 0, \dots, m, \quad (4.58)$$

constitutes, under a condition to be specified below, such a set. To prove this we have to show that a point  $q_k$  of the form (4.58) remains after one iteration of the mapping  $G$  of this form, generally with a different  $k$ . Notice first that a given point belonging to the support of  $G_1$  and to the support of  $G_2$  has two images (as a result of the overlapping of the branches) that will differ by the quantity  $\frac{\lambda}{2}\varepsilon$ . Hence the latter has to be of the form (4.58)

$$\frac{\lambda}{2}\varepsilon = \frac{e}{m} \quad (4.59)$$

where  $e$  is a positive integer satisfying eq. (4.56). Secondly, for a point belonging at the same time to the support of  $G_2$  and to the support of  $G_3$  the difference in the images now implies that  $\frac{\lambda}{2}$  also be of the form (4.58)

$$\frac{\lambda}{2} = \frac{n}{m} \quad (4.60)$$

where  $n$  is a positive integer such that eq. (4.55) is satisfied. Notice that dividing eq. (4.59) by eq. (4.60) one gets

$$\varepsilon = \frac{e}{n}. \quad (4.61)$$

Third and last, the part  $\lambda^2(1 - 2\varepsilon)q_k$  appearing in eq. (4.57) also has to be of the form (4.58)

$$4 \frac{n^2}{m^2} \left(1 - 2 \frac{e}{n}\right) \frac{k}{m} = \frac{\text{integer}}{m}. \quad (4.62)$$

Now eq. (4.62) is to be satisfied for  $k = 0, \dots, m$ . The necessary and sufficient condition is that it be true for  $k = 1$

$$4 \frac{n^2}{m^2} \left(1 - 2 \frac{e}{n}\right) = p \quad (4.63)$$

where  $p$  is a positive integer. The constraints (4.55) and (4.56) imply that

$$p < \frac{4n^2}{m^2} \leq 4. \quad (4.64)$$

So to proceed we have to show that there exists, within the appropriate ranges, integers  $e$ ,  $n$  and  $m$  such that  $p$  is an integer. Solving eq. (4.63) for  $\frac{n}{e}$  one gets

$$\frac{n}{e} = 1 + \sqrt{1 + \frac{p}{4} \left(\frac{m}{e}\right)^2}. \quad (4.65)$$

Suppose the solution for  $e = 1$  is  $n = n^*$ ,  $m = m^*$

$$n^* = 1 + \sqrt{1 + \frac{p}{4} (m^*)^2}, \quad (4.66)$$

so that the parameters  $\lambda$  and  $\varepsilon$  take on the value

$$\lambda^* = 2 \frac{n^*}{m^*}, \quad \varepsilon^* = \frac{1}{n^*}. \quad (4.67)$$

Now the solutions for  $e = 2, 3, \dots$  are  $n = en^*$ ,  $m = em^*$ . Hence the parameters  $\lambda$  and  $\varepsilon$  are still given by eq. (4.67). Accordingly we can limit ourselves to  $e = 1$  and from eq. (4.64) to  $p = 1, 2$  and  $3$ . The following table lists the solutions of eq.

(4.66) for  $m < 10000$ .

$p$	$m^*$	$n^*$	$\lambda^*$	$\varepsilon^*$
2	4	4	2	0.25
2	24	18	1.5	0.055555
2	140	100	1.4286	0.01
2	816	578	1.4166	0.001730
2	4756	3364	1.4146	0.000297
3	8	8	2	0.125
3	30	27	1.8	0.037037
3	112	98	1.75	0.010204
3	418	363	1.7368	0.002755
3	1560	1352	1.7333	0.000740
3	5822	5043	1.7324	0.000198

(4.68)

Notice that the value  $\lambda^*$ ,  $\varepsilon^*$  appearing in this table all satisfy

$$\varepsilon < \frac{1}{2} - \frac{1}{4\lambda} \quad (4.69)$$

implying that the eigenvalues of the jacobian of this transformation are greater than one in absolute value, and thus that the mapping  $\Phi$  is expanding in all directions. Let us also mention that there exists Markov partitions for  $G$  corresponding to chaotic repellers as is the case for instance for  $m^* = 2$ ,  $n^* = 3$  ( $\lambda^* = 3$ ,  $\varepsilon^* = \frac{1}{3}$ ).

#### 4.2.4 Bernoulli and anti-Bernoulli maps for $\varepsilon = \frac{1}{4}$

In this section we consider in detail the case  $\lambda = 2$ ,  $\varepsilon = \frac{1}{4}$ , for which the mapping  $G$  admits a Markov partition delimited by the points

$$q_k = \frac{k}{4} \quad k = 0, \dots, 4. \quad (4.70)$$

Our aim is first to construct explicitly the 2-d Markov partition for the coupled system  $\Phi$  of eq (4.14). We then determine the topological transition matrix and the transition matrix  $\mathbf{W}$  of the generalized master equation which enables us to compute

explicitly the invariant density of the coupled system as well as time-dependent properties.

In section 4.2.2 we have seen that the first iterate of a segment

$$y = q_k \quad (4.71)$$

is a collection of  $M$  segments of the straight line

$$y' = \frac{\varepsilon}{1-\varepsilon} x_1 + \frac{1-2\varepsilon}{1-\varepsilon} g(q_k), \quad (4.72)$$

where  $M$  is the number of branches of  $f$ . Here  $M = 2$  and these segments coincide as can be seen from eqs. (4.36)-(4.37) because the map  $f$  has the property

$$f(x) = f\left(x - \frac{1}{2}\right) \quad \frac{1}{2} \leq x \leq 1. \quad (4.73)$$

The following table gives the independent term of eq. (4.72) for each element  $q_k$  delimiting the Markov partition.

$q$	$\frac{1-2\varepsilon}{1-\varepsilon} g_1(q)$	$\frac{1-2\varepsilon}{1-\varepsilon} g_2(q)$
0	0	
$\frac{1}{4}$	$\frac{1}{3}$	
$\frac{1}{2}$	$\frac{2}{3}$	0
$\frac{3}{4}$		$\frac{1}{3}$
1		$\frac{2}{3}$

(4.74)

Now the iterate of eq. (4.72) is the second iterate of eq. (4.71) which, by definition (eq. (4.50)), is given by the mapping  $G$

$$y'' = G(q_k) = \{q_l\}. \quad (4.75)$$

Notice that since  $G$  is multivalued  $l$  takes on a number of values which is equal to

the number of supports of the branches of  $G$  that  $q_k$  is on. Eq. (4.57) for  $G$  becomes

$$G(q) = \begin{cases} G_1(q) = 2q + \frac{1}{2} & 0 \leq q < \frac{1}{4} \\ G_2(q) = 2q + \frac{1}{4} & 0 \leq q < \frac{3}{8} \\ G_3(q) = 2q - \frac{1}{4} & \frac{1}{8} < q \leq \frac{1}{2} \\ G_4(q) = 2q - \frac{1}{2} & \frac{1}{4} < q \leq \frac{1}{2} \\ G\left(q - \frac{1}{2}\right) & \frac{1}{2} \leq q \leq 1. \end{cases} \quad (4.76)$$

This mapping is displayed in fig. 4.2 and leads to the following table.

$q$	$G_1(q)$	$G_2(q)$	$G_3(q)$	$G_4(q)$
0	$\frac{1}{2}$	$\frac{1}{4}$		
$\frac{1}{4}$		$\frac{3}{4}$	$\frac{1}{4}$	
$\frac{1}{2}-$			$\frac{3}{4}$	$\frac{1}{2}$
$\frac{1}{2}+$	$\frac{1}{2}$	$\frac{1}{4}$		
$\frac{3}{4}$		$\frac{3}{4}$	$\frac{1}{4}$	
1			$\frac{3}{4}$	$\frac{1}{2}$

(4.77)

Here  $\frac{1}{2}-$  means that we take the point  $\frac{1}{2}$  to be in the cell which is on its left whereas  $\frac{1}{2}+$  stands for the right hand side.

Let us turn to the segments

$$x = q_k, \quad (4.78)$$

the first iterate of which is

$$x' = \frac{\varepsilon}{1-\varepsilon} x_2 + \frac{1-2\varepsilon}{1-\varepsilon} f(q_k). \quad (4.79)$$

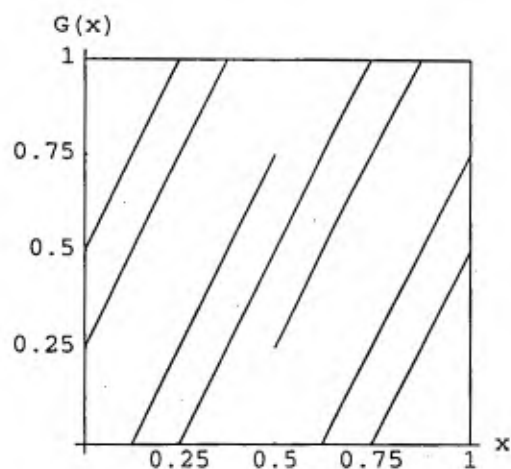


Figure 4.2: Mapping  $G$  of eq. (4.76).

One has the following table.

$q$	$\frac{1-2\varepsilon}{1-\varepsilon} f_1(q)$	$\frac{1-2\varepsilon}{1-\varepsilon} f_2(q)$
0	$\frac{2}{3}$	
$\frac{1}{4}$	$\frac{1}{3}$	
$\frac{1}{2}$	0	$\frac{2}{3}$
$\frac{3}{4}$		$\frac{1}{3}$
1		0

(4.80)

Notice that the set of independent terms is the same as for  $g$  but because of the negative slope of  $f$  it is gone through in the reverse order. The second iterate of eq. (4.78) by  $\Phi$  is now given by the mapping  $F$

$$x'' = F(q_k). \quad (4.81)$$

It turns out that for  $\lambda = 2$  the mapping  $F$  and  $G$  are identical

$$F \equiv G \quad \text{iff } \lambda = 2, \quad (4.82)$$

entailing that the points of eq. (4.70) also delimit a Markov partition for  $F$  and that the table (4.77) is valid for  $F$  as well.

We are now in the position to determine the 2-d Markov partition of the full mapping  $\Phi$  of eq. (4.14). Let us denote respectively by  $X_k$ ,  $Y_k$ ,  $U_l$  and  $V_l$  the segments contained in the unit square of the following straight lines

$$\begin{aligned} x = \frac{k}{4}, & & y = \frac{k}{4} & & k = 0, \dots, 4 \\ x = \frac{1}{3}y + \frac{l}{3}, & & y = \frac{1}{3}x + \frac{l}{3} & & l = 0, 1, 2. \end{aligned} \quad (4.83)$$

From the tables (4.74), (4.77), (4.80) we know that the set of all these segments is invariant under  $\Phi$

$$\begin{aligned} \Phi : \{X_k, Y_k, U_l, V_l\} &\rightarrow \{X_k, Y_k, U_l, V_l\} & k = 0, 1, 2, 3, 4 \\ & & l = 0, 1, 2. \end{aligned} \quad (4.84)$$

The domains  $S_i$  delimited by these segments are thus mapped onto each other under  $\Phi$  and constitute the elements of the 2-d Markov partition (cf eq. (4.17)). This partition is displayed in fig. 4.3. The topological transition matrix can now be determined up to some permutations depending on the way we order the elements of the 2-d partition. Notice that we need only consider the 22 elements that are in the rhomb delimited by  $V_0, V_2, U_0, U_2$  since it is the image of the unit square under  $\Phi$ . Tables (4.74), (4.80) yield directly

$$\begin{aligned} \Phi : X_0 &\rightarrow U_2 & \Phi : Y_0 &\rightarrow V_0 \\ \Phi : X_1 &\rightarrow U_1 & \Phi : Y_1 &\rightarrow V_1 \\ \Phi : X_{2-} &\rightarrow U_0 & \Phi : Y_{2-} &\rightarrow V_2 \\ \Phi : X_{2+} &\rightarrow U_2 & \Phi : Y_{2+} &\rightarrow V_0 \\ \Phi : X_3 &\rightarrow U_1 & \Phi : Y_3 &\rightarrow V_1 \\ \Phi : X_4 &\rightarrow U_0 & \Phi : Y_4 &\rightarrow V_2. \end{aligned} \quad (4.85)$$

From the table (4.77) one deduces that the image of  $U_l$  is contained in two  $X_k$ . On the other hand the image of  $U_l$  restricted to one quadrant is a segment of just one  $X_k$ . The value of  $k$  can be determined from eq. (4.85). Indeed it suffices to find a point of  $U_l$  which is also on, say,  $X_i$  and  $Y_j$ .  $X_k$  must then go through the image of

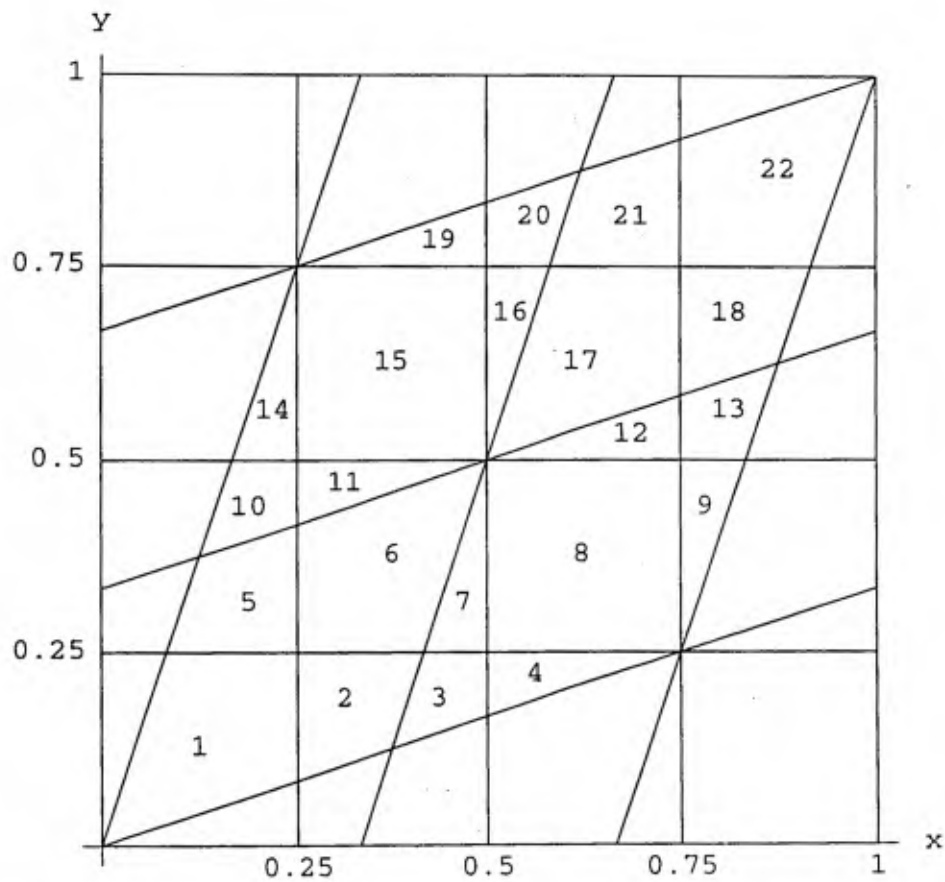


Figure 4.3: 2-d Markov partition for the mapping of eq. (4.14) where  $g$  is the Bernoulli map,  $f$  the anti-Bernoulli map and  $\epsilon = \frac{1}{4}$ .

$X_i$  and  $Y_j$ . Idem for  $V_i$ . With the following shorthand notation

$$\begin{aligned}
 RR &\equiv [0, \frac{1}{2}] \otimes [0, \frac{1}{2}] \\
 RL &\equiv [0, \frac{1}{2}] \otimes [\frac{1}{2}, 1] \\
 LR &\equiv [\frac{1}{2}, 1] \otimes [0, \frac{1}{2}] \\
 LL &\equiv [\frac{1}{2}, 1] \otimes [\frac{1}{2}, 1],
 \end{aligned} \tag{4.86}$$

one has

$$\begin{aligned}
 \Phi : U_0|_{RR} &\rightarrow X_3 & \Phi : V_0|_{RR} &\rightarrow Y_1 \\
 \Phi : U_0|_{RL} &\rightarrow X_2 & \Phi : V_0|_{LR} &\rightarrow Y_2 \\
 \Phi : U_1|_{RR} &\rightarrow X_1 & \Phi : V_1|_{RR} &\rightarrow Y_3
 \end{aligned}$$

$$\begin{aligned}
\Phi : U_1|_{LL} &\rightarrow X_3 & \Phi : V_1|_{LL} &\rightarrow Y_1 \\
\Phi : U_2|_{LR} &\rightarrow X_2 & \Phi : V_2|_{RL} &\rightarrow Y_2 \\
\Phi : U_2|_{LL} &\rightarrow X_1 & \Phi : V_2|_{LL} &\rightarrow Y_3 .
\end{aligned} \tag{4.87}$$

Consider for instance the element  $S_1$  delimited by  $V_0, Y_1, U_0, X_1$ . From eqs. (4.85),(4.87) it follows that

$$\Phi : \{V_0|_{RR}, Y_1, U_0|_{RR}, X_1\} \rightarrow \{Y_1, V_1, X_3, U_1, \} , \tag{4.88}$$

which according to our numbering (see fig. 4.3) delimits the 3 elements of the partition  $S_7, S_8, S_{12}$ . According to eq. (4.17) this yields the first line of the following topological transition matrix

$$\mathbf{A} = \begin{pmatrix}
0 & 0 & 0 & 0 & 0 & 0 & 1 & 1 & 0 & 0 & 0 & 1 & 0 & 0 & 0 & 0 & 0 & 0 & 0 & 0 \\
0 & 0 & 0 & 0 & 0 & 1 & 0 & 0 & 0 & 0 & 0 & 0 & 0 & 0 & 0 & 0 & 0 & 0 & 0 & 0 \\
0 & 0 & 0 & 0 & 1 & 0 & 0 & 0 & 0 & 0 & 0 & 0 & 0 & 0 & 0 & 0 & 0 & 0 & 0 & 0 \\
0 & 0 & 0 & 0 & 0 & 0 & 0 & 0 & 0 & 0 & 0 & 1 & 1 & 0 & 0 & 0 & 0 & 0 & 0 & 0 \\
0 & 0 & 0 & 0 & 0 & 0 & 0 & 0 & 0 & 0 & 0 & 0 & 0 & 0 & 0 & 1 & 0 & 0 & 0 & 0 \\
0 & 0 & 0 & 0 & 0 & 0 & 0 & 0 & 0 & 1 & 0 & 0 & 0 & 1 & 1 & 0 & 0 & 0 & 0 & 0 \\
0 & 0 & 0 & 0 & 0 & 0 & 0 & 0 & 0 & 1 & 0 & 0 & 0 & 1 & 0 & 0 & 0 & 0 & 0 & 0 \\
0 & 0 & 0 & 0 & 0 & 0 & 0 & 0 & 0 & 0 & 0 & 0 & 0 & 0 & 0 & 1 & 1 & 0 & 0 & 1 \\
0 & 0 & 0 & 0 & 0 & 0 & 0 & 0 & 0 & 0 & 0 & 0 & 0 & 0 & 0 & 1 & 0 & 0 & 0 & 1 \\
0 & 0 & 0 & 0 & 0 & 0 & 0 & 0 & 0 & 0 & 0 & 0 & 0 & 0 & 0 & 0 & 0 & 0 & 0 & 1 \\
0 & 0 & 0 & 0 & 0 & 0 & 0 & 0 & 0 & 0 & 0 & 0 & 0 & 0 & 0 & 0 & 0 & 0 & 1 & 0 \\
0 & 0 & 1 & 1 & 0 & 0 & 0 & 0 & 0 & 0 & 0 & 0 & 0 & 0 & 0 & 0 & 0 & 0 & 0 & 0 \\
0 & 1 & 0 & 0 & 0 & 0 & 0 & 0 & 0 & 0 & 0 & 0 & 0 & 0 & 0 & 0 & 0 & 0 & 0 & 0 \\
0 & 0 & 1 & 0 & 0 & 0 & 1 & 0 & 0 & 0 & 0 & 0 & 0 & 0 & 0 & 0 & 0 & 0 & 0 & 0 \\
1 & 1 & 0 & 0 & 1 & 1 & 0 & 0 & 0 & 0 & 0 & 0 & 0 & 0 & 0 & 0 & 0 & 0 & 0 & 0 \\
0 & 0 & 0 & 0 & 0 & 0 & 0 & 0 & 1 & 0 & 0 & 0 & 1 & 0 & 0 & 0 & 0 & 0 & 0 & 0 \\
0 & 0 & 0 & 0 & 0 & 0 & 1 & 1 & 0 & 0 & 0 & 1 & 0 & 0 & 0 & 0 & 0 & 0 & 0 & 0 \\
0 & 0 & 0 & 0 & 0 & 1 & 0 & 0 & 0 & 0 & 0 & 0 & 0 & 0 & 0 & 0 & 0 & 0 & 0 & 0 \\
0 & 0 & 0 & 0 & 0 & 0 & 0 & 0 & 0 & 0 & 1 & 1 & 0 & 0 & 0 & 0 & 0 & 0 & 0 & 0 \\
0 & 0 & 0 & 0 & 0 & 0 & 0 & 0 & 0 & 0 & 0 & 0 & 0 & 0 & 0 & 0 & 1 & 0 & 0 & 0 \\
0 & 0 & 0 & 0 & 0 & 0 & 0 & 0 & 0 & 0 & 0 & 0 & 0 & 0 & 0 & 1 & 0 & 0 & 0 & 0 \\
0 & 0 & 0 & 0 & 0 & 0 & 0 & 0 & 0 & 1 & 0 & 0 & 0 & 1 & 1 & 0 & 0 & 0 & 0 & 0
\end{pmatrix} \tag{4.89}$$

Notice that it contains only 44 non-zero elements. The transition matrix  $\mathbf{W}$  of the generalized master equation (4.24) for piecewise constant densities is given by eq. (4.26),

$$\mathbf{W} = \frac{1}{2} \mathbf{A}^T \tag{4.90}$$

where  $T$  stands for the transpose. Its eigenvalues are

$$1, \pm \frac{\sqrt{2}}{2}, \pm \frac{1}{2}, \pm \frac{i}{2}, 0. \quad (4.91)$$

It is worth mentioning that there is a Jordan block of order 2 associated to the eigenvalue  $-\frac{1}{2}$ . Hence time correlation functions are to be computed as discussed in Sec. 2.4. Note that for linear observables one has to resort to the transition matrix  $\mathbf{W}$  given by eq. (4.28) which yields here

$$\mathbf{W} = \left( \begin{array}{c|c|c} \frac{1}{2} a_{ji} & \frac{1}{4} \Delta_{\alpha_j} a_{ji} & -\frac{1}{4} \delta_{\beta_j} a_{ji} \\ \hline 0 & -\frac{3}{8} a_{ji} & -\frac{1}{8} a_{ji} \\ \hline 0 & -\frac{1}{8} a_{ji} & \frac{3}{8} a_{ji} \end{array} \right). \quad (4.92)$$

Its eigenvalues are in addition to eq. (4.91)

$$\pm \frac{3}{8}, \pm \frac{3\sqrt{2}}{16}, \pm \frac{3}{16}, \pm \frac{3i}{16}. \quad (4.93)$$

The eigenvector associated to the eigenvalue unity of eq. (4.91) is

$$\mathbf{c} = \text{col} \left( 1, 2, 2, \frac{4}{3}, 2, 3, \frac{8}{3}, 2, \frac{4}{3}, 2, \frac{8}{3}, \frac{8}{3}, 2, \frac{4}{3}, 2, \frac{8}{3}, 3, 2, \frac{4}{3}, 2, 2, 1 \right). \quad (4.94)$$

It yields according to eq. (4.19) an analytical expression for the invariant density  $\rho(x, y)$  which is displayed in fig. 4.4. From eq. (4.94) one deduces that  $\rho(x, y)$  is symmetric with respect to both  $y = x$  and  $y = 1 - x$ . This leads to the following expression for the invariant 1-d reduced probability density  $\rho(x)$

$$\rho(x) = \begin{cases} \frac{8}{3} x & 0 \leq x < \frac{1}{12} \\ \frac{17}{3} x - \frac{1}{4} & \frac{1}{12} \leq x < \frac{1}{6} \\ \frac{11}{3} x + \frac{1}{12} & \frac{1}{6} \leq x < \frac{1}{4} \\ -\frac{1}{9} x + \frac{19}{12} & \frac{1}{4} \leq x < \frac{5}{12} \\ -\frac{10}{9} x + 2 & \frac{5}{12} \leq x < \frac{1}{2} \\ \rho(1-x) & \frac{1}{2} \leq x \leq 1. \end{cases} \quad (4.95)$$

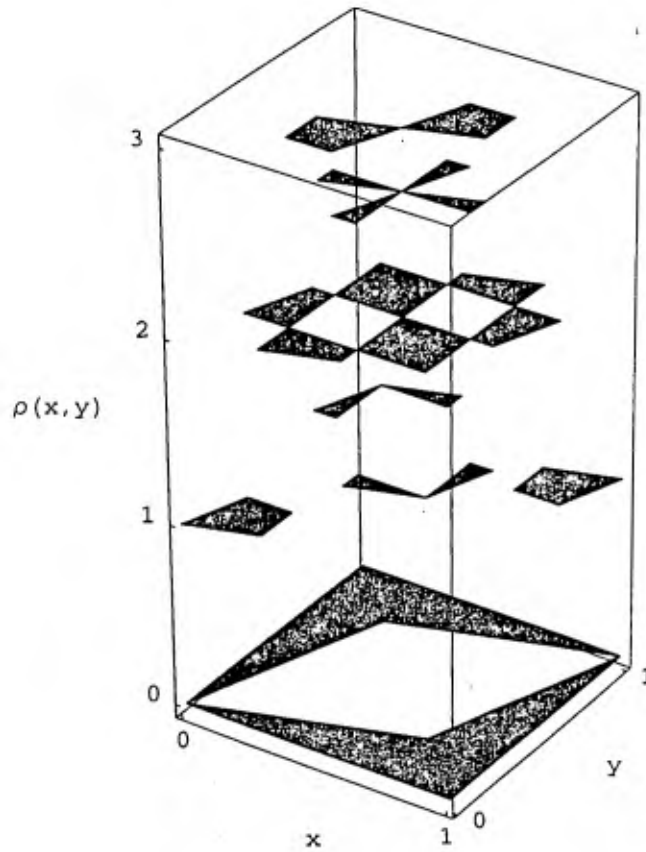


Figure 4.4: Invariant probability density  $\rho(x, y)$  for the mapping of eq. (4.14) where  $g$  is the Bernoulli map,  $f$  the anti-Bernoulli map and  $\varepsilon = \frac{1}{4}$ .

It is displayed in fig. 4.5. Notice that although we are coupling two fully chaotic maps with uniform invariant density the resulting 1-d marginal is not uniform on  $[0, 1]$ .

### 4.3 Coupled map lattices

Our aim here is to consider a CML with an arbitrary number  $N$  of elements. We propose the following CML

$$z_i^{n+1} = f_i \left( z_i^n + \frac{\varepsilon}{2} [z_{i-1}^n + z_{i+1}^n] \right) \quad (4.96)$$

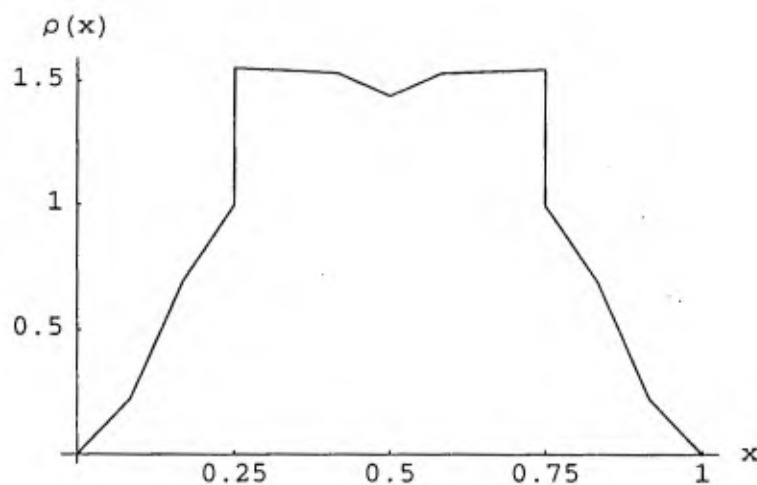


Figure 4.5: Invariant 1-d reduced probability density  $\rho(x)$  given by eq. (4.95) for the mapping of eq. (4.14) where  $g$  is the Bernoulli map,  $f$  the anti-Bernoulli map and  $\varepsilon = \frac{1}{4}$ .

where  $z_i^n \in [0, 1]$ ,  $\varepsilon \in [0, 1]$ ,  $n$  being the discrete time and  $i = 1, \dots, N$  a site of a 1-d ring. The maps  $f_i$  have the following property

$$f_i(1+z) = f_i(z) \quad z \in [0, 1]. \quad (4.97)$$

As above we are interested in individual maps  $f_i$  that are chaotic and such that no trajectory escapes  $[0, 1]$ .

In the next section we define reduced distribution functions and derive their evolution equations which take the form of a BBGKY type of hierarchy. We then show for a class of fully chaotic maps with uniform invariant density that the 1-d reduced probability density of the coupled system remains uniform for all values of the coupling constant  $\varepsilon$

### 4.3.1 Reduced probability densities and BBGKY hierarchy

In the framework of a statistical description of the CML (4.96) the central object is the Perron-Frobenius operator which evolves the probability density  $\rho_n(z_1, \dots, z_N)$  according to

$$\rho_{n+1}(z_1, \dots, z_N) = \mathcal{P}\rho_n(z_1, \dots, z_N)$$

$$= \int_I dy_1 \dots \int_I dy_N \rho_n(y_1, \dots, y_N) \delta \left( z_1 - f_1 \left( y_1 + \frac{\varepsilon}{2} [y_2 + y_N] \right) \right) \dots \delta \left( z_N - f_1 \left( y_N + \frac{\varepsilon}{2} [y_{N-1} + y_1] \right) \right) . \quad (4.98)$$

Now since  $N$  - the size of the ring - is arbitrary the full probability density is a high-dimensional object, possibly infinite-dimensional. As a consequence, one is interested in reduced distribution functions also called marginals

$$\rho_n(z_1, \dots, z_s) \equiv \int_I dz_{s+1} \dots \int_I dz_N \rho_n(z_1, \dots, z_N) \quad s = 1, \dots, N-1 . \quad (4.99)$$

For the sake of notation we shall not indicate  $s$  explicitly in the left handside of eq. (4.99). Its value is clear from the number of arguments of  $\rho$ . In particular, for  $s = 1$  one has

$$\rho_n(z_1) \equiv \int_I dz_2 \dots \int_I dz_N \rho_n(z_1, \dots, z_N) . \quad (4.100)$$

The equations of evolution of these  $s$ -point distribution functions are obtained by integrating the Perron-Frobenius equation (4.98) for the full probability density over all variables but  $z_1, \dots, z_s$ . One obtains in this way a hierarchy of equations, each involving a higher order reduced probability density

$$\begin{aligned} \rho_{n+1}(z_1, \dots, z_s) &= \mathcal{P}_s \rho_n(z_1, \dots, z_s) \\ &= \int_I dy_1 \dots \int_I dy_s \int_I dy_{s+1} \int_I dy_N \rho_n(y_1, \dots, y_s, y_{s+1}, y_N) \\ &\quad \delta \left( z_1 - f_1 \left( y_1 + \frac{\varepsilon}{2} [y_2 + y_N] \right) \right) \dots \delta \left( z_s - f_s \left( y_s + \frac{\varepsilon}{2} [y_{s-1} + y_{s+1}] \right) \right) , \end{aligned} \quad (4.101)$$

where  $\mathcal{P}_s$  is the  $s$ -point Perron-Frobenius operator. This hierarchy is of the type of the BBGKY hierarchy encountered in statistical mechanics [Ba75]. In the sequel we shall focus on the 1-d reduced distribution function whose evolution equation is

$$\rho_{n+1}(z_1) = \int_I dy_1 \int_I dy_2 \int_I dy_N \rho_n(y_1, y_2, y_N) \delta \left( z_1 - f_1 \left( y_1 + \frac{\varepsilon}{2} [y_2 + y_N] \right) \right) . \quad (4.102)$$

Hence taking into account eq. (4.97)

$$\begin{aligned} \rho_{n+1}(z_1) &= \sum_{\alpha} \frac{1}{|f_1'(f_{1\alpha}^{-1}(z_1))|} \int_I dy_2 \int_I dy_N \left\{ \rho_n \left( f_{1\alpha}^{-1}(z_1) - \frac{\varepsilon}{2} [y_2 + y_N], y_2, y_N \right) \right. \\ &\quad \left. + \rho_n \left( 1 + f_{1\alpha}^{-1}(z_1) - \frac{\varepsilon}{2} [y_2 + y_N], y_2, y_N \right) \right\} \chi_{f_1(C_{\alpha})}(z_1) , \end{aligned} \quad (4.103)$$

where  $f_{1\alpha}$  denotes the  $\alpha$ -th monotone branch of  $f_1$  and  $C_{\alpha}$  its support.

### 4.3.2 Invariant 1-d marginal for piecewise linear full maps

In this section we consider the case where the maps  $f_i$  are piecewise linear full maps with an arbitrary number of branches  $M_i > 1$ . For this class of maps, including for example the Bernoulli or the tent map, we show that the invariant 1-d reduced distribution function  $\rho(z_1)$ ,

$$\mathcal{P}_1 \rho(z_1) = \rho(z_1) \quad (4.104)$$

is uniform on  $[0, 1] \forall \varepsilon$

$$\rho(z_1) = \chi_{[0,1]}(z_1) . \quad (4.105)$$

To prove this let us assume that

$$\rho_n(z_1, z_2, z_N) = \chi_{[0,1]}(z_1) \chi_{[0,1]}(z_2) \chi_{[0,1]}(z_N) , \quad (4.106)$$

which entails that

$$\rho_n(z_1) = \chi_{[0,1]}(z_1) . \quad (4.107)$$

Notice first that of the two terms appearing in the right hand side of eq. (4.103), for any  $\alpha$ , only one will contribute since both arguments  $f_{1\alpha}^{-1}(z_1) - \frac{\varepsilon}{2}[y_2 + y_N]$  and  $1 + f_{1\alpha}^{-1}(z_1) - \frac{\varepsilon}{2}[y_2 + y_N]$  cannot be in  $[0, 1]$  at the same time (except when the first one is 0). Suppose now that  $\forall y_2, y_N \in [0, 1]$  one of these arguments is in  $[0, 1]$ . Hence,  $\forall \alpha$ , using eq. (4.106)

$$\begin{aligned} & \int_I dy_2 \int_I dy_N \left[ \rho_n \left( f_{1\alpha}^{-1}(z_1) - \frac{\varepsilon}{2}[y_2 + y_N], y_2, y_N \right) \right. \\ & \left. + \rho_n \left( 1 + f_{1\alpha}^{-1}(z_1) - \frac{\varepsilon}{2}[y_2 + y_N], y_2, y_N \right) \right] = 1 . \end{aligned} \quad (4.108)$$

It follows from eq. (4.103) that

$$\rho_{n+1}(z_1) = \sum_{\alpha} \frac{1}{|f_1'(f_{1\alpha}^{-1}(z_1))|} . \quad (4.109)$$

Now for a piecewise linear full map  $f_1$  one has

$$\sum_{\alpha} \frac{1}{|f_1'(f_{1\alpha}^{-1}(z_1))|} = \sum_{k=1}^{M_1} \frac{1}{|\Lambda_k^{(1)}|} = 1 \quad (4.110)$$

where  $\Lambda_k^{(1)}$  is the slope of the  $k$ -th branch of  $f_1$ . As a consequence

$$\rho_{n+1} = \chi_{[0,1]}(z_1) . \quad (4.111)$$

It remains thus to show that  $\forall y_2, y_N \in [0, 1]$  there will be a  $y_1$  in  $[0, 1]$ . This is what we do in the rest of this section. Let us denote by  $\theta$  the quantity  $y_1 + \frac{\varepsilon}{2}(y_2 + y_N)$  which is the argument of  $f_1$  in eq. (4.102),

$$\theta \equiv y_1 + \frac{\varepsilon}{2}(y_2 + y_N) \quad (4.112)$$

Since the variables  $y_1, y_2$  and  $y_N$  vary from 0 to 1,  $\theta$  ranges from 0 to  $1 + \varepsilon$ ,

$$0 \leq \theta \leq 1 + \varepsilon. \quad (4.113)$$

We shall distinguish the case  $0 \leq \theta \leq 1$  from the case  $1 \leq \theta \leq 1 + \varepsilon$  where use has to be made of eq. (4.97).

•  $0 \leq \theta \leq 1$  :

Subtracting the quantity  $-\frac{\varepsilon}{2}(y_2 + y_N)$  from  $\theta$  one gets the following inequalities

$$-\varepsilon \leq \theta - \frac{\varepsilon}{2}(y_2 + y_N) \leq 1. \quad (4.114)$$

Since the quantity which is bounded above and below is precisely  $y_1$  and  $y_1 \in [0, 1]$ , eq. (4.114) is to be replaced by

$$0 \leq \theta - \frac{\varepsilon}{2}(y_2 + y_N) \leq 1. \quad (4.115)$$

This can be rewritten as

$$\frac{1}{\varepsilon}(\theta - 1) \leq \frac{1}{2}(y_2 + y_N) \leq \frac{\theta}{\varepsilon}. \quad (4.116)$$

Now  $\frac{1}{2}(y_2 + y_N) \in [0, 1]$  so that the lower bound is to be replaced by zero and the upper one by 1 for  $\theta > \varepsilon$ . One thus gets

$$\begin{cases} 0 \leq \theta \leq \varepsilon : & 0 \leq \frac{1}{2}(y_2 + y_N) \leq \frac{\theta}{\varepsilon} \\ \varepsilon \leq \theta \leq 1 : & 0 \leq \frac{1}{2}(y_2 + y_N) \leq 1 \end{cases} \quad (4.117)$$

This means that for a given  $\theta$  as  $\frac{1}{2}(y_2 + y_N)$  varies in the appropriate range there will be a  $y_1$  in  $[0, 1]$  (cf eq. (4.115)). Now  $\theta$  enters eq. (4.102) via the Dirac delta distribution. This entails that  $f_1(\theta) = z_1$  so that  $\theta$  itself is the preimage of  $z_1$  by the branch  $\alpha$  of  $f_1$ ,

$$\theta = f_{1\alpha}^{-1}(z_1). \quad (4.118)$$

Since  $f_1$  is a full map such a preimage exists for any  $z_1 \in [0, 1]$  and is contained in  $[0, 1]$ . It follows that given a  $z_1 \in [0, 1]$  eq. (4.117) becomes

$$\begin{cases} 0 \leq f_{1\alpha}^{-1}(z_1) \leq \varepsilon : & 0 \leq \frac{1}{2}(y_2 + y_N) \leq \frac{1}{\varepsilon} f_{1\alpha}^{-1}(z_1) \\ \varepsilon \leq f_{1\alpha}^{-1}(z_1) \leq 1 : & 0 \leq \frac{1}{2}(y_2 + y_N) \leq 1 \end{cases} \quad (4.119)$$

•  $1 \leq \theta \leq 1 + \varepsilon$  :

Subtracting  $-\frac{\varepsilon}{2}(y_2 + y_N)$  from  $\theta$  one gets now

$$1 - \varepsilon \leq \theta - \frac{\varepsilon}{2}(y_2 + y_N) \leq 1, \quad (4.120)$$

which can be rewritten as

$$\frac{1}{\varepsilon}(\theta - 1) \leq \frac{1}{2}(y_2 + y_N) \leq \frac{1}{\varepsilon}(\theta - 1) + 1. \quad (4.121)$$

In this expression the upper bound is greater than or equal to 1 so that it can be replaced by 1. Let us define  $\theta'$  through

$$\theta' \equiv \theta - 1. \quad (4.122)$$

Eq. (4.121) becomes then

$$\frac{\theta'}{\varepsilon} \leq \frac{1}{2}(y_2 + y_N) \leq 1, \quad (4.123)$$

where

$$0 \leq \theta' \leq \varepsilon. \quad (4.124)$$

Now because of property (4.97) one has

$$f_1(\theta) = f_1(\theta - 1) = f_1(\theta'). \quad (4.125)$$

It follows from eq. (4.102) that

$$\theta' = f_{1\alpha}^{-1}(z_1). \quad (4.126)$$

Hence eq. (4.123) becomes

$$\frac{1}{\varepsilon} f_{1\alpha}^{-1}(z_1) \leq \frac{1}{2}(y_2 + y_N) \leq 1, \quad (4.127)$$

for

$$0 \leq f_{1\alpha}^{-1}(z_1) \leq \varepsilon. \quad (4.128)$$

Combining eqs. (4.119) and (4.127) yields

$$0 \leq \frac{1}{2}(y_2 + y_N) \leq 1 \text{ if } 0 \leq f_{1\alpha}^{-1}(z_1) \leq 1. \quad (4.129)$$

For a full map this is the case  $\forall \alpha$  and  $\forall z_1 \in [0, 1]$ . We thus arrive at the conclusion that  $\forall z_1 \in [0, 1]$  the variables  $y_2, y_N$  are both integrated over the whole interval  $[0, 1]$ , which is what was left aside to prove that the invariant 1-d projection of the full probability density is uniform on  $[0, 1]$ .

## 4.4 Conclusions

In this chapter we have constructed Markov partitions for two diffusively coupled piecewise linear maps enabling us to cast the Perron-Frobenius equation into a generalized master equation. We have introduced a CML of the form

$$z_i^{n+1} = f_i \left( z_i^n + \frac{\varepsilon}{2} [z_{i-1}^n + z_{i+1}^n] \right) \quad i \in L, \quad (4.130)$$

with  $f_i$  satisfying

$$f_i(1+z) = f_i(z) \quad z \in [0, 1]. \quad (4.131)$$

Here the lattice  $L$  is infinite or finite with periodic boundary conditions. Contrary to the diffusively coupled maps considered above, this CML has the nice property that the invariant 1-d marginal of the coupled system is uniform when the individual piecewise linear maps have uniform invariant density. It can be written in an alternative form through the change of variables

$$\mathbf{x}^n = \mathbf{D} \mathbf{z}^n \quad (4.132)$$

where the matrix  $\mathbf{D}$  is given by

$$D_{ij} = \delta_{ij} + \frac{\varepsilon}{2} (\delta_{i,j-1} + \delta_{i,j+1}) \quad i, j \in L. \quad (4.133)$$

In the new variables the CML (4.130) becomes

$$x_i^{n+1} = f_i(x_i^n) + \frac{\varepsilon}{2} [f_{i-1}(x_{i-1}^n) + f_{i+1}^n(x_{i+1}^n)] \quad i \in L. \quad (4.134)$$

This form is reminiscent of the standard diffusive coupling considered in Sec. 4.1 eq. (4.9). It differs in two ways. First the domain of definition here is not  $\otimes_{i \in L} [0, 1]$  in the  $\mathbf{x}$  but in the  $\mathbf{z}$  variables which is smaller. Outside this domain there are new branches of the maps which ensure that the property (4.131) is satisfied. Secondly, there is no factor  $(1 - \varepsilon)$  in front of  $f_i$  in eq. (4.134). A consequence of this is that summing over  $i$  the left and right hand sides of eq. (4.134) one gets an  $\varepsilon$ -dependent right hand side which implies that there is nothing like the conservation of mass here contrary to the standard diffusive coupling.

It is remarkable that one can go from a representation like eq. (4.130) to one like eq. (4.134) by a simple change of variables since, at first sight, they seem to correspond to different physical pictures. Indeed, in (4.130) diffusion occurs first and then the new state is transformed by the local dynamics whereas the two processes occur in the reverse order for eq. (4.134).

Notice that this change of variables can be done for standard diffusive coupling as well provided one takes now the usual diffusion matrix. The interest is that  $\otimes_{i \in L} [0, 1]$  in the  $\mathbf{z}$  variables is invariant under the mapping and that the reduced distribution functions now involve integrations in different directions. This results in objects that are in some sense less singular. However it is not sufficient to get uniform invariant 1-d marginal for the coupled system as is the case for the type of CML proposed here.

At present only the 1-d projection of a coupled system involving one class of maps has been computed. It would be desirable to extend this work to phenomenologically richer maps such as the logistic maps as well as to higher order projections, in particular in connection with the possibility to set up reduced, mean field types of description, free of heuristic approximations.



## Chapter 5

# Nonequilibrium thermodynamics of dynamical systems: entropy production and phase space volume contraction

### 5.1 Introduction

Recently, a number of relationships linking phase-space dynamics to thermodynamic quantities like entropy production and Onsager coefficients have been put forward [EvCoMo90, GaCo95, Ga96, Ru96]. In their general setting they are concerned with an initially isolated conservative system subjected subsequently to a dissipative perturbation, describing the combined effect of an external constraint and of a thermostat. As such a system possesses a (generally multifractal) attractor it will undergo on average a contraction of the phase space volume,

$$\lim_{t \rightarrow \infty} \overline{\frac{d}{dt} \ln \Delta\Gamma(t)} = \sum_i \sigma_i < 0 \quad (5.1)$$

where  $\sigma_i$  are the (mean) Lyapunov exponents [Ot93]. The rate of this contraction  $\left| \overline{d \ln \Delta\Gamma(t) / dt} \right|$  is then *defined* by some authors as the entropy production of the dynamical system on the grounds of its positivity. Alternatively in certain types of thermostatted Hamiltonian systems it is shown to be equal in the nonequilibrium steady state to the work per unit time performed on the system by the external constraints, which is in turn formally identical to the expression of entropy production as given by irreversible thermodynamics [EvMo90].

As well known phase space contraction is also given by the time derivative of the Gibbs entropy,

$$S_G = - \int dx \rho(\mathbf{x}, t) \ln \rho(\mathbf{x}, t) \quad (5.2)$$

where  $\mathbf{x} = \{x_i\}$  denotes the set of phase space coordinates, provided that the rate of change of the probability density  $\rho$  is evaluated from the Liouville equation,

$$\lim_{t \rightarrow \infty} \frac{dS_G}{dt} = \sum_i \sigma_i < 0. \quad (5.3)$$

One is then led immediately to the paradoxical conclusion that in such systems Gibbs entropy decreases without limit for long times and becomes eventually unbounded thereby precluding the existence of a steady state value,  $\lim_{t \rightarrow \infty} S_G = -\infty$ . This is to be related to the singularity of the invariant density  $\rho_s$ , confined on an object - the attractor - whose dimensionality is strictly less than that of the embedding phase space.

Inasmuch as irreversible thermodynamics, in particular the distinction between entropy flux and entropy production, must be generated from a balance equation describing how entropy evolves in time, the result summarized in (5.3) seems to preclude the possibility to build a self-consistent thermodynamics of the above defined thermostatted systems. It is indeed not clear why one can plainly use the expression of entropy production of classical irreversible thermodynamics, which finds its origin in quite different assumptions such as local equilibrium and the Gibbs entropy postulate. One is thus led to inquire whether the connection between entropy production and phase space volume contraction (or equivalently Lyapunov exponents) stipulated in recent literature is an intrinsic property, a matter of definition or the result of the particular algorithm devised for thermostating the system. One might even argue that under the setting of eqs. (5.1)-(5.3) there is no place for entropy production at all : as the system collapses toward the attractor it merely experiences a (negative) entropy flux, reflecting the fact that time going on its localization in phase space becomes increasingly sharper.

The difficulties summarized above are sufficiently compelling to warrant an alternative approach and a complementary viewpoint. Our objective in the present work is to outline a step in this direction accounting for the following features :

- to provide a link between phase-space dynamics and thermodynamic-like quantities,

- to be free of the singularities of the entropy pointed out in connection with eq. (5.3),
- to generate, in a self-consistent manner, a thermodynamic formalism bearing a direct link with the entropy production of classical irreversible thermodynamics.

The general formulation, based on the introduction of fluctuating forces along with the action of the dissipative perturbation, is laid down in Sec. 5.2. In Sec. 5.3 a balance equation for the information entropy is derived, from which two alternative forms of (information) entropy production are identified. A more explicit form of these terms is derived in Secs. 5.4 and 5.5 for the particular classes of thermostatted and mesoscopic systems respectively, leading to an explicit relation with thermodynamic entropy production. The main conclusions are drawn in Sec. 5.6.

## 5.2 Setting

In what follows we shall be concerned with systems whose state vector  $\mathbf{x} = (x_1, \dots, x_n)$  satisfies the following generic form of evolution equations

$$\frac{d\mathbf{x}}{dt} = \mathbf{F}(\mathbf{x}, \mu) + \mathbf{R}(t) . \quad (5.4)$$

The evolution operator  $\mathbf{F}$ , the control parameter  $\mu$  and the stochastic forcing  $\mathbf{R}$  are designed to account for the following situations :

- i) the evolution operator  $\mathbf{F}$  is a dissipative operator, in the sense of

$$\overline{\text{div } \mathbf{F}^t} < 0 \quad t \geq t_0 . \quad (5.5)$$

It may describe the evolution of a set of macroscopic observables, or the evolution of microscopic degrees of freedom of an initially conservative system put subsequently in contact with a thermostat and subjected to a dissipative perturbation removing it from equilibrium.

- ii) the control parameter  $\mu$  monitors the thermodynamic behavior of the system,

$$\mu = \mu_e + h , \quad (5.6)$$

$\mu_e$  being the equilibrium value and  $h$  the deviation from equilibrium.

iii) the stochastic forcing  $\mathbf{R}$  may

- be of external origin, its role being solely to regularize the singularities of the invariant density  $\rho_s$  associated to the dissipative character of  $\mathbf{F}$ ,
- account for the thermodynamic fluctuations around the average values of the observables associated with the dissipative perturbation added to the initial conservative dynamics, in which case it should satisfy appropriate fluctuation-dissipation relationships,
- account for the interaction between the system and external reservoirs (heat baths, etc).

In either case,  $\mathbf{R}$  will be modeled as a multi-Gaussian white noise,

$$\begin{aligned}\langle R_i(t) \rangle &= 0 \\ \langle R_i(t) R_j(t') \rangle &= \varepsilon Q_{ij} \delta(t - t'),\end{aligned}\quad (5.7)$$

$Q_{ij}$  being a positive definite matrix and  $\varepsilon$  a strength parameter.

Eqs. (5.4) and (5.7) define a Markov process of the diffusion type and induce a Fokker-Planck equation [DeMa62] for the evolution of the probability density  $\rho(x, t)$

$$\begin{aligned}\frac{\partial \rho}{\partial t} &= - \sum_i \frac{\partial}{\partial x_i} F_i \rho + \frac{\varepsilon}{2} \sum_{ij=1}^n Q_{ij} \frac{\partial^2 \rho}{\partial x_i \partial x_j} \\ &= \mathcal{L} \rho + \frac{\varepsilon}{2} \sum_{ij} Q_{ij} \frac{\partial^2 \rho}{\partial x_i \partial x_j}\end{aligned}\quad (5.8)$$

where  $\mathcal{L}$  is the Liouville operator.

We will often be interested in the properties of eq. (5.8) in the "weak noise" limit  $\varepsilon \rightarrow 0$ . It is well known that in this limit one may seek for solutions of the form [Va81]

$$\rho = Z^{-1} \exp \left[ \frac{1}{\varepsilon} \phi(\mathbf{x}, t) + o(1) \right] \quad (5.9)$$

where  $Z$  is the normalization factor and  $\phi$  is referred to as the stochastic potential. Substituting into (5.8) and keeping only dominant terms in  $\varepsilon$  one obtains in the steady state

$$\frac{1}{2} \sum_{ij} Q_{ij} \frac{\partial \phi_s}{\partial x_i} \frac{\partial \phi_s}{\partial x_j} = \sum_i F_i \frac{\partial \phi_s}{\partial x_i} \quad (5.10)$$

It can be shown for large classes of systems that  $\phi_s$  and hence the invariant density  $\rho_s$  are smooth as long as  $\varepsilon$  is not strictly zero. This reflects the regularizing action of the stochastic forcing anticipated earlier in the present section.

### 5.3 The information entropy and its balance

As was stressed in Sec. 1.5 in a discrete state stationary stochastic process entropy can be defined uniquely once the Shannon-Khinchin postulates are adopted [BeSc93]. It represents the information (amount of data) necessary to localize the state of the system in a phase space cell of linear dimension  $\delta$  and is given by

$$S_I = \sum_i P_i \ln P_i \quad (5.11)$$

where the index  $i$  stands for the state and  $P_i$  for its probability. As the resolution  $\delta$  gets finer  $P_i$  tends to  $\rho\delta$  where  $\rho$  is the corresponding density. Eq. (5.11) shows then that  $S_I$  contains a singular part in  $\ln \frac{1}{\delta}$ , plus a regular contribution depending solely on  $\rho$ . As the singular part is independent of the dynamics it can be used as reference value and one obtains the continuous version of (5.11),

$$S_I = - \int d\mathbf{x} \rho(\mathbf{x}, t) \ln \rho(\mathbf{x}, t) . \quad (5.12)$$

Having a definition of (information) entropy  $S_I$  and an evolution equation for  $\rho$  one can now derive a balance equation for  $S_I$ , identify entropy production-like terms bearing the signature of dynamics in phase space and compare them with the entropy production of irreversible thermodynamics. We first observe from (5.8) and (5.12) that

$$\frac{dS_I}{dt} = - \int d\mathbf{x} \left[ - \sum_i \frac{\partial}{\partial x_i} F_i \rho + \frac{\varepsilon}{2} \sum_{ij} Q_{ij} \frac{\partial^2 \rho}{\partial x_i \partial x_j} \right] \ln \rho . \quad (5.13)$$

The right hand side of this relation can be transformed by performing partial integrations. Dropping boundary terms (a legitimate procedure since the probability density tends rapidly to zero as  $|\mathbf{x}| \rightarrow \infty$ ) one obtains after some straightforward manipulations the following form of information entropy balance

$$\frac{dS_I}{dt} = \int d\mathbf{x} \rho \operatorname{div} \mathbf{F} + \frac{\varepsilon}{2} \sum_{ij} Q_{ij} \int d\mathbf{x} \frac{1}{\rho} \frac{\partial \rho}{\partial x_i} \frac{\partial \rho}{\partial x_j} . \quad (5.14)$$

The second term in (5.14) is positive definite on the grounds of the positive definiteness of the matrix  $Q_{ij}$ , while the first one has no definite sign. This suggests to identify the latter to (information) entropy flux and the former to (information) entropy production  $P_I$ , given by the relation

$$P_I = \frac{\varepsilon}{2} \sum_{ij} Q_{ij} \int d\mathbf{x} \frac{1}{\rho} \frac{\partial \rho}{\partial x_i} \frac{\partial \rho}{\partial x_j} . \quad (5.15)$$

A more explicit representation of  $P_I$  can be obtained in the steady state and in the limit  $\varepsilon \ll 1$  using expressions (5.9)-(5.10). We obtain

$$P_I = \frac{1}{2\varepsilon} \sum_{ij} Q_{ij} \int dx \rho_s \frac{\partial \phi_s}{\partial x_i} \frac{\partial \phi_s}{\partial x_j} = \int dx \sum_i F_i \frac{\partial \rho_s}{\partial x_i} \quad (5.16)$$

or, after a partial integration,

$$P_I = - \int dx \rho_s \operatorname{div} \mathbf{F} = - \overline{\operatorname{div} \mathbf{F}^\infty} = - \sum_i \sigma_i + O(\varepsilon) > 0 \quad (5.17)$$

where  $\sigma_i$  are the Lyapunov exponents of the deterministic system (eqs. (5.4) in the absence of noise). We have thus shown that information entropy production as defined by (5.15) is equal to the negative sum of Lyapunov exponents or equivalently (cf. eq. (5.1)) to the rate of phase space volume contraction, plus a correction vanishing with the noise strength [NiDa96]. This result is rather remarkable since it would seem at first sight from (5.15) that  $P_I$  should tend to zero as  $\varepsilon \rightarrow 0$ . The fact that it nevertheless gives a finite contribution in this limit reflects the non-analytic dependence of the probability density in  $\varepsilon$ , eq. (5.9).

In short we have established, through  $P_I$ , a link between thermodynamically inspired quantities and the quantifiers of the underlying dynamics in phase space, free of the difficulties outlined in the Introduction. Still, no connection with the entropy production of irreversible thermodynamics has been made at this stage since the distance from equilibrium has not been explicitly displayed. To achieve this we decompose the diffusion term in the Fokker-Planck equation (eq. (5.8)) in a new way exhibiting the equilibrium distribution  $\rho_e$ , using the identity

$$\frac{\partial^2 \rho}{\partial x_i \partial x_j} = \frac{\partial}{\partial x_i} \left( \frac{\partial \ln \rho_e}{\partial x_j} \right) \rho + \frac{\partial}{\partial x_i} \rho_e \frac{\partial}{\partial x_j} \frac{\rho}{\rho_e}. \quad (5.18)$$

The information entropy balance, eqs. (5.13) and (5.14) now yields

$$\begin{aligned} \frac{dS_I}{dt} = - \int dx \ln \rho & \left[ - \sum_i \frac{\partial}{\partial x_i} F_i \rho + \frac{\varepsilon}{2} \sum_{ij} Q_{ij} \frac{\partial}{\partial x_i} \left( \frac{\partial \ln \rho_e}{\partial x_j} \rho \right) \right] \\ & - \frac{\varepsilon}{2} \sum_{ij} Q_{ij} \int dx \ln \rho_e \frac{\partial}{\partial x_i} \rho_e \frac{\partial}{\partial x_j} \frac{\rho}{\rho_e} \\ & - \frac{\varepsilon}{2} \sum_{ij} Q_{ij} \int dx \rho \left( \frac{\partial}{\partial x_i} \ln \frac{\rho}{\rho_e} \right) \left( \frac{\partial}{\partial x_j} \ln \frac{\rho}{\rho_e} \right). \end{aligned} \quad (5.19)$$

We notice that the first, second and third terms in this relation are respectively of zeroth, first and second order with respect to the deviation from equilibrium. Performing partial integrations as before one obtains

$$\begin{aligned} \frac{dS_I}{dt} = & \overline{\text{div } \mathbf{F}} + \frac{\varepsilon}{2} \sum_{ij} Q_{ij} \int d\mathbf{x} \rho \left[ -\frac{\partial \ln \rho_e}{\partial x_i} \frac{\partial \ln \rho_e}{\partial x_j} + 2 \frac{\partial \ln \rho}{\partial x_i} \frac{\partial \ln \rho_e}{\partial x_j} \right] \\ & + \frac{\varepsilon}{2} \sum_{ij} Q_{ij} \int d\mathbf{x} \rho \left( \frac{\partial}{\partial x_i} \ln \frac{\rho}{\rho_e} \right) \left( \frac{\partial}{\partial x_j} \ln \frac{\rho}{\rho_e} \right) . \end{aligned} \quad (5.20)$$

This new decomposition of the rate of change of information entropy features now a part  $P'_I$  (the third term in the r.h.s.) which is both positive definite and of second order in the deviation from equilibrium, thereby fulfilling the principal condition required on entropy production. Neglecting terms of order higher than two by approximating

$$\ln \frac{\rho}{\rho_e} = \ln \left( 1 + \frac{\delta\rho}{\rho_e} \right) \approx \frac{\delta\rho}{\rho_e} \quad (5.21)$$

$\delta\rho$  being the deviation from equilibrium, one obtains

$$P'_I = \frac{\varepsilon}{2} \sum_{ij} Q_{ij} \int d\mathbf{x} \rho_e \left( \frac{\partial}{\partial x_i} \frac{\delta\rho}{\rho_e} \right) \left( \frac{\partial}{\partial x_j} \frac{\delta\rho}{\rho_e} \right) \geq 0 . \quad (5.22)$$

On the other hand, the first term in the r.h.s. of (5.20) has no definite sign and contains, in principle, contributions of all orders in the deviation from equilibrium. In the steady state  $dS_I/dt = 0$  and the contribution of this term and of the second one in (5.20) must cancel that of  $P'_I$ . The role of the second term in this balance is, then, to remove the contributions of all but second orders in  $\delta\rho$  contained in  $\overline{\text{div } \mathbf{F}}$ . We may therefore write, in the steady state

$$P'_I = -\overline{\text{div } \mathbf{F}}^\infty - (\text{terms of 0th and 1st order in } \delta\rho) \quad (5.23)$$

or (cf (5.17))

$$P'_I = -\sum_i \sigma_i - (\text{terms of 0th and 1st order in } \delta\rho) . \quad (5.24)$$

This establishes a connection between irreversible thermodynamics on the one side, and phase space dynamics on the other. At this stage this connection cannot be made more explicit, as our analysis encompasses a very wide class of dynamical systems. In the next two sections more explicit forms of entropy balance are derived for the specific cases of thermostatted systems and mesoscopic systems.

## 5.4 Thermostatted systems

Thermostatted systems have recently attracted considerable attention since they provide an interesting way to incorporate the nonequilibrium constraints in the form of an external "mechanical" force added to the equations of evolution of the microscopic degrees of freedom [Ho85, HoHoPo87, EvMo90, PoHo97].

To express the action of a thermostat in our formulation we decompose the deterministic part  $\mathbf{F}$  in eq. (5.4) into the sum of a contribution  $\mathbf{F}_0 = \mathbf{F}(\mathbf{x}, \mu_e)$  to which  $\mathbf{F}$  reduces in the absence of nonequilibrium constraint ( $h = 0$  in eq.(5.6)) and of a contribution  $h \left( \frac{\partial \mathbf{F}}{\partial \mu} \right)_{\mu_e} = h\mathbf{F}_1$  associated to the action of the constraint. Eq. (5.4) becomes then

$$\frac{d\mathbf{x}}{dt} = \mathbf{F}_0(\mathbf{x}) + h\mathbf{F}_1(\mathbf{x}) + \mathbf{R}(t). \quad (5.25)$$

The variables  $x_i$  now represent the coordinates  $\mathbf{q}_i$  and moment  $\mathbf{p}_i$  of a system of particles in contact with a reservoir. The equilibrium part  $\mathbf{F}_0$  together with the fluctuating forces  $\mathbf{R}$  ensure that in the limit  $h = 0$  the system is driven irreversibly to canonical equilibrium.

The Fokker-Planck equation associated to (5.25) reads

$$\begin{aligned} \frac{\partial \rho}{\partial t} = & - \sum_i \frac{\partial}{\partial x_i} \left[ F_{0i} - \frac{1}{2} \sum_j Q_{ij} \left( \frac{\partial \ln \rho_e}{\partial x_j} \right) \right] \rho \\ & - h \sum_i \frac{\partial}{\partial x_i} F_{1i} \rho + \frac{1}{2} \sum_{ij} Q_{ij} \frac{\partial}{\partial x_i} \rho_e \frac{\partial}{\partial x_j} \rho \end{aligned} \quad (5.26)$$

where the contribution of the diffusion part has been decomposed as in eq. (5.18). In equilibrium  $h = 0$  and  $\rho = \rho_e$ . The second and third term in the r.h.s. of eq. (5.26) vanish then identically, entailing that the first term must also vanish. This imposes a relation between the parameters appearing in the functions  $F_{0i}$  and the matrix  $Q_{ij}$ , which can be looked at as the manifestation of a fluctuation-dissipation type of theorem (we assume for simplicity that  $Q_{ij}$  is not affected by the nonequilibrium constraint). More explicitly, one has

$$- \sum_i \frac{\partial}{\partial x_i} \phi_i \rho_e = 0 \quad (5.27)$$

where the "effective" vector field  $\phi_i$  governing the dynamics around equilibrium is given by

$$\phi_i = F_{0i} - \frac{1}{2} \sum_j Q_{ij} \frac{\partial \ln \rho_e}{\partial x_j}. \quad (5.28)$$

Now, Eq. (5.27) must be compatible with the equilibrium limit of the full-scale (microscopic) Liouville equation in the absence of constraint

$$\rho_e \sim \exp(-\beta H), \quad (5.29)$$

$H$  being the total energy. We conclude that  $\phi_i$  must have a symplectic structure and, in particular, be divergence-free,

$$\operatorname{div} \phi = 0. \quad (5.30)$$

The underlying dynamics associated with the drift term in eq. (5.26) is therefore phase space volume-conserving, and the modified diffusion term in this equation provides the proper way to account for the fluctuations around such an equilibrium conservative dynamics. Finally, the term in  $h$  in (5.26), expresses the non-equilibrium part of the dynamics, which will be modeled as a dissipative (phase space volume-contracting) process,

$$\overline{\operatorname{div} \mathbf{F}_1^t} < 0 \quad t \geq t_0. \quad (5.31)$$

We come now to the information entropy balance. Differentiating eq. (5.12) with respect to time and using eq. (5.26) we obtain

$$\begin{aligned} \frac{dS_I}{dt} = & -\frac{d}{dt} \int dx \rho \ln \rho_e - \int dx \ln \frac{\rho}{\rho_e} \\ & \left[ -\sum_i \frac{\partial}{\partial x_i} \phi_i \rho - h \sum_i \frac{\partial}{\partial x_i} F_{1i} \rho + \frac{1}{2} \sum_{ij} Q_{ij} \frac{\partial}{\partial x_i} \rho_e \frac{\partial}{\partial x_j} \frac{\rho}{\rho_e} \right]. \end{aligned} \quad (5.32)$$

The new element is now that in isoenergetically thermostatted systems the first term vanishes identically, owing to the conservation of the mean value of total energy  $H$  (cf. (5.29)). The remaining part of (5.32) is then automatically of second order in the deviation from equilibrium, in particular since the action of  $-\sum_i \frac{\partial}{\partial x_i} \phi_i$  on  $\rho_e$  gives zero: the zeroth and first order terms in (5.24) are therefore absent. We may give to this part a more explicit form by expanding the logarithm to first order in  $h\delta\rho = \rho - \rho_e$  and by performing partial integration. Noticing that the action of the part in  $\phi_i$  gives a vanishing result one obtains

$$\begin{aligned} \frac{1}{h^2} \frac{dS_I}{dt} = & \int dx \delta\rho \operatorname{div} \mathbf{F}_1 + \int dx \left( \sum_i F_{1i} \frac{\partial \ln \rho_e}{\partial x_i} \right) \delta\rho + \\ & \frac{\varepsilon}{2} \sum_{ij} Q_{ij} \int dx \rho_e \left( \frac{\partial}{\partial x_i} \frac{\delta\rho}{\rho_e} \right) \left( \frac{\partial}{\partial x_j} \frac{\delta\rho}{\rho_e} \right). \end{aligned} \quad (5.33)$$

We thus recover the entropy production term  $P'_I$ , eq. (5.22), together with a more explicit expression of the remaining, entropy flux like terms,  $J'_I$ , as compared to eq. (5.20),

$$\frac{1}{h^2} J'_I = \int dx \delta\rho \operatorname{div} \mathbf{F}_1 - \beta \int dx \sum_i \mathbf{F}_{1i} \frac{\partial H}{\partial x_i} \delta\rho. \quad (5.34)$$

Here the first part represents the rate of phase-space volume contraction to the second order, whereas the second part can be viewed as the average of the work per unit time of the external forcings acting (tangentially) along the different degrees of freedom  $i$ . In the steady state

$$P'_I = -J'_I \quad (5.35)$$

providing an explicit relation between irreversible thermodynamics and phase space dynamics.

As a first illustration of the foregoing we consider Brownian motion in an external field [DeMa62],

$$m \frac{dv}{dt} = -\zeta v + eE + R(t) \quad (5.36)$$

where  $m$  is the mass,  $e$  the charge and the coefficient  $\zeta$  expresses the effect of friction exerted on the particle by the host fluid, which acts like a heat bath at constant temperature  $T$ . The correspondence with the general form (5.25) leads to the identification  $F_0 = (-\zeta/m)v$ ,  $F_1 = \frac{eE}{m}$ . The flux term  $J'_I$  in eq. (5.34) becomes

$$J'_I = -\frac{1}{kT} \int_{-\infty}^{\infty} dv eE v \delta\rho \quad (5.37)$$

where the integrand represents the work per unit time performed on the particle by the external force.

The Fokker-Planck equation corresponding to (5.36) can be solved straightforwardly, yielding

$$\rho_e = \left( \frac{m}{2\pi kT} \right)^{1/2} e^{-\frac{mv^2}{2kT}}, \quad \delta\rho = \rho_e \frac{meE}{\zeta kT} v \quad (5.38)$$

where use was made of the fluctuation-dissipation relation [DeMa62, Va81]  $Q = \frac{\zeta kT}{m^2}$ . Inserting into eq. (5.37) one obtains in the steady state

$$J'_I = -\frac{e^2 E^2}{\zeta kT}, \quad P'_I = -J'_I = \frac{e^2 E^2}{\zeta kT} \quad (5.39)$$

which is exactly the entropy production of irreversible thermodynamics for this system.

It is worth noting that the "effective" vector field  $\phi$  corresponding to this dynamical system is trivial. Indeed, using the above given explicit forms of  $\rho_e$  and  $Q$  one finds from eq. (5.28)

$$\phi = -\frac{\zeta}{m}v - Q\frac{\partial}{\partial v}\left(-\frac{mv^2}{2kT}\right) = 0. \quad (5.40)$$

This at first sight surprising result is due to the absence of inertial terms in the field-free limit of eq. (5.36). The Fokker-Planck equation for this system reduces thus actually to the last two terms of eq. (5.26),

$$\frac{\partial\rho}{\partial t} = -\frac{eE}{m}\frac{\partial\rho}{\partial v} + \frac{\zeta kT}{m^2}\frac{\partial}{\partial v}\rho_e\frac{\partial\rho}{\partial v}. \quad (5.41)$$

A similar structure will arise in all problems involving purely dissipative evolution laws.

We next consider the more involved case of the Sllod equations modelling shear flow [EvMo84], as applied to two coupled degrees of freedom :

$$\begin{aligned} \frac{dx}{dt} &= v_x + \gamma y \\ \frac{dy}{dt} &= v_y \\ \frac{dv_x}{dt} &= F_x - \gamma v_y - \alpha v_x \\ \frac{dv_y}{dt} &= F_y - \alpha v_y. \end{aligned} \quad (5.42)$$

Here  $x, y$  denote the coordinates and  $v_x, v_y$  the associated velocities (we take for simplicity  $m = 1$ ).  $\gamma$  stands for the shear,  $\alpha$  accounts for the interactions with the reservoir and  $F_x, F_y$  are conservative forces of internal origin. We do not consider, at this stage, the fluctuating forces accompanying the dissipative perturbation.

The divergence of the vector field associated to eqs. (5.42) is

$$\frac{\partial\dot{x}}{\partial x} + \frac{\partial\dot{y}}{\partial y} + \frac{\partial\dot{v}_x}{\partial v_x} + \frac{\partial\dot{v}_y}{\partial v_y} = -2\alpha. \quad (5.43)$$

Requiring that the total energy  $\frac{1}{2}(v_x^2 + v_y^2 + \phi)$  (with  $F_x = -\frac{\partial V}{\partial x}$ , etc) remains constant one finds that  $\alpha$  is related to the nonequilibrium constraint  $\gamma$ ,

$$\alpha(v_x^2 + v_y^2) = -\gamma(F_x y + v_x v_y). \quad (5.44)$$

The equilibrium part of eqs. (5.42) consists thus entirely of "inertial" contributions and is described by a conservative vector field. It is the analog, for this problem, of the "effective" vector field  $\phi$  (eq. (5.28) which contrary to the Brownian motion case is now non-trivial. The entropy flux term (eq. (5.34)) reads

$$J'_I = -2\bar{\alpha} - \frac{1}{kT} \int dx dy dv_x dv_y \left[ \frac{\partial \phi}{\partial x} \gamma y - (\gamma v_y + \alpha v_x) v_x - \alpha v_y^2 \right] \delta \rho \quad (5.45)$$

or, using (5.44) and (5.35),

$$J'_I = -2\bar{\alpha} = 2\gamma \overline{(F_{xy} + v_x v_y) / (v_x^2 + v_y^2)} = -P'_I \quad (5.46)$$

where the average is taken with  $\delta \rho$ . The computation of this correction to  $\rho_e$  requires an explicit modelling of the fluctuating forces and hence of the diffusion part of the Fokker-Planck equation (5.26) and is beyond the scope of the present work. Suffice it to observe here that the numerator in eq. (5.46) is nothing but the definition of the momentum flux of the system. Eq. (5.46) exhibits therefore the product of the average of this flux multiplied by the shear  $\gamma$ . This is just minus the entropy production of irreversible thermodynamics for this system. We have therefore here a clearcut connection between thermodynamic and phase space quantities in the form of a strict equality between entropy production and phase space volume contraction.

## 5.5 Mesoscopic systems

We next turn to the case where  $\mathbf{x}$  stands for a set of macroscopic observables and  $\mathbf{R}$  for the thermodynamic fluctuations. In the small noise limit  $\varepsilon \rightarrow 0$  considered in Sec. 5.3  $\rho$  is expected to be peaked sharply around the attractor of the deterministic (noiseless) evolution equations. We express this by decomposing  $\mathbf{x}$  as

$$\mathbf{x} = \bar{\mathbf{x}} + \delta \mathbf{x} \quad , \quad \frac{|\delta \mathbf{x}|}{|\bar{\mathbf{x}}|} \ll 1 \quad (5.47)$$

and by limiting the expansion of the rate function  $\mathbf{F}(\mathbf{x}, \mu)$  in eq. (5.4) around  $\bar{\mathbf{x}}$  to its linear terms,

$$\dot{\delta \mathbf{x}} = \mathbf{l} \delta \mathbf{x} + \mathbf{R}(t) \quad (5.48)$$

where

$$l_{ij} = \left( \frac{\partial F_i}{\partial x_j} \right)_{\bar{\mathbf{x}}} \quad (5.49)$$

Here  $\bar{\mathbf{x}}$  is the macroscopic state (average or more generally most probable value of the probability density) evolving according to

$$\dot{\bar{\mathbf{x}}} = \mathbf{F}(\bar{\mathbf{x}}, \mu). \quad (5.50)$$

The Fokker-Planck equation induced by (5.48) reads then

$$\frac{\partial \rho}{\partial t} = - \sum_{ij} \frac{\partial}{\partial \delta x_i} l_{ij} \delta x_j \rho + \frac{\varepsilon}{2} \sum_{ij} Q_{ij} \frac{\partial^2 \rho}{\partial \delta x_i \partial \delta x_j}. \quad (5.51)$$

Inasmuch as the macroscopic steady state  $\bar{\mathbf{x}}_s$  is stable, eq. (5.51) admits a stationary solution in the form of a multivariate Gaussian distribution

$$\rho(\delta \mathbf{x}, t) = \frac{\sqrt{g/\varepsilon}}{(2\pi)^{n/2}} \exp \left[ -\frac{1}{2\varepsilon} \sum_{ij} g_{ij} \delta x_i \delta x_j \right] \quad (5.52)$$

where the matrix  $\mathbf{g}$  is given by [NiPr77]

$$\mathbf{1} \mathbf{g}^{-1} + (\mathbf{1} \mathbf{g}^{-1})^T = -\mathbf{Q} \quad (5.53)$$

$g$  being its determinant.

So far we have not specified the thermodynamic status of our system and, in particular, its distance from thermodynamic equilibrium. Operationally this distance is monitored by the control parameter  $\mu$  present in the evolution laws (eq. (5.4)), which may account for the interaction of the system with external reservoirs and/or for the direct action of an external field. At equilibrium ( $\mu = \mu_e$ ) eq. (5.52) reduces to

$$\rho_e(\delta \mathbf{x}_e) = \frac{\sqrt{g^e/\varepsilon}}{(2\pi)^{n/2}} \exp \left[ -\frac{1}{2\varepsilon} \sum_{ij} g_{ij}^e \delta x_i^e \delta x_j^e \right] \quad (5.54)$$

where  $g_{ij}^e$  is related to the deviation  $\Delta S$  of thermodynamic entropy from its equilibrium value due to a fluctuation through [DeMa62]

$$g_{ij}^e = - \left( \frac{\partial^2 \Delta S}{\partial \delta x_i \partial \delta x_j} \right). \quad (5.55)$$

We are here interested in the linear response to a weak nonequilibrium constraint  $h$ ,

$$\begin{aligned} \rho &= \rho_e + h \delta \rho + o(h^2) \\ \mu &= \mu_e + h \quad \left| \frac{h}{\mu_e} \right| \ll 1. \end{aligned} \quad (5.56)$$

As a rule, the effect of the constraint will be twofold :

(i) The macroscopic state  $\bar{\mathbf{x}}$  is shifted from the equilibrium value  $\mathbf{x}_e$ ,

$$\bar{\mathbf{x}} = \mathbf{x}_e + h\mathbf{x}^{(1)} + \dots \quad (5.57)$$

hence

$$\delta\mathbf{x} = \delta\mathbf{x}_e - h\mathbf{x}^{(1)} \quad (5.58)$$

Substituting (5.57) in eq. (5.50) and expanding around  $\mathbf{x}_e$  and  $\mu_e$  to first order in  $h$  yields

$$\mathbf{x}^{(1)} = -\ell_e^{-1} \left( \frac{\partial F}{\partial \mu} \right)_e \quad (5.59)$$

(ii) The matrix  $\mathbf{g}$  and its determinant  $g$  will deviate from their equilibrium values

$$\begin{aligned} \mathbf{g} &= \mathbf{g}_e + h\mathbf{g}^{(1)} \\ g &= g_e + hg^{(1)} \end{aligned} \quad (5.60)$$

as a result of the nonequilibrium corrections to the Jacobian matrix  $\mathbf{l}$  and to the noise correlation matrix  $\mathbf{Q}$  in eq. (5.53)

$$\begin{aligned} \mathbf{l} &= \mathbf{l}_e + h\mathbf{l}^{(1)} + \dots \\ \mathbf{Q} &= \mathbf{Q}_e + h\mathbf{Q}^{(1)} + \dots \end{aligned} \quad (5.61)$$

Carrying out these expansions systematically in eqs. (5.52) and (5.53) we finally obtain

$$\delta\rho = \left( \frac{g^{(1)}}{2g_e} + \frac{1}{2\varepsilon} \sum_{ij} g_{ij}^e (\delta x_i^e x_j^{(1)} + \delta x_j^e x_i^{(1)}) - \frac{1}{2\varepsilon} \sum_{ij} g_{ij}^{(1)} \delta x_i^e \delta x_j^e \right) \rho_e \quad (5.62)$$

We are now in the position to evaluate the information entropy production  $P'_I$ , eq. (5.22). Adopting the Onsager definition of the thermodynamic force  $X_i$  associated to  $x_i$ ,

$$X_i = \frac{\partial \Delta S}{\partial x_i} = - \sum_k g_{ik}^e x_k \quad (5.63)$$

and noting that the part  $Q_{ij}^e$  of  $Q_{ij}$  is twice the Onsager matrix  $L_{ij}$  of phenomenological coefficients [Va81] we obtain, to the leading order in the noise strength  $\varepsilon$

$$P'_I = \frac{1}{\varepsilon} \sum_{ij} L_{ij} \bar{X}_i^{(1)} \bar{X}_j^{(1)} + O(h^3, \varepsilon^0) \quad (5.64)$$

This is nothing but the Gibbsian form of entropy production of irreversible thermodynamics [Va81]. Notice that the factor  $\frac{1}{\varepsilon}$  accounts for the extensivity of entropy production as it is proportional to the volume of the system.

## 5.6 Conclusions

We have developed a thermodynamic approach to the class of dynamical systems amenable to a Fokker-Planck type of description based on the balance equation of information entropy. Entropy flux and entropy production-like terms depending on the characteristics of the dynamics in phase space, particularly the rate of phase space volume contraction, have been identified. Their connections with irreversible thermodynamics have been explored on two case studies pertaining to thermostatted and to mesoscopic systems.

Our principal motivation for augmenting the deterministic description by the addition of stochastic forcings is that nonequilibrium constraints reflect the interaction of a system with external reservoirs. Such an interaction involves, as a rule, a reduced description of the reservoirs; it is therefore most naturally modeled by a dissipative term, in which case it needs also to be complemented by explicit consideration of the fluctuations. This procedure which in many respects resembles classical coarse-graining leads, for free, to the regularization of the invariant probabilities and introduces a source term in the entropy balance, counteracting in the steady state the sink term which was the only one appearing in eq. (5.3). Furthermore, in the absence of the nonequilibrium constraint this description generates quite naturally the correct canonical equilibrium limit. This important condition, at the basis of the very concept of "thermostatting", is usually not fulfilled in the work reported in the literature where at equilibrium one obtains the microcanonical distribution. In this respect the case of the Sllod equations should be investigated further. In our view thermostatting should already be active in equilibrium, and this can only be achieved if the evolution operator  $F(\mathbf{x}, \mu_e)$  is dissipative. It is only at the level of the "effective" vector field  $\phi$ , eq. (5.28), that the conservative character of the underlying microscopic dynamics will show up.

Future work in this area should aim at establishing the link between irreversible thermodynamics and phase space dynamics for more representative systems and on a still more explicit basis. For instance, in most realistic systems, Lyapunov exponents and contraction rates fluctuate considerably along the invariant manifolds. The repercussions of these fluctuations on thermodynamic properties would certainly be worth elucidating. Of special interest are also multivariate, spatially extended systems possessing a large number of Lyapunov exponents. The extent to which all the exponents contribute to macroscopic level properties like entropy production is

largely unknown, and one might advance that only a few of them - presumably the slowest ones - would play an important role.

## Chapter 6

# Conclusions and perspectives

In this thesis we have been concerned with the probabilistic description of a wide class of dynamical systems emulating a variety of situations of interest. The generalized spectral decomposition of the Perron-Frobenius operator has been derived when it involves Jordan forms and a connection with transitions in the decay modes has been established. We have computed time correlation functions for models of homoclinic systems whose relevance is confirmed by experimental data and showed that they provide a characterization of the different types of homoclinic attractors.

We have also addressed the inverse problem of designing dynamical systems with prescribed probabilistic properties. One-dimensional chaotic maps with arbitrary invariant density and correlation function featuring one time scale can be constructed. It would be very useful to extend these results to correlation functions with two time scales which are frequently observed.

Simple models of spatially extended systems in the form of coupled map lattices giving rise to spatio-temporal chaos have been studied. In addition to having constructed Markov partitions for two coupled piecewise linear maps we have proposed a model for which the invariant one-dimensional reduced probability density for a lattice of arbitrary size can be computed. In this context, one direction of research is to explore the possibility of setting up reduced, mean field types of description, free of heuristic approximations for these systems.

On the other hand, in this thesis we have attempted to bring new perspectives to an old problem of statistical mechanics which has the strange privilege to stimulate and nourish passionate discussions related to its foundations, particularly in connection with irreversibility. Ever since the time of Boltzmann it has been customary to see the scientific community vacillating between extreme, mutually contradicting

positions. To day, in one end of the spectrum one will find researchers asserting that the problem of irreversibility has found its definitive solution in the hands of Boltzmann, and that its connection with the complexity of the underlying dynamics is rather tenuous. In the opposite end other researchers point to the need to extend classical and quantum dynamics in order to incorporate explicitly irreversibility - a fundamental, everyday reality.

We have adopted a "middle of the road" attitude which amounts to inquiring whether one can relate quantitatively the thermodynamic properties of a system at the macroscopic level to the characteristics of phase space dynamics at the microscopic level, accepting at the outset full validity of the basic laws governing this dynamics. Starting from a probabilistic description a thermodynamic approach has been developed based on the balance equation of information entropy for the class of dynamical systems amenable to a Fokker-Planck type of description. Entropy flux and entropy production-like terms containing information on the characteristics of the dynamics in phase space have been obtained, and their connections with irreversible thermodynamics have been explored.

Future work in this area should aim at establishing the link between irreversible thermodynamics and phase space dynamics for more representative systems and on a still more explicit basis. Of special interest are multivariate, spatially extended systems. The number of Lyapunov exponents of these systems is very large, and one may wonder whether only a few "dominant" such exponents-presumably the slowest ones - would count for macroscopic-level properties like entropy production. Furthermore, in most real-world systems Lyapunov exponents and contraction rates fluctuate considerably along the invariant manifolds. The repercussions of these fluctuations as far as irreversible thermodynamics is concerned would be worth elucidating.

## Bibliography

- [AbSt68] Abramowitz, M. and Stegun, I. A.. *Handbook of mathematical functions*. Dover, New York, 1968.
- [AlMaGaNi96] D. Alonso, D. MacKernan, P. Gaspard and G. Nicolis. Statistical approach to nonhyperbolic chaotic systems. *Phys. Rev. E*, **54**, 2474, 1996.
- [ArArRi90] F. Argoul, A. Arnéodo and P. Richetti. Symbolic dynamics in the Belousov-Zhabotinski reaction: an experimental and theoretical approach to Shil'nikov chaos. In *Spatial inhomogeneities and transient behaviour in chemical kinetics*, Manchester University Press, Manchester, 1990.
- [ArAv68] V. Arnold and A. Avez. *Ergodic problems of classical mechanics*. Benjamin, New York, 1968.
- [ArAuCv90] R. Artuso, E. Aurell and P. Cvitanovic. Recycling of strange sets. II. Applications. *Nonlinearity*, **3**, 325, 1990.
- [BaKe90] V. Baladi and G. Keller. Zeta functions and transfer operators for piecewise monotone transformations. *Commun. Math. Phys.*, **127**, 459, 1990.
- [BaNiNi97] V. Balakrishnan, G. Nicolis and C. Nicolis. Recurrence time statistics in chaotic dynamics. I. Discrete time maps. *J. Stat. Phys.*, **86**, 191, 1997.
- [Ba75] R. Balescu. *Equilibrium and nonequilibrium statistical mechanics*. Wiley, New York, 1975.
- [BaDa95] A. Baranovsky and D. Daems. Design of one-dimensional chaotic maps with prescribed statistical properties. *Int. J. Bifur. Chaos*, **5**, 1585, 1995.
- [Ba96] F. Baras. Stochastic analysis of limit cycle behavior in spatially extended systems. *Phys. Rev. Lett.*, **77**, 1398, 1996.

- [BeSc93] C. Beck and F. Schlögl. *Thermodynamics of chaotic systems*. Cambridge University Press, Cambridge, 1993.
- [Bl93] M. Blank. Singular effects in chaotic dynamical systems. *Russian Acad. Sci. Dokl. Math.*, **47**, 1, 1993.
- [Bl97] M. Blank. Generalized phase transitions in finite coupled map lattices. *Physica D*, **103**, 34, 1997.
- [BrTeVo96] W. Breyman, T. Tél and J. Vollmer. Entropy production for open dynamical systems. *Phys. Rev. Lett.*, **77**, 2945, 1996.
- [BrTeVo97] W. Breyman, T. Tél and J. Vollmer. Entropy balance, time reversibility and mass transport in dynamical systems. To appear in *Chaos*, **8**, 1998.
- [BrKu95] J. Bricmont and A. Kupiainen. Coupled analytic maps. *Nonlinearity*, **8**, 379, 1995.
- [BrKu96] J. Bricmont and A. Kupiainen. High temperature expansions and dynamical systems. *Commun. Math. Phys.*, **178**, 703, . 1996
- [BrKu97] J. Bricmont and A. Kupiainen. Infinite-dimensional SRB measures. *Physica D*, **103**, 18, 1997.
- [Bu95] L. A. Bunimovich. Coupled map lattices: one step forward and two steps back. *Physica D*, **86**, 248, 1995.
- [Bu97] L. A. Bunimovich. Coupled map lattices: some topological and ergodic properties. *Physica D*, **103**, 1, 1997.
- [BuSi88] L. A. Bunimovich and Ya. G. Sinai. Spacetime chaos in coupled map lattices. *Nonlinearity*, **1**, 491, 1988.
- [ChEyLeSi93a] N. I. Chernov, G. L. Eyink, J. L. Lebowitz and Ya. G. Sinai. Derivation of Ohm's law in a deterministic mechanical model. *Phys. Rev. Lett.*, **70**, 2209, 1993.
- [ChEyLeSi93b] N. I. Chernov, G. L. Eyink, J. L. Lebowitz and Ya. G. Sinai. Steady-state electrical conduction in the periodic Lorentz gas. *Commun. Math. Phys.*, **154**, 569, 1993.

- [ChLe97] N. I Chernov and J. L. Lebowitz. Stationary nonequilibrium states in boundary-driven Hamiltonian systems: shear flow. *J. Stat. Phys.*, **86**, 953, 1997.
- [Co96] P. Collet. *Leçons sur les systèmes étendus*, Ecole polytechnique, 1996.
- [Da96] D. Daems. Non-diagonalizability of the Frobenius-Perron operator and transition between decay modes of the time autocorrelation function. *Chaos, Solitons & Fractals*, **7**, 1753, 1996.
- [DaGrLvPr98] D. Daems, S. Grossmann, V. S. L'vov and I. Procaccia. Continued fraction representation of temporal multiscaling in turbulence. In preparation.
- [DaNi94] D. Daems and G. Nicolis. Probabilistic approach to homoclinic chaos. *J. Stat. Phys.*, **76**, 1287, 1994.
- [DaNi98a] D. Daems and G. Nicolis. Entropy production and phase-space volume contraction. Submitted to *Phys. Rev. E*.
- [DaNi98b] D. Daems and G. Nicolis. Coupled map lattices: exact results. In preparation.
- [De84] R. J. Deissler. One-dimensional strings, random fluctuations and complex chaotic structures. *Phys. Lett. A*, **100**, 451, 1984.
- [DeMa62] S. de Groot and P. Mazur. *Nonequilibrium thermodynamics*. North Holland, Amsterdam, 1962.
- [Dr97] D. J. Driebe. Jordan blocks in a one-dimensional Markov map. *Computers Math. Applic.*, **34**, 103, 1997.
- [Dr98] D. J. Driebe. *Fully chaotic maps and broken time symmetry*. Kluwer Academic Publishers, London, 1998.
- [EcRu85] J. P. Eckmann and D. Ruelle. Ergodic theory of chaos and strange attractors. *Rev. Mod. Phys.*, **57**, 617, 1985.
- [ErMi82] S. M. Ermakov and G. A. Mikailov. *Statistical modelling*. Nauka, Moscow, 1982.

- [EvCoMo90] D. J. Evans, E. G. D. Cohen and G. P. Morris. Viscosity of a simple fluid from its maximal Lyapunov exponents. *Phys. Rev. A*, **42**, 5990, 1990.
- [EvCoMo93] D. J. Evans, E. G. D. Cohen and G. P. Morris. Probability of Second Law Violations in Shearing Steady States. *Phys. Rev. Lett.*, **71**, 2401, 1993.
- [EvMo84] D. J. Evans and G. P. Morris. Nonlinear-response theory for steady planar Couette flow. *Phys. Rev. A*, **30**, 1528, 1984.
- [EvMo90] D. Evans and G. Morris. *Statistical mechanics of nonequilibrium liquids*. Academic, London, 1990.
- [FaCrFrPaSh80] D. Farmer, J. Crutchfield, J. Froehling, N. Packard and R. Shaw, Power spectra and mixing properties of strange attractors. *Ann. N. Y. Acad. Sci.*, **357**, 453, 1980.
- [Fe78] M. Feigenbaum. Quantitative universality for a class of nonlinear transformations. *J. Stat. Phys.*, **19**, 25, 1978.
- [Fe79] M. Feigenbaum. The universal metric properties of nonlinear transformations. *J. Stat. Phys.*, **21**, 669, 1979.
- [Fe96] B. Fernandez. Existence and stability of steady fronts in bistable coupled map lattices. *J. Stat. Phys.*, **82**, 931, 1996.
- [Fe97] B. Fernandez. PhD thesis, Université de la Méditerranée, 1997.
- [FeRa97] B. Fernandez and L. Raymond. The propagating fronts in a bistable CML. *J. Stat. Phys.*, **86**, 337, 1997.
- [Ga96] G. Gallavotti. Chaotic hypothesis: Onsager reciprocity and fluctuation-dissipation theorem. *J. Stat. Phys.*, **84**, 899, 1996.
- [GaCo95] G. Gallavotti and E. G. D. Cohen. Dynamical ensembles in nonequilibrium statistical mechanics. *Phys. Rev. Lett.*, **74**, 2964, 1995.
- [Ga82] P. Gaspard. Mémoire, Université Libre de Bruxelles, 1982.
- [Ga87] P. Gaspard. PhD thesis, Université Libre de Bruxelles, 1987.

- [Ga92] P. Gaspard.  $r$ -adic one-dimensional maps and the Euler summation formula. *J. Phys. A Math. Gen.*, **25**, L483, 1992.
- [Ga97a] P. Gaspard. Chaos and hydrodynamics. *Physica A*, **240**, 54, 1997.
- [Ga97b] P. Gaspard. Entropy production in open volume-preserving systems. *J. Stat. Phys.*, **88**, 1215, 1997.
- [GaKaNi84] P. Gaspard, R. Kapral and G. Nicolis. Bifurcation phenomena near homoclinic systems: a two-parameter analysis. *J. Stat. Phys.*, **35**, 697, 1984.
- [GaNiPrTa95] P. Gaspard, G. Nicolis, A. Provata and S. Tasaki. Spectral signature of the pitchfork bifurcation: Liouville equation approach. *Phys. Rev. E*, **51**, 74, 1995.
- [Ga98] P. Gaspard. *Chaos, scattering and statistical mechanics*. Cambridge University Press, Cambridge, 1998.
- [GeNi93] P. Geysmans and G. Nicolis. Thermodynamic fluctuations and chemical chaos in a well-stirred reactor: a master equation analysis. *J. Chem. Phys.*, **99**, 8964, 1993.
- [Gi94] T. Gilbert. Mémoire, Université Catholique de Louvain, 1994.
- [GoKr69] I. C. Gohberg and M. G. Krein. *Introduction to the theory of linear nonselfadjoint operators*. American Mathematical Society, Providence, 1969.
- [GrTh77] S. Grossmann and S. Thomaé. Invariant distributions and stationary correlation functions of one-dimensional discrete processes. *Z. Naturforsch.*, a **32**, 1353, 1977.
- [HaSa92] H. Hasegawa and W. Saphir. Decaying eigenstates for simple chaotic systems. *Phys. Lett. A*, **162**, 471, 1992.
- [HoHoPo87] B. Holian, W. Hoover and H. Posch. Canonical dynamics of the Nosé oscillator: stability, order, and chaos. *Phys. Rev. Lett.*, **59**, 10, 1987.
- [Ho85] W. Hoover. Canonical Dynamics: Equilibrium phase-space distribution. *Phys. Rev. A*, **31**, 1695, 1985.

- [Ju98] W. Just. Analytical approach for piecewise linear coupled map lattices. *J. Stat. Phys.*, **90**, 727, 1998.
- [Ka84] K. Kaneko. Period doubling of kink-antikink patterns, quasiperiodicity of antiferro-like structures and spatial intermittency in coupled logistic lattice - Toward a prelude of a field-theory of chaos. *Prog. Theor. Phys.*, **72**, 480, 1984.
- [Ka89a] K. Kaneko. Pattern dynamics in spatiotemporal chaos. Pattern selection, diffusion of defect and pattern competition intermittency. *Physica D*, **34**, 1, 1989.
- [Ka89b] K. Kaneko. Self-consistent Perron-Frobenius operator for spatiotemporal chaos. *Phys. Lett. A*, **139**, 47, 1989.
- [Ka93] K. Kaneko, ed., *Theory and applications of coupled map lattices*, Wiley, New York, 1993.
- [KeKu92] G. Keller and M. Künzle. Transfer operators for coupled map lattices. *Ergod. Th. & Dynam. Syst.*, **12**, 297, 1992.
- [KeKuNo92] G. Keller, M. Künzle and T. Nowicki. Some phase transitions in coupled map lattices. *Physica D*, **59**, 39, 1992.
- [KeNo92] G. Keller and T. Nowicki. Spectral theory, zeta functions and the distribution of periodic points for Collet-Eckmann maps. *Commun. Math. Phys.*, **149**, 31, 1992.
- [KoSa72] A. A. Kosyakin and E. A. Sandler. Ergodic properties of a class of piecewise smooth transformations of the interval. *Isvest. Vus. Math.*, **3**, 32, 1972.
- [Ku93] M. Künzle. PhD thesis, Universität Erlangen, 1993.
- [LaMa85] A. Lasota and M. C. Mackey. *Probabilistic properties of deterministic systems*. Cambridge University Press, Cambridge, 1985.
- [Lo94] J. Losson. PhD thesis, MacGill University, 1994.
- [LoMa94a] J. Losson and M. C. Mackey. Statistical cycling in two diffusively coupled maps. *Physica D*, **72**, 324, 1994.

- [LoMa94b] J. Losson and M. C. Mackey. Statistical cycling in coupled map lattices. *Phys. Rev. E*, **50**, 843, 1994.
- [LoMiMa95] J. Losson, J. G. Milton and M. C. Mackey. Phase transitions in networks of chaotic elements with short and long range interactions. *Physica D*, **81**, 177, 1995.
- [Ma92] D. MacKernan. Dissipative deterministic chaotic dynamics between the Lyapunov time and the long time limit: a probabilistic description. In T. Bountis, ed., *Chaotic dynamics: theory and practice*, Plenum Press, New York, 1992.
- [Ma95] D. MacKernan. Local and global statistical properties of deterministic chaos. *Nuovo Cimento*, **17 D**, 863, 1995.
- [Ma97] D. MacKernan. PhD thesis, Université Libre de Bruxelles, 1997.
- [MaNi94] D. MacKernan and G. Nicolis. Generalized Markov coarse graining and spectral decompositions of chaotic piecewise linear maps. *Phys. Rev. E*, **50**, 988, 1994.
- [MaHo92] M. Mareschal and B. Holian, eds., *Microscopic simulations of complex hydrodynamic phenomena*, Plenum Press, New York, 1992.
- [Ma91] D. Mayer. Continued fractions and related transformations. In T. Bedford et al., eds., *Ergodic theory, symbolic dynamics and hyperbolic spaces*, Oxford Science Publications, Oxford, 1991.
- [MoSoOs81] H. Mori and B. So and T. Ose. Time-correlation functions of one-dimensional transformations. *Prog. Theor. Phys.*, **66**, 4, 1981.
- [Ni95] G. Nicolis. *Introduction to Nonlinear Science*. Cambridge University Press, Cambridge, 1995.
- [NiDa96] G. Nicolis and D. Daems. Nonequilibrium thermodynamics of dynamical systems. *J. Phys. Chem.*, **100**, 19187, 1996.
- [NiDa98] G. Nicolis and D. Daems. Probabilistic and thermodynamic aspects of dynamical systems. *Chaos*, **8**, 311, 1998.

- [NiMaTi91] G. Nicolis, S. Martinez and E. Tirapegui. Finite coarse-graining and Chapman-Kolmogorov equation in conservative dynamical systems. *Chaos, Solitons and Fractals*, **1**, 1, 1991.
- [NiNi88] G. Nicolis and C. Nicolis. Master-equation approach to deterministic chaos. *Phys. Rev. A*, **38**, 427, 1988.
- [NiNiWa92] C. Nicolis, G. Nicolis and Q. Wang. Sensitivity to initial conditions in spatially distributed systems. *Int. J. Bifur. Chaos*, **2**, 263, 1992.
- [NiOpNi97] G. Nicolis, M. Op de Beeck and C. Nicolis. Dynamics of coarse-grained variables in spatially extended systems. *Physica D*, **103**, 73, 1997.
- [NiPiMa92] G. Nicolis, J. Piasecki and D. MacKernan. Toward a probabilistic description of deterministic chaos. In G. Györgi, I. Kondor, L. Savári and T. Tél, eds., *From phase transitions to chaos*, World Scientific, Singapore, 1992.
- [NiPr77] G. Nicolis and I. Prigogine. *Self-organization in nonequilibrium systems*. Wiley, New York, 1977.
- [Op94] M. Op de Beeck. Mémoire, Université Libre de Bruxelles, 1994.
- [Ott93] E. Ott. *Chaos in dynamical systems*. Cambridge University Press, Cambridge, 1993.
- [OttGrYo90] E. Ott and C. Grebogi and J. A. Yorke. Controlling chaos. *Phys. Rev. Lett.*, **64**, 1196, 1990.
- [PoHo97] H. Posch and W. Hoover. Time-reversible dissipative attractors in three and four phase-space dimensions. *Phys. Rev. E*, **55**, 6803, 1997.
- [Pr49] I. Prigogine. Le domaine de validité de la thermodynamique des phénomènes irréversibles. *Physica*, **15**, 272, 1949.
- [Pr61] I. Prigogine. *Introduction to thermodynamics of irreversible processes*. Freeman, San Francisco, 1961.
- [Pr80] I. Prigogine. *From being to becoming*. Wiley, New York, 1980.
- [Ri87] P. Richetti. PhD thesis, Université de Bordeaux, 1987.

- [Ru76] D. Ruelle. A measure associated with axiom-A attractors. *Amer. J. Math.*, **98**, 619, 1976.
- [Ru96] D. Ruelle. Positivity of entropy production in nonequilibrium statistical mechanics. *J. Stat. Phys.*, **85**, 1, 1996.
- [ShMaRo84] A. N. Sharkovsky, Y. L. Maistrenko and E. Y. Romanenko. *Differential equations and their applications*. Naukova Dumka, Kiev, 1984.
- [Sh65] L. P. Shil'nikov. A case of the existence of a countable number of periodic motions. *Sov. Math. Dokl.*, **6**, 163, 1965.
- [Sh70] L. P. Shil'nikov. A contribution to the problem of the structure of an extended neighborhood of a rough equilibrium state of saddle-focus type. *Math. USSR Sbornik*, **10**, 91, 1970.
- [TaAn94] S. Tasaki and I. Antoniou. Generalized spectral decomposition for the  $r$ -adic Renyi map. In P. Clément and G. Lumer, eds., *Evolution equations, control theory and biomathematics*, Marcel Dekker, New York, 1994.
- [Te88] R. Temam. *Infinite dimensional dynamical systems in mechanics and physics*. Springer, New York, 1988.
- [Va81] N. Van Kampen. *Stochastic processes in physics and chemistry*. North Holland, Amsterdam, 1981.
- [Vo93] D. L. Volevich. The Sinai-Bowen-Ruelle measure for a multidimensional lattice of interacting hyperbolic mappings. *Russian Acad. Sci. Dokl. Math.*, **47**, 117, 1993.
- [Vo94] D. L. Volevich. Construction of an analogue of Bowen-Ruelle-Sinai measure for a multidimensional lattice of interacting hyperbolic mappings. *Russian Acad. Math. Sbornik*, **79**, 347, 1994.
- [VoTeBr97a] J. Vollmer, T. Tél and W. Breyman. Equivalence of irreversible entropy production in driven systems: an elementary chaotic map approach. *Phys. Rev. Lett.*, **79**, 2759, 1997.

- [VoTeBr97b] J. Vollmer, T. Tél and W. Breymann. Entropy balance in the presence of drift and diffusion currents: an elementary chaotic map approach. To appear in *Phys. Rev. E*, **58**, 1998.
- [WaKa84a] I. Waller and R. Kapral. Spatial and temporal structures in systems of coupled nonlinear oscillators. *Phys. Rev. A*, **30**, 2047, 1984.
- [WaKa84b] I. Waller and R. Kapral. Synchronization and chaos in coupled nonlinear oscillators. *Phys. Lett. A*, **105**, 163, 1984.

